Aalto University
School of Chemical
Engineering

RIINA AROMAA

RARE EARTH ELEMENTS DISTRIBUTION KINETICS IN COPPER MATTE-SLAG SYSTEM

Master´s Programme in Chemical, Biochemical and Materials Engineering

Major in Sustainable Metals Processing

Master's thesis for the degree of Master of Science in Technology submitted for inspection, Espoo, 24 September, 2019.

Supervisor Prof. Ari Jokilaakso

Instructor M.Sc. Lassi Klemettinen

Aalto University
School of Chemical
Engineering

Aalto University, P.O. BOX 11000, 00076 AALTO
www.aalto.fi

Abstract of master's thesis

Author Riina Aromaa

Title of thesis Rare earth elements distribution kinetics in copper matte-slag system

Degree Programme Master's programme in Chemical, Biochemical and Materials Engineering

Major Sustainable Metals Processing

Thesis supervisor Ari Jokilaakso

Thesis advisor(s) / Thesis examiner(s) Lassi Klemettinen

Date 24.09.2019 **Number of pages** 89+29 **Language** English

Abstract

The use of rare earth elements (REE) is increasing due to the increasing use of hybrid electric vehicles (HEV) and green technology applications. As a result, the in-use stocks of REEs and the amount of end-of-life (EoL) products containing REEs are growing annually. Almost all primary REEs are produced in China. The EU has categorized REEs as being some of the most critical elements mainly since the rest of the world is dependent on China to supply them. The production of REEs is also riddled by the balance problem which leads to overproduction of some REEs and underproduction of others. Recycling of REEs could help alleviate the criticality of REEs and eliminate the balance problem. Currently, however, no REEs are functionally recycled.

This thesis studied the time-dependent behaviour of REEs in copper matte-slag system in copper matte smelting conditions. The literature review investigated the resources, production and recycling of REEs as well as the distribution of elements during copper matte smelting. Of the sources for secondary REEs, nickel metal hydride (Ni-MH) batteries were studied more closely. The experimental part focused on the behaviour of REEs in simulated copper flash smelting conditions. The REEs chosen for this work were lanthanum and neodymium, and experiments were conducted in air and argon atmospheres. Sample characterization was conducted using scanning electron microscope energy dispersive X-ray spectroscopy (SEM-EDS), electron probe microanalyser (EPMA) and laser ablation inductively coupled plasma mass spectrometry (LA-ICP-MS).

The results of this work indicated that the REEs strongly favour the slag phase and the distribution into the slag phase begins almost instantly when the system reaches high temperatures. With increasing contacting time, the REEs distribute more strongly into the slag phase.

Keywords REE, Ni-MH batteries, kinetics, copper smelting

Aalto-yliopisto
Kemian tekniikan
korkeakoulu

Aalto-yliopisto, PL 11000, 00076 AALTO
www.aalto.fi

Diplomityön tiivistelmä

Tekijä Riina Aromaa

Työn nimi Harvinaisten maametallien jakautumisen kinetiikka kuparikivi-kuona systeemissä

Koulutusohjelma Master's programme in Chemical, Biochemical and Materials Engineering

Pääaine Sustainable Materials Processing

Työn valvoja Ari Jokilaakso

Työn ohjaaja(t)/Työn tarkastaja(t) Lassi Klemettinen

Päivämäärä 24.09.2019 **Sivumäärä** 89+29 **Kieli** Englanti

Tiivistelmä

Hybridiajoneuvojen ja vihreän teknologian sovellusten määrä on kasvussa ja niiden mukana lisääntyy myös harvinaisten maametallien käyttö. Näiden mukana kasvaa vuosittain harvinaisten maametallien määrä yhteiskunnassa ja elinkaarensa päähän tulevien, harvinaisia maametalleja sisältävien tuotteiden määrä. Lähes kaikki primaariset harvinaiset maametallit tuotetaan Kiinassa. Muu maailma on harvinaisten maametallien suhteen riippuvainen Kiinasta ja se on suurin syy siihen, että EU on luokitellut harvinaiset maametallit kriittisimpien alkuaineiden joukkoon. Harvinaisten maametallien tuotantoon liittyy myös tasapaino-ongelma, joka johtaa joidenkin maametallien ylituotantoon ja toisten alituotantoon. Harvinaisten maametallien kierrätys voisi vähentää niiden kriittisyyttä ja poistaa tasapaino-ongelman, mutta niiden kierrätys on tällä hetkellä käytännössä olematonta.

Tässä diplomityössä tutkittiin harvinaisten maametallien ajasta riippuvaista käyttäytymistä kuparikivi-kuona systeemissä kupariliekkisulatusuunissa vallitsevissa olosuhteissa. Kirjallisuusosassa tarkasteltiin harvinaisten maametallien lähteitä, tuotantoa ja kierrätystä sekä aineiden jakautumista kupariliekkisulatusprosessissa. Harvinaisten maametallien sekundaarisista lähteistä Ni-MH akkuihin syvennyttiin tarkemmin. Kokeellisessa osassa tukittiin harvinaisten maametallien jakautumista kivi- ja kuonafaasien välillä ilma- ja argonatmosfäärissä. Harvinaisista maametalleista tähän työhön valittiin lantaani ja neodyymi. Näytteiden koostumuksen analysointiin käytetyt metodit olivat SEM-EDS, EPMA ja LA-ICP-MS.

Työn tuloksista ilmeni, että harvinaiset maametallit suosivat vahvasti kuonafaasia ja niiden jakautuminen kuonafaasiin alkaa lähes välittömästi, kun systeemi saavuttaa korkean lämpötilan. Pidemmillä kontaktiajoilla harvinaiset maametallit jakautuvat vielä vahvemmin kuonafaasiin.

Avainsanat Harvinaiset maametallit, Ni-MH akut, kinetiikka, liekkisulatus

Preface

This master's thesis has been actualised at Aalto University School of Chemical Engineering at the Department of Chemical and Metallurgical Engineering. The work was completed as a part of the SYMMET project.

This thesis was supervised by prof. Ari Jokilaakso from the research group for metallurgy. I'd like to express my gratitude for his insightful advice and help throughout this work. This thesis was instructed by M.Sc. Lassi Klemettinen, who I want to sincerely thank for all his help, guidance and valuable feedback regarding this thesis.

I also wish to thank the members of the metallurgy and metallurgical thermodynamics and modelling groups for their help and support.

I want to thank my family who have always given me their support throughout my studies and especially my dad, who is probably the reason I ended up studying this field. Lastly, I want to thank Janne, who has patiently been through all the highs and lows of this project with me.

Riina Aromaa

24.9.2019

Symbols and Abbreviations

EDS	Energy dispersive X-ray spectroscopy
EoL	End-of-life
EPMA	Electron probe microanalyser
HEV	Hybrid electric vehicle
LA-ICP-MS	Laser ablation inductively coupled plasma mass spectrometry
K	Equilibrium constant
$L^{m/s}$	Distribution coefficient (matte/slag)
Ni-MH	Nickel metal hydride
PCB	Printed circuit board
ppm	parts per million
REE	Rare earth element
REO	Rare earth oxide
SEM	Scanning electron microscope
t_e	Equilibration time
WEEE	Waste electronic and electrical equipment
wt-%	Weight percentage
α	Activity
γ	Activity coefficient

Table of contents

1 Introduction

Technological advancement has led to an increased need for rare earth elements (REE), which are used in a multitude of high-tech applications and green technologies. As a result of increased use, the in-use stocks of REEs are growing and an increasing number of REE containing products are discarded each year.

One of the important applications for REEs are Ni-MH (Nickel metal hydride) batteries, which are used in hybrid electric vehicles (HEV). The number of HEVs sold globally has been steadily growing. The in-use stocks of Ni-MH batteries are significant and growing as more HEVs are taken into use. Considering all applications, the use of REEs is growing, owing mostly to their use in NdFeB permanent magnets which are essential for many green technologies such as wind turbines.

The REE reserves are spread around the world but nearly all REEs are produced in China. The low price of REEs produced in China has led to difficulties for projects outside China to be feasible.

The primary production of REEs is affected by the balance problem. REEs are found together in nature in varying concentrations. Their relative concentrations are most often not the same as the demand for distinct REEs. This leads to overproduction of some REEs and underproduction of others.

REEs have been determined by the EU to be some of the most critical elements. This is mainly due to the EU being dependent on China to supply its demand for REEs. REEs are also difficult to replace in their applications, making them essential for the production of many high technology applications.

Recycling of REE containing products is one of the ways that could help alleviate the supply risk of REEs. Recycling could also remove the balance problem as REE containing products contain REEs in similar concentrations to the demand. Currently, basically no REEs are functionally recycled, and when REE containing products are recycled, REEs are usually lost in the process.

Understanding the thermodynamic behaviour of the valuable elements of a product is essential to obtain process parameters that are suitable for recycling and recovery of the valuables. The distribution of base elements and reactions during copper matte smelting have been studied in detail [1]. Previous research concerning the behaviour of REEs in copper matte slag systems is limited. The equilibrium distribution of REEs in a copper matte-slag system has been investigated but the study did not look at distribution kinetics [2].

At the moment REEs are not functionally recycled and more studies are needed on the possible avenues of recycling. One possible method of recycling REEs is in pyrometallurgical processes. Knowledge of thermodynamic factors is essential to determine the behaviour of elements in a system. Currently, the equilibrium distribution of REEs in a copper matte-slag system is known but how it is reached is not.

The goal of this thesis was to experimentally measure the time dependency of REE distribution during copper matte smelting. Experiments were conducted in air and argon atmospheres to simulate different conditions in the flash smelting furnace.

This thesis consists of two parts: the literature review and the experimental part. The literature review looked at primary and secondary REEs, their sources, production and criticality. From the sources of secondary REEs, Ni-MH batteries were investigated in more detail. Different recycling processes were studied as well as the distribution of elements during copper matte smelting. The experimental part introduces the experimental and analytical methods. The results are discussed and compared to results from the literature review.

2 Primary REEs

2.1 Resources

REEs are defined as the 15 lanthanide elements and Sc and Y. Although in practice scandium is often removed from the definition due to its different behaviour. One of the lanthanides, promethium, is also very rare and not found in nature since it has a very short half-life. [3]

REEs can be divided into heavy and light REE elements. Light REEs consist of lanthanides La, Ce, Pr, Nd and Sm and heavy REEs of lanthanides Eu, Gd, Tb, Dy, Ho, Er, Tm, Yb and Lu as well as Y. Heavy REEs often occur together in nature as do light REEs. Geological deposits of light REEs are more common than those of heavy REEs. [3]

Around 200 different REE bearing minerals are known but only a small number of them are commercially significant. Bastnäsite and monazite are the minerals most often mined for light REE elements while xenotime is mined for heavy REEs. [4] REEs never occur alone in nature but are instead always accompanied by other REEs in different concentrations.

REEs almost always occur in nature in the +3 valence state, in other words in the form of REE_2O_3 oxide. Ce and Eu make up two exceptions. Cerium may be in the +4 valence state and form CeO_2 in oxidizing environments. Oxidizing environments include weathered deposits and seawater deposits. Eu may be found in the +2 valence state in reducing environments. [3]

REEs can be found in several types of deposits, mainly in either hard rock deposits or placer sands. Placer deposits are more numerous. [5] REEs are also produced as co-products or by-products with other minerals and it is possible to extract them from some wastes [3]. Extraction of REEs as by-products or co-products is more common than mining REEs as the main mineral [5]. Geological deposits of REEs can be divided into four main groups: carbonatites, alkaline igneous systems, ion-adsorption clay

deposits, and monazite-xenotime-bearing placer deposits. Light REEs are mainly produced from carbonatites and placer deposits while the main source for heavy REEs are ion-adsorption clay deposits. [6]

Ion-exchange clay deposits in China are nearly the only deposits of heavy REEs that are currently being extracted [7]. The deposits are usually small and have a low grade of REEs but they are relatively rich in heavy REEs [3]. In ion adsorption style deposits radioactive elements are washed away by weathering while heavy REEs are selectively ion-adsorbed into the clay layer. This type of deposit has currently only been found in southern China and some parts of Southeast Asia since it is formed under specific climate and geological conditions. Ion-exchange clay types of deposits are superior in the sense that they contain very few radioactive elements and the REEs can be easily separated. [8]

Carbonatite type deposits can be found in e.g. China, the United States, Australia and Vietnam. The amount of REE oxides in carbonatite deposits is usually medium to large but with a high grade. Carbonatites are the main economic source of REEs. Two of the most well-known REE mines, Bayan Obo in China and Mountain Pass in the US, both mine carbonatite type deposits. Bayan Obo is the largest REE deposit in the world. [3] The REEs found in carbonatite type deposits are almost exclusively light ones [5].

Alkaline rocks are found in the Russian Kola Peninsula, Greenland and Canada. Compared to carbonatite deposits, alkaline rock deposits have a larger amount but a lower grade of REEs. They also have a higher proportion of heavy REEs. [3]

Placer deposits or mineral sands are found in India, Australia and South Africa. The grade of REEs is usually low in placer deposits and the REEs are usually by-products. Monazite and xenotime are some of the minerals which may be concentrated in placer deposits but monazite from placer deposits tends to have more radioactive elements than monazite from carbonatite deposits. [3]

The abundance of REEs in the earth's crust varies. The most abundant is cerium at 66 ppm at the same level as copper. The least abundant is thulium at 0.5 ppm which is

close to thallium (0.7 ppm). [9] The light REEs cerium, lanthanum and neodymium are the most abundant in the earth's crust while heavier REEs, such as lutetium and thulium are rarer. As stated by the Oddo-Harkins rule, REEs with odd atomic numbers are more abundant in the crust than REEs with even atomic numbers. [3]

The U.S. Geological Survey [6] reported that the world reserves of REEs in 2017 were estimated to be 120 million tons. The largest reserves are located in China with 44 million tons with Brazil and Vietnam coming second with about half of that at 22 million tons each. Other countries with significant reserves include Australia, Canada, Greenland, India, Malawi, Malaysia, Russia, South Africa and United States. [6]

Eggert et al. [10] reported that the REE resources outside of China grew significantly between the years 2010 and 2015 following the REE crisis, when China reduced its export quotas and REE prices rose significantly. The resources outside China were 13.4 million metric tons in 2010 whereas in 2015 the same figure was 100.2 million tons. According to Eggert et al. [11] much of these are located in Canada and Greenland. [10]

2.2 Production

In 2017 the world production of REEs from primary resources was 130,000 metric tons. China was by far the largest producer with 105,000 tons. China has controlled the REE production and market for the last few decades. The second largest producer in 2017 was the United States with 20,000 tons. Other producer countries were Australia, India, Malaysia, Russia, Thailand and Vietnam with production quantities ranging from 100 to 3,000 tons. [6] However, estimates for mining production of REEs can be quite varied depending on, if the illegal mining operations in China are taken into account. Some sources estimate that the illegal production may be as high as 30 % of the Chinese national production quotas. [12]

The extraction rates of REEs have experienced some periods of strong growth. From 1990 the production of REEs has more than doubled, reaching 130,000 tons in the 2000s. The strongest growth in the extraction rates was between 2002 and 2008.

Then the average growth was up to 6 % per year. Since then, however, the extraction rates have remained somewhat similar at around 130,000 tons. The REE crisis can be seen also in the production numbers as a dip but they quickly returned to the pre-crisis values of around 130,000 tons per year. [12] The yearly world mine production values from 1990 to 2017 are presented in Figure 1.

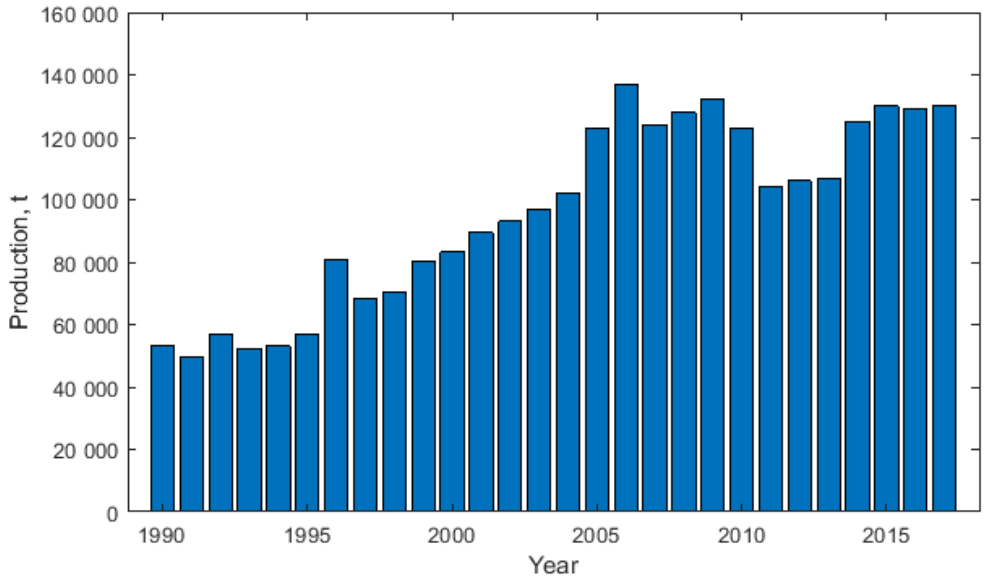

Figure 1 REE world mine production 1990-2017. 1990 [13], 1991-1995 [14], 1996-2000 [15], 2001-2005 [16], 2006-2010 [17], 2011-2015 [18], 2016-2017 [6].

One challenge rising from the different crustal abundances of REEs and their occurrence together in nature is the so called balance problem where the production and demand of different REEs is unbalanced. Primary production may produce more than necessary of a less in demand REE without necessarily matching the demand of a higher in demand REE. One example is of La, Ce, Nd, Dy and Pr which occur together in nature but the amounts of La and Ce are higher than those of Nd, Dy and Pr. The demand for Nd, Dy and Pr is higher than the demand for La and Ce which means that La and Ce are overproduced while trying to match the demand for Nd and Pr. [19, 20] The balance problem emerged when the newer applications of REEs such as lamp phosphors required pure REEs. Older applications used mixtures of REEs such as mischmetal, which did not lead to such a large disparity between supply and demand as most REEs that were produced were also consumed. [12] Mischmetal is an alloy of

REEs and the individual elements are present in the same proportion as which they naturally occur in bastnäsite or monazite [5].

The environmental costs associated with primary REE production may often be significant. Some new mining operations have faced backlash due to concerns about adverse effects on the environment and health. Mining of REEs is associated with the release of contaminants such as dust and heavy metals. 2000 tons of toxic waste and 1000 tons of ammonium sulfate and heavy metals contaminated wastewater are produced when one ton of REEs are processed. More negative effects include soil erosion, flooding and loss of biodiversity as well as pollution of air, soil and water. [21]

Mining of REEs is mainly done in countries with environmental and health regulations that are less strict. Especially illegal mining in China does not in any way comply with regulations. Many elephants such as poor ventilation of dusty work area, poor hygiene and improper use or absence of personal protective equipment increase the likelihood of exposure. Long-term exposure to REE dusts may cause severe lung issues.

Another challenging quality of primary REEs is that they are often found associated with uranium or thorium mineralization. Uranium ores often contain significant amounts of REEs and vice versa. Some particular challenges in processing REE ores can rise from this co-deposition with radio-nuclides. REE mining is often associated with formation of uranium or thorium-rich waste and radioactive stockpiles. [21]

2.3 World trade

The main exporter of REEs and compounds by far is China which has held a monopoly on REEs for the last few decades. USA, Japan, Germany, Austria and France are among the largest importers. Many of the largest importers do not have any REE mining and are thus completely reliant of Chinese exports. [3]

The largest exporters of REEs in any form in 2017 measured by value were China, Malaysia, Japan, Vietnam and France. Any form in this case refers to REEs in all stages

of the value chain. The main exporters measured by weight of REEs were China, Australia, Malaysia, Myanmar and Russia. [22] The largest exporters by value and weight are given in Table 1.

Table 1 Largest exporters of REEs by value and weight [22].

Exporter	Value (m $)	Exporter	Weight (kt)
China	501	China	43.6
Malaysia	247	Australia	28.9
Japan	199	Malaysia	25.5
Vietnam	163	Myanmar	20
France	100	Russia	10.3

The largest importers of REEs in any form in 2017 by value were Japan, United States, China, Vietnam and Germany. The largest importers measured by weight were China, Malaysia, Japan, United States and Estonia. [22] The largest importers by value and weight are given in Table 2.

Table 2 The largest importers of REEs by value and weight [22].

Importer	Value (m $)	Importer	Weight (kt)
Japan	570	China	35.8
USA	298	Malaysia	29.6
China	214	Japan	29.6
Vietnam	116	USA	12.5
Germany	107	Estonia	8.7

The largest single trade flows are naturally found between the largest exporters and the largest importers. The largest single trade flows are given in Table 3. It is interesting to note that China is involved in more than half of the largest trade flows.

Table 3 The largest trade flows of REEs by value and weight [22].

Trade flow	Value (m $)	Trade flow	Weight (kt)
China to Japan	209	Australia to Malaysia	28.8
Vietnam to Japan	155	Myanmar to China	20
Malaysia to China	131	China to Japan	16
China to USA	103	Malaysia to China	12.3
Australia to Malaysia	75	China to USA	9.6

Some trends in the REEs trade can be seen in the global trade flows. If a country is a large exporter by weight but not a large exporter by value, it most likely means that the country exports products from the beginning of the value chain, such as concentrates. One example of such a country is Australia where the environmental legislation is relatively strict compared to some less developed countries. This has given birth to a business model where REEs are mined in Australia but exported to other countries, such as Malaysia, for smelting [8]. The largest trade flow by weight is from Australia to Malaysia which would support this.

After smelting in Malaysia the product is again exported [8]. This is supported by the fact that Malaysia is both one of the largest importers of REEs as one of the largest exporters. By value the trade flow from Malaysia to China is larger than the trade flow from Australia to Malaysia but measured by weight the situation is reversed [22]. The value of the REE products is thus increasing while it is in Malaysia. Malaysia was also one of the fastest growing importers and exporters between the years 2012 to 2017 [22]. This likely speaks for this being a recent trend rather than one that has been the standard for a long time.

Japan is one of the largest consumers of REEs but there is no mining of REEs within the country. Japan is on the list of large exporters by value but not by weight meaning that they process REEs higher up in the value chain. Japan imports large quantities of

REEs at a relatively high value. It is on both lists for the largest importers but is higher up on the list of importers by value. Japan is thus likely importing REEs in an already quite refined form and then using them to produce REE containing consumer products such as mobile phones or electric vehicles.

Europe is largely absent from the lists of largest exporters and importers supporting the statement that there is very little REEs related production within the EU. France is listed as one of the largest exporters by value. This is probably due to the company Solvay which separates REEs and thus functions somewhat higher up in the value chain. Estonia is listed as one of largest importers by weight, most likely because of the company Silmet.

Silmet was not too long ago acquired by a company from the United States and any products were likely to be exported. However, the company that acquired it has since gone bankrupt. Currently the largest streams to Silmet are coming from Russia, likely from the Lovozero deposits. Most of the production in Estonia is still being exported and the main importing countries are the U.S. and Japan, although a fair share of it is going to Germany as well. Most of the EU production of REE containing products, such as NdFeB permanent magnets, fluorescent lamps and Ni-MH batteries is taking place in Germany.

A lot of the mined REEs are going to China since only a few REE separation plants exist outside of it. Much of the competence is located in China. The only major separation plants outside China are the Silmet plant in Estonia, the Solvay Rhodia plant in France and the Lynas Advanced Materials Plant in Malaysia. China has also managed to make it economical to perform value added manufacturing in China since restrictions are placed on exports but not consumption within its borders. [23]

The total value of the global REE trade was 2.1 billion $ in 2017. It is significantly less than the highest value of almost 7 billion from around 2010. [22] This is, however, not a result of reduced trading since the total weight of REEs traded globally reached 180 kt in 2017 whereas in 2010 it was 110 kt [22]. The recent trends in REE trade are

presented in Figure 2. The figure shows the effect of the reduction in Chinese export quotas which raised the prices of REEs through the roof creating the so called REE crisis. After the crisis the weight of traded REEs rose steadily while the value of the traded material decreased [22].

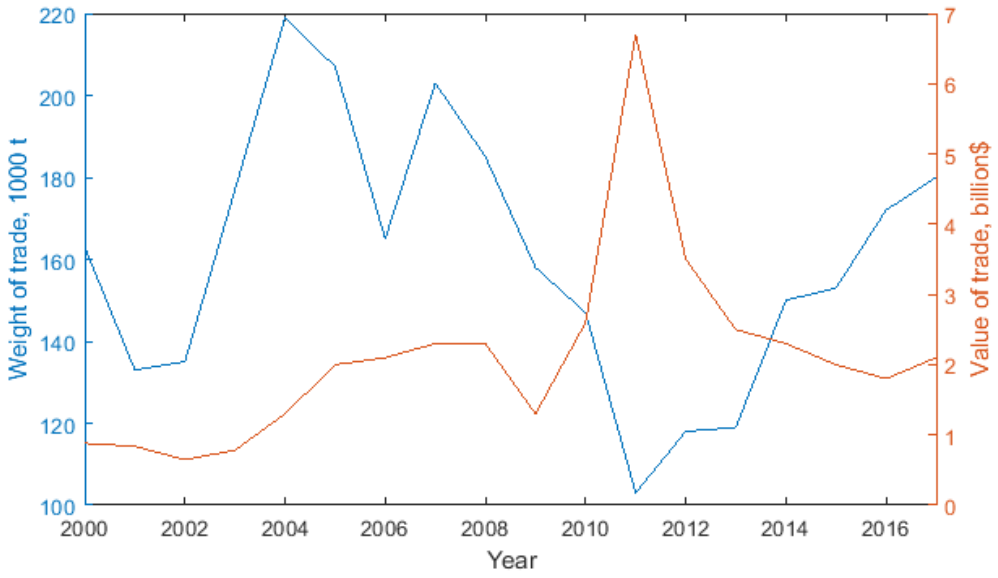

Figure 2 Recent REE trade by weight and value, adapted from [22].

2.4 Criticality

Criticality can be thought of as a measure of supply risk and demand. Criticality of a raw material can be measured in a number of ways and most commonly it involves defining the supply risk and economical importance of the raw material. The more in demand the material is and the more restricted its supply is, the more critical the material becomes. [19]

Evaluations can be done on a number of levels and the results will vary based on the chosen scale. The criticality of an element globally might not be the same as the criticality of the same element for a country or a region. The same applies for short-term and long-term analyses. Factors that are often considered when doing criticality studies are geological deposits, geographic locations of deposits and processing facilities, social issues, regulatory structures, geopolitics, environmental issues, recycling potential, sustainability and substitutability. [19]

2.4.1 Criticalities of REEs

The criticality of REEs on the global scale has been investigated by Nassar et al. [24] based on supply risk, environmental implications and vulnerability to supply restriction. They found REEs as a group to be less critical than some other elements e.g. silver on the global scale although previously the criticality of REEs has been thought of as being one of the highest. [24]

Supply risk can be evaluated based on three components: the geological, technological and economic component, the social and regulatory component, and the geopolitical component. Nassar et al. [24] found that the REEs had similar supply risks due to the fact that they occur together in the same ore bodies and geographic locations. They noted, however, also that the balance problem may be of some importance in different supply and demand scenarios. [24]

Environmental implications can be evaluated using life cycle analysis. REEs impact the environment through their extraction and processing, which requires energy and water while also generating polluting emissions to air, water and soil. On a scale from 0 to 100 the results of Nassar et al. [24] for different REEs ranged from very low (4.2) for lanthanum to moderately low (34.4) for lutetium. The differences reflect economic allocations of environmental burdens based on elemental distributions in concentrate and price averages. [24]

Vulnerability to supply restriction can be evaluated globally by using two components: importance and substitutability [25, 24]. Nassar et al. [24] found significant variation in the vulnerability to supply restrictions for different REEs. On a scale from 0 to 100, some, such as Sm, scored as low as 15.1 but others scored as high as 50.6. Eu, Er and Dy have the largest vulnerability for supply restriction on the global level. The differences reflect the variation in uses and the potential for substitution of the different elements. For Eu which scored the highest, the main use is in phosphors and its substitution is generally not possible. [24]

When changing the boundary of the criticality study from global to just the European Union, REEs become more critical. The European Commission evaluated criticality on

the basis of substitutability, economic importance and reliance on importation. Based on these criteria REEs are considered to be the most critical by the EU. [25] This criticality result is different from the global case studied by Nassar et al. [24] mainly due to the fact that EU is completely reliant on importation of REEs to supply the demand. There is no significant extraction of REEs within the EU and the recycling of post-consumer products containing REEs is currently minimal. [25]

The European Commission [25] used the substitution index as a measure of the difficulty of substituting the material. Value for the index was calculated for economic importance and supply risk parameters. The economic importance was calculated based on technical and cost performance of the substitutes and the supply risk based on global production and criticality as well as co-production and by-production of the substitutes. The economic importance of light and heavy REEs was calculated to be 0.90 and 0.96, respectively. The values for supply risk for light and heavy REEs were 0.93 and 0.89, respectively. On a scale from 0 to 1, 1 would be least substitutable and REEs are thus considered highly critical. [25]

A review article by Pell et al. [19] of several criticality studies at several different levels found most REEs to be critical and several to be extremely critical in regards to the supply risk. The economic importance of the REEs as a whole was not as large as their supply risk but most were still categorized as being critical in regards to the economic importance as well. The study also applied an economic resource scarcity potential to the evaluation of criticality on a global scale. Their findings included that Nd and Dy had the highest criticality and most need to broaden the supply chain while Ce was overproduced and available in excess. Nd and Dy have also a relatively high economic importance compared to the other REEs. [19]

The criticality of specific REE elements is changing as their use in applications is either increasing or decreasing. Some heavy REEs, previously considered to be some of the most critical, have been surpassed by other light REEs. This is due to their main application being fluorescent lamps, the use of which is declining. On the other hand, some light REEs such as neodymium are used in applications with increasing

production volumes, such as NdFeB permanent magnets. [12] Especially carbon lean technology applications, such as wind turbines and electric vehicles increase the demand for Nd.

2.4.2 Reasons

There are many reasons why REEs are among some of the most critical elements. The Chinese monopoly on REE production, the widespread use of REEs and the difficulty of replacing them are among the most important.

Many REEs cannot be substituted in the applications they are used in [20]. There either are no substitutes or the substitutes do not perform as well as the REEs. Some substitutes may also be as expensive as the REE they are used to replace. [3] The difficulty in substituting REEs increases their criticality and supply risk. [25]

The main global producer of REEs is China which produces 95 % of all REEs [21]. China controls the amount of REEs it allows to be exported and it has reduced export quotas in the past [19]. There is significant internal demand and use by industries on all levels of the value chain within China as well [26]. These make up some of the biggest threats to global supply of REEs.

There is very little mining of REEs outside of China and some countries are therefore losing the ability and infrastructure to extract and process ores containing REEs and manufacture REE products. Currently the world demand of REEs is supplied by China but there has been an increase in domestic REE manufacturing industries in China which could have an effect on the amount of REEs it exports to the world. There is a risk of domestic demand in China surpassing the production, or the global demand of REE increasing significantly. This combined with the difficulty of opening new mines and achieving permits creates doubt about the continued global supply of REEs. [27]

The issue for the EU is that there is currently very little REE related production on any level of the value chain. There is currently no extraction of REE oxides. Solvay in France and Silmet in Estonia are the only European operators with business in separation of REE oxides. Together they currently conduct 3-5 % of the global REE

oxides separation. LCM in the United Kingdom and again Silmet in Estonia are the only companies in the EU working with metal fabrication of REEs. Together they have a 1 % share of global production in the field. There are a few companies, mostly in Germany, working with the manufacture of NdFeB permanent magnets, Ni-MH batteries and fluorescent lamps. The share of global production, however, is small, 6-9 % at best for the manufacture of fluorescent lamps, the share of production for NdFeB magnets and Ni-MH batteries is even smaller, 1-2 % and <1 %, respectively. [28]

Challenges exist for REE production outside China. The owner of the Mountain Pass mine which was reopened in 2012, Molycorp, filed for bankruptcy less than three years after starting up production again. The owner of Mount Weld, Lynas, experienced similar difficulties but pulled through although its current existence is not without struggle. A major component in this struggle is the fact that both mines are rich in the non-critical light REEs. [23] The cheaper production of REEs in China is keeping prices too low for many projects outside China to be lucrative.

The production costs in each country are affected by several factors, including the environmental regulations on smelting. The regulations may increase the expenses related to waste disposal and treatment. Also, while the energy costs in USA and Australia are relatively low compared to e.g. Japan, the cost of labor is high. Differences are found related to the cost of raw materials needed for smelting which are high in the US but low in Australia. [8]

The balance problem also contributes to the criticality of REEs. The current demand is most unbalanced compared to the supply for neodymium, dysprosium, terbium and erbium. At least for the near future there will continue to be shortages of these elements. [29] This is mostly due to the balance problem and lack of recycling and the high use of these elements in consumer products.

The demand of REEs is expected to grow. They are crucial in the change to a carbon-lean energy system. REEs are increasingly being used in green energy applications such as wind turbines. [29] REEs are also used in alternative energy vehicles, hybrid

electric vehicles and electric vehicles which are becoming increasingly more popular. This affects the demand of neodymium in particular as it is used in the electric motor permanent magnets and the permanent magnets used in wind turbines. [30] Most of the increase in the demand of REEs in the near future can thus be attributed to the increasing use of NdFeB permanent magnets [28].

2.4.3 Solutions

There are many ways to tackle the criticality of REEs. Most include some way of reducing supply risk or decreasing the economic importance of the REEs. They include diversification of the supply, stockpile build-up, recycling and developing new materials and technologies to replace the REEs. [8]

Diversification of supply is necessary for geopolitical reasons. China has for decades had basically a monopoly on the mining of REEs. Not many years ago 95 % of REEs production came from China. China stills accounts for basically all of the production of REEs but the recent trend has been somewhat positive in regards to the diversification of supply. The Mount Weld mine in Australia has been recently opened and is one of the major producers of REEs outside China.

There are several projects on extracting REEs outside China in the feasibility and pre-feasibility phases. A few possible new mining projects exist also in Europe, the most likely to be taken into production being in Sweden or Greenland. If even one of the possible projects in the EU would enter production, it would have a significant influence on the supply of many REEs.

Some attempts have been made to diversify the supply of REEs and contracts have been signed by Siemens and Molycorp as well as Lynas and some Japanese companies. However, these companies are only able to survive if their customers are willing to pay a higher price for their product in order to help alleviate the supply risk that is associated with the REEs. [28]

Increased primary production might support increased recycling as well. Increased primary production would increase the capacity for separation of REEs which in turn

could increase the ability of recycling REEs from end-of-life (EoL) products. [7] Increasing the amount of REEs recycled is essential to ensure the security of supply [20]. Recycling of REEs could reduce the geopolitical aspects of supply risk by diversifying the supply [27].

Some countries keep stockpiles of valuable or critical elements. Stockpiles act as a buffer against possible supply restrictions or the possibility of prices rising significantly. China has planned to create so called strategic reserves of REEs by setting aside 300,000 tons of REEs and creating a stockpile in Inner Mongolia where the Bayan Obo mine is located. [31] Stockpiles of less in demand REEs are also formed because of the disparity between the supply and demand of certain REEs [12].

Substituting REEs in some of their applications would reduce their demand and criticality. Some REEs have been substituted in their applications following the high price increase of REEs after the decrease in Chinese export quotas. The price increase acted as a catalyst to drive the research to replace the REEs with a cheaper material. For example NeFeB permanent magnets can be replaced by other magnets but they are not as effective and larger magnets are required to perform the same function. Similarly the REE mixture in Ni-MH batteries can be replaced by another alloy but only with a decrease in the hydrogen storage properties.

Substitution may be done in several ways. One is element-for-element substitution in which one element is substituted for another. Second is technology-for-element substitution in which a new production technology allows for less of the critical element to be used. Third method is grade-for-grade substitution in which e.g. a magnet is substituted for the same type of magnet that just has less of the critical element and thus does not exhibit as good properties. Fourth is product-for-product substitution in which e.g. a magnet is replaced by another type of magnet that perhaps has lower performance or larger size. The broadest type of substitution is system-for-system in which the whole working function is changed. E.g. wind turbines no longer use gearboxes and their function has been replaced by magnets. [10]

Even though REEs are chemically very similar and they share many similarities, their characteristics and behaviours are different. This means that REEs sometimes cannot be substituted with another REE even though they are very similar. If it could be done it would be very beneficial as some REEs experience overproduction while the supply of others cannot match their demand.

Recycling is one major way in which the criticality of REEs can be reduced. In-use stocks of REE containing consumer products are increasing and with them the possibility of supply from EoL consumer products. In the short term the waste flows are unlikely to contribute much to the REE supply but in the long term the amounts of EoL products containing REEs will increase sharply [29]. A lot of research is also being done in the area of recovery of REEs and recycling of products containing REEs [32, 33]. However, the recovery of REEs from them would require functional recycling of the REEs which is not the case currently. Developing economic processes to functionally recycle REEs would lessen the need for primary raw materials and recycling would help alleviate the balance problem. The composition of REEs in EoL products is more similar to the demand of different REEs and recycling could help with the overproduction by producing REEs in more similar ratios as to what is their demand.

3 Secondary REEs

3.1 Sources

Besides primary reserves, REEs are also found in several waste streams and EoL consumer products. These can be significant secondary sources of REEs. REEs from secondary sources can be used in the production of REE products similarly to primary REEs.

New scrap is scrap that is formed during fabrication and manufacturing processes. These waste streams are often less complex than those formed from EoL consumer products. [34] New scrap formed for example during magnet manufacturing includes rejected magnets or residues from grinding [4]. Expected formation of scrap during manufacturing of magnets is 20-30 % of the manufacturing volume [35]. All is likely recovered since new scrap is often recycled straight back to the process where it was produced.

REEs are also found in industrial process residues such as red mud (bauxite residue), mine tailings, metallurgical slags and ash that is produced in thermal power and incineration plants. Light and middle REEs are concentrated into the phosphogypsum waste that is produced during the wet phosphoric acid process. REEs may be present in the coal or ore used in blast furnace smelting of iron ore. They then concentrate into the slag which could be considered a possible source of REEs. REEs are also found in coal fly ash which contains the whole range of REEs compared to primary ores which only contain a selection of them. In mine tailings REEs are typically found in low concentrations but the volumes of mine tailings produced are massive. In Bayan Obo, the largest REE producer in the world, REEs are recovered from mine tailings that are formed as a by-product of iron mining. [4]

Old scrap or post-consumer scrap consist of products that have reached the EoL phase and have been taken out of use [34]. REEs can be recovered from several post-consumer scraps such as fluorescent lights, magnets, batteries, and spent catalysts. Phosphors in fluorescent or compact fluorescent lamps and cathode ray tubes

contain significant amounts of heavy REEs such as Eu, Tb and Y. Spent NdFeB and SmCo magnets are rich sources of Nd and Sm, respectively. [4] Ni-MH batteries contain significant amount of e.g. La and Ce with 10 % of La and 6 % of Ce annual production being used in Ni-MH batteries [36].

Most of the global REE consumption, around 60 %, is going into mature markets such as catalysts, glassmaking, lighting and metallurgy and the rest to developing markets such as battery alloys, ceramics and permanent magnets. In the mature markets around 80 % of the REEs used consist of lanthanum and cerium whereas dysprosium, neodymium and praseodymium account for around 85 % of the REEs used in the developing market segments. [37] However, the use of REEs in the developing markets is increasing and the largest increases of REE demand are due to their use in carbon lean technology applications.

3.2 In-use stocks

In-use stocks of many REEs are constantly growing as the flow into use is larger than the flow of EoL products removed from use [38]. Stockpiles of waste electronical and electrical equipment (WEEE) and the portable batteries they contain are constantly growing while their possibility to contribute to the REE supply remains untapped [26]. Du and Graedel [38] calculated the approximate stocks of ten more commonly used REEs in anthropogenic sources in 2007. They reported e.g. that 86,200 t of La, 143,600 t of Ce, 50,100 t of Pr, and 136,800 t of Nd had accumulated into in-use stocks between 1995 and 2007. [38] To compare, the current annual world mine production of REEs is 130,000 tons [6].

The most promising post-consumer scrap for recycling is spent Ni-MH batteries and NdFeB permanent magnets from EoL products. They contain REEs in significant amounts and are widely used in different applications and products which means that they are highly available in the anthroposphere.

The in-use stocks of NdFeB permanent magnets have been growing due to their use in emerging green technology applications such as wind turbines and electric

vehicles, as well as electronic and electric products. Their lifetimes may vary from 2-3 years in consumer electronics all the way to 10-20 years in wind turbines. Similarly their weight varies from less than 1 g in small consumer products to 1-2 tons in wind turbines. Around 26,000 tons of REOs, mostly neodymium, are used annually in the production of NdFeB magnets. 51,000 tons of NdFeB magnets were used in 2012. [39]

In 2008 12,100 metric tons of REE oxides were used in battery alloys [37]. Ni-MH batteries seem to have only recently become significant end-uses for REEs and their stocks have recently started to grow. The batteries were commercialized in the beginning of the 1990s [40]. The amount of electric vehicles and hybrid electric vehicles which are major users of Ni-MH batteries that contain large amounts of REEs, has started to rise during the last decade and can be expected to keep increasing. This results in a major increase in the in-use stocks of REEs as well. Their EoL volumes will, however, likely remain low for some time due to the low amount of hybrid and electric vehicles currently in use and the long lifetime of more than ten years of the batteries. [41]

REE containing Ni-MH batteries may sometime in the future be replaced by Li-ion batteries which would reduce the demand for REEs for battery alloys. It would also have an impact on the growth of in-use stocks of REEs. The main use for Ni-MH batteries is in hybrid electric cars. [37] In Japan the rechargeable batteries market share of Ni-MH batteries reached its peak value of 50 % in 2000 and drastically decreased over the following years before leveling at approximately 20 %. The share of Li-ion batteries on the other hand has been constantly rising since their arrival on the market. They have dominated the rechargeable batteries market since 2003 when their market share reached that of Ni-MH batteries. [40] Of course, this would not have an impact on the other end-uses of REEs and their criticality would only be affected to a certain degree.

It has been estimated that in 2007 the in-use stocks of REEs were four times the amount of the annual extraction [11]. The amount of in-use stocks is high enough

that recycling of REEs from end-use products could be a significant contributor to the demand of REEs. One of the benefits of recycling would be that it could provide a possible solution to the balance problem as the disparity between the economic market demand and the composition of the raw material does not exist [32]. Recycled material also would not be associated with radioactive elements in the way that primary REEs are.

3.3 Ni-MH batteries

3.3.1 Use

Ni-MH batteries are used in a wide variety of applications ranging from small portable batteries to large battery packs of HEVs. Portable Ni-MH batteries have been used in mobile phones, computers, camcorders and other portable devices. They are also often used in electrical tools such as cordless drills. Ni-MH batteries are also used in industrial standby applications such as energy storage for telecommunication. HEVs are the main application of Ni-MH batteries and HEV Ni-MH batteries account for 53 % of all Ni-MH batteries. [5]

There are many advantages associated with Ni-MH batteries. They have a long useful life and are safe to operate compared to e.g. Li-ion batteries. They are also safe to use during recharging and tolerate some abusive over discharging and over recharging. The ability to tolerate some over discharge is essential in battery packs for HEVs since some cells may be over discharged due to capacity mismatch. They have large energy and power capacities per unit mass and unit volume. They require low maintenance and have a wide operating temperature range (-30 to +70 ^{o}C). Compared to previously commonly used Ni-Cd batteries, Ni-MH batteries are made of environmentally acceptable and recyclable materials. [42]

The main disadvantage associated with the Ni-MH batteries is its energy capacity compared to Li-ion batteries. They can only store about two-thirds as much energy

per kilogram as Li-ion batteries. This is why Ni-MH batteries are often used in hybrid electric vehicles while Li-ion batteries dominate the fully electric vehicle market. [42]

3.3.2 In-use stocks

Ni-MH batteries have ca. 28 % share of the rechargeable battery market [43]. The Ni-MH batteries reached their peak share of the market in 2000 and their market share has since been decreasing. Li-ion batteries took over the leading market share in 2002. The market share of Ni-MH batteries has been somewhat steady but even though the market share is not growing, the amount of batteries put on the market is steadily doing so due to the use of Ni-MH batteries in hybrid electric vehicles which are becoming more popular. [40] Today the annual consumption of Ni-MH batteries is 160,000 tons, 190,000 tons and 800,000 tons in portable batteries, industrial batteries and automotive batteries, respectively. [44]

In 2011, 40 tons of REEs were discarded with the portable rechargeable batteries in WEEE in Germany alone. [45] Globally in 2016 93,000 tons of portable batteries were discarded from use and collected. More than twice that amount was put on the market. While the amount of portable batteries and accumulators put on the market has been quite steady between 2009 and 2016, the collection rate has been constantly rising. [46] The increased collection rate directly translates into more REEs from Ni-MH batteries as well being available for recovery.

Another important source of Ni-MH batteries in addition to portable batteries are the Ni-MH batteries used in hybrid electric vehicles. More than half of the usage of Ni-MH batteries is in hybrid electric vehicles. The amount of REEs contained in a typical hybrid electric vehicle's Ni-MH battery is around 2.6 kg. For example, every Toyota Prius contains 2.5 kg of REEs in its battery pack [32].

Japan has been one of the first countries where electric vehicles have gained significant popularity. The amount of HEV in use in Japan in 2010 was 1.4 million and it has been estimated to rise to 18-24 million by year 2030. This would account to 23.5-31.5 % of all vehicles in use. As of 2030 an estimated 0.51-0.65 million HEVs will

have reached the EoL stage in Japan. The recovery potential of REEs from the Ni-MH batteries of EoL HEVs is thus estimated to rise from 73 tons in 2010 to 2900 tons in 2030. [47] In the EU in 2016 there were almost 272 million HEVs. That is a growth of 14 million compared to 2012. [48] The number of new registered hybrid electric vehicles in the EU was 7.2 million in 2016 [49].

The average useful life of Ni-MH batteries varies much and depends on the application that it is used in. The lifetime of the batteries used in portable electronics may be as short as 2-3 years but the lifetimes of batteries used in hybrid electric vehicles are ten times that at 20-30 years. Significant and growing quantities of spent Ni-MH batteries are discarded every year and make up a valuable stock of secondary REEs.

3.3.3 Structure and composition

The main parts of a Ni-MH battery are cathode, anode, electrolyte, separator and the casing. REEs in the battery are found in the anode which is a hydrogen storage alloy based on mischmetal and nickel alloys. The cathode consists of nickel, coated with nickel hydroxides. The electrolyte in Ni-MH batteries is a potassium solution. The separator is usually polyamide or polypropylene fleece or gauze. When the battery is assembled it is fitted into a steel case. [50]

Currently most Ni-MH anodes are based on REE alloys. The key property in Ni-MH battery anodes is their ability to store hydrogen. The REE mixtures are used in the batteries for their exceptional hydrogen storage properties. The most common type of REE based Ni-MH battery anode is the AB_5 type where A stands for pure La or mischmetal and B is one or more early transition elements such as Ni. The AB_5 type alloy can form hydrides up to AB_5H_6. A volume unit of AB_5 type alloy can store more hydrogen than the same volume unit of liquid hydrogen. [5] Other types of hydrogen absorbing alloys are also used in Ni-MH batteries but they are in some way lacking compared to the REE based alloys. Some suffer from slow activation and poor rate capabilities in certain environments, while others are difficult to produce or are

thermodynamically too stable with sluggish kinetics to be practically used in batteries. [42]

The typical REE amount in a Ni-MH battery varies between 6-10 % depending on the shape of the battery [50, 4]. Although one study [51] found that as much as 17 % of the Ni-MH battery consisted of REEs and another [52] reported 13-16 w-% mischmetal. The consensus, however, seems to be that rechargeable nickel metal hydride (Ni-MH) batteries contain around 10 % REEs [20, 45]. The REE amount in Ni-MH battery anode powder can be 34 weight-% [26]. Typical REE contents in Ni-MH batteries depending on the battery type are given in Table 4.

Table 4 REE contents of different Ni-MH batteries, adapted from Meshram et al. [4].

Type of battery	Button	Cylindrical	Prismatic	HEV
% of REEs	6-8 %	8-10 %	7-8 %	7 %

Half of the REEs used in battery alloys is La (52.5 %), the rest are Ce, Pr, Nd and Y (31.0, 4.0, 11.0 and 1.5 %, respectively). Typical REE composition of a Ni-MH battery is 3.7, 2.1, 0.4 and 0.8 weight-% of La, Ce, Pr and Nd, respectively. [7] The typical REE composition of a portable Ni-MH battery is also presented in Table 5.

Table 5 Content of major REEs in mischmetal and Ni-MH batteries, adapted from Guyonnet et al. [7].

	La	Ce	Pr	Nd
In the mischmetal	52.5 %	31.0 %	4.0 %	11.0 %
In an Ni-MH battery	3.7 %	2.1 %	0.4 %	0.8 %

The battery chemistry of a Ni-MH battery is depicted in reaction equations 1, 2 and 3. Reaction equation 1 describes the anode reaction, 2 describes the cathode reaction and 3 describes the sum reaction. M denotes AB_5 where A is a mixture of REEs and B is one or more early transition elements such as Ni. [41]

$$H_2O + M + e^- \leftrightarrow OH^- + MH \quad (1)$$

$$Ni(OH)_2 + OH^- \leftrightarrow NiO(OH) + H_2O + e^- \quad (2)$$

$$M + Ni(OH)_2 \leftrightarrow MH + NiO(OH) \quad (3)$$

In a fully charged state the material on the positive electrode is nickel oxy-hydroxide and the material on the negative electrode is a metal hydride. During charging of the battery, the nickel oxy-hydroxide on the positive electrode reacts with hydroxide in the electrolyte according to the reaction equation 2 to produce NiO(OH) and water. Similarly during charging the metal alloy on the negative electrode reacts with water according to the reaction equation 1 to form a metal hydride. The sum reaction during charging is given by the reaction equation 3. The charging reaction is exothermic. [53]

4 Recycling

The recycling process of EoL-products can be divided into several steps. The first one is collection which needs the cooperation of several entities such as consumers, governments and companies to be efficient. Next step is the dismantling of products to classify and separate valuable materials followed by pretreatment such as crushing. The last step is the recovery of valuable materials from pretreated scrap using suitable processes. To achieve a high overall recycling and recovery rate, each step is critical and all need to have high recovery rates.

Pyrometallurgical and hydrometallurgical processes can be used separately or together to recover REEs from spent battery scrap. There have been methods developed for the pyrometallurgical and hydrometallurgical processing of specifically Ni-MH batteries [2]. However, designing a recycling process only for one type of battery may be technically difficult and economically unpractical [40]. This makes it attractive to study the behaviour of trace elements in base metal processes and the suitability of the processes for recycling of the trace elements. Ni-MH batteries are in the industry mostly used in primary processes as secondary raw materials and base metals are recovered while trace elements such as REEs are allowed to be lost with slag [2].

4.1 Pretreatment

Recycling of REEs may currently require extensive dismantling of the energy storage scrap before they can be fed into recycling processes designed to recover REEs and other valuable materials. [20] Mechanical separation is thus often required before pyrometallurgical and especially hydrometallurgical processing [2].

Minerals processing operations can be used to reduce the volume of battery scrap and to liberate their valuables. The physical separation processes used in minerals processing are well established and relatively low cost and they can be combined flexibly to separate different fractions from different raw materials. Since the valuable components of the batteries are encased in a hard shell, dismantling the

case gives better access to the valuable components inside. Once the electrodal materials are exposed, the metallic materials can be extracted by pyrometallurgical or hydrometallurgical processes. Physical separation steps will decrease the amount of impurities that are fed into the processes. This may, in turn, reduce the costs associated with the processes and improve their selectivity thus improving the amount of valuable elements recovered. [40]

One way to dismantle the outer shell is by crushing. This reduces the scrap volume and breaks up the structure of the battery so that the different materials may be separated. This improves the following recycling steps of fine grinding and magnetic separation and reduces the scrap volume. Spent batteries are a very heterogeneous process stream which means that the crushers used must be high speed with a high reduction ratio in order to truly liberate the different battery components. [40]

EoL electronic scrap is typically shredded as a whole except for hazardous components and materials which are removed pre-shredding [54]. Shredding of the batteries produces three fractions: fluff, which consists of plastic and paper, metals, which consists of base metals such as Cu, Al and Fe, and black mass, which contains anode and cathode materials.

There are risks with battery shredding, including risk of explosion, fire or release of hazardous volatile organic compounds [41]. Crushing of Ni-MH batteries may lead to self-ignition as moisture comes in contact with the hydrogen alloy powder and causes short circuiting [40]. Deactivation may be beneficial to reduce the risks involved with crushing and shredding the batteries. The used batteries may be frozen with e.g. liquid nitrogen to de-activate them and to embrittle the steel case. Another way to deactivate them is to submerge them in an inert gas.

The EoL battery may be heat treated to remove plastic materials. The plastic and organic materials in the battery have little value other than their energy value. Their value as fuel, however, can only be made use of in the pyrometallurgical processing of the battery scrap; they are only a hindrance in the hydrometallurgical processes.

If the treatment method of the battery scrap is going to be hydrometallurgical, it is beneficial to remove the plastic materials during pretreatment.

After crushing some of the fine electrodal material may be adhered to coarser material. It requires extensive grinding to remove the powder form electrolyte active materials from their supporting substrates. Ultrasonic vibration can be used to separate them into different fractions. [40]

After liberation the valuable components of the batteries may be concentrated using magnetic, electrostatic and gravity separation [40]. Sieving may be used to separate the REE containing anode powder from the rest of the bulkier materials. [55] More ways to separate the materials include magnetic separation to remove the iron containing fraction such as the broken steel case [40]. The plastic fraction may be separated using mechanical classification [50].

4.2 Hydrometallurgical treatment

Several hydrometallurgical methods have been developed specifically to recover the valuable materials from EoL Ni-MH batteries. They are usually preceded by some type of mechanical separation to remove the hard casing which surrounds the valuable materials and separate the iron and plastic from the valuable electrode materials. Several purely hydrometallurgical processes exist for the recovery of REEs from Ni-MH batteries but they may also be used after pyrometallurgical processing to recover valuables from e.g. slag. Some examples of possible hydrometallurgical Ni-MH treatment processes are provided next.

Zhang et al. [56] leached electrode materials off battery scrap using sulfuric acid. Solvent extraction and precipitation using oxalic acid were used to recover the REEs from the leach solution. The REE oxalates were then transformed into REE oxides using calcination. The total yield of REEs was almost 94 wt-% and the purity of the final REO product was more than 99 %. [56]

Li et al. [57] separated and recovered nickel, cobalt and REEs from spent Ni-MH batteries. The electrode materials were leached using sulfuric acid which lead to the

separation of the REE from the rest of the metals due to the low solubility of REE sulphates. Solvent extraction with P204 separated other metals from nickel and cobalt. REEs were stripped from the organic phase using HCl and the REEs remaining in the leach residue as sulphates were transformed into hydroxides using NaOH. They were then redissolved as pure chlorides. [57]

Yang et al. [58] added oxalic solution to the filtrate formed after leaching with HCl and filtration and REE oxalates were precipitated. A final product of 99 % pure REE oxides was obtained after the removal of impurities with the addition of ammonia, filtering, washing with dilute HCl and calcining. The total REE recovery was 95 %. [58]

Rodriguez and Mansur [59] leached nickel and cobalt from Ni-MH residue using sulfuric acid. The REEs were separated by precipitation by pH adjustment using NaOH. Only 50 % of the REEs were removed. Solvent extraction was used to separate nickel and cobalt from the leach liquor. [59]

Pietrelli et al. [60] leached Ni-MH battery waste using sulfuric acid. REEs were selectively precipitated as sodium RE double sulfates. Around 80 % of the REEs contained in the batteries were recovered. [60]

Innocenzi and Veglio [61] used two consecutive leaching steps with sulfuric acid to dissolve nearly all lanthanum and cerium present in Ni-MH powders obtained from an industrial scale grinding process. 99 % of REEs were recovered after selective precipitation with sodium hydroxide and filtration to obtain a solid REE concentrate. [61]

Hydrometallurgical processes to recover the valuable materials in Ni-MH batteries involve acid leaching with various acids to dissolve the elements of interest [62]. Sulfuric acid and hydrochloric acid have been studied and have provided good results. Selective precipitation and solvent extraction have both been used to recover the valuable elements from the leach liquor [56, 57, 54, 59, 60, 61]. After leaching REEs are often precipitated as oxalates, hydroxides or sulfates after which they can be converted to the desired form. The described hydrometallurgical methods of recovering REEs from spent Ni-MH batteries are gathered in Table 6.

Table 6 Hydrometallurgical recovery of REEs from spent Ni-MH batteries.

Ref	Leaching	Recovery after leaching	Conversions	REE Recovery	Purity
[56]	H_2SO_4	Solvent extraction, precipitation as oxalates	Calcination of oxalate into oxide	93.6 %	99.8 %
[57]	H_2SO_4	Precipitation as hydroxides, solvent extraction with P204	Hydroxides redissolved with HCl as chlorides	97.8 %	-
[58]	HCl	Precipitation as oxalates	Calcination of oxalates into oxides	95 %	99 %
[59]	H_2SO_4	Precipitation as hydroxides,	-	50 %	-
[60]	H_2SO_4	Precipitation as double sulfates	-	80 %	87 %
[61]	H_2SO_4	Precipitation as hydroxides	-	99 %	-

There are several advantages and disadvantages associated with hydrometallurgical treatment of waste Ni-MH batteries. One important advantage is that it is possible to reach very high recovery rates of REEs. Hydrometallurgical processes are, however, difficult to use in practice due to their complexity [50]. Complex series of solvent extraction, selective precipitation and stripping are necessary after leaching to recover the valuable materials from the leach liquor. Advantages of hydrometallurgical processes include low investment costs and the possibility of recycling several different waste fractions. Disadvantages include the large consumption of chemicals associated with hydrometallurgical processing. Also many manual operations are required before the hydrometallurgical processes to dismantle the batteries and separate the different components. [32]

4.3 Pyrometallurgical treatment

Some methods for recovery of valuable materials from Ni-MH batteries involve also pyrometallurgical processing. Pyrometallurgical processes require less pretreatment of scrap but most need to be followed by hydrometallurgical treatment methods to recover all valuables. Pyrometallurgical methods proposed for the recovery of Ni-MH batteries include electroslag refining, liquid-metal extraction, glass-slag method and direct remelting [63]. Some examples of possible pyrometallurgical treatment processes for Ni-MH batteries are provided next.

Maroufi et al. [26] investigated the recovery of REE oxides from EoL Ni-MH batteries by thermal isolation via an oxidation-reduction process. The REEs did not remain in the metallic phase but distributed mainly to the oxide phase. Maroufi et al. investigated two processes, in the first process the anode powder of a Ni-MH battery was oxidized in air and then reduced by metallic iron at 1550 ^{o}C for 90 minutes in an inert atmosphere. In the second process the anode powder was mixed with hematite and heat treated in the same conditions as the first. The result in both cases was that the REEs separated in oxide form. The first case resulted in a purer oxide phase with higher REE concentration. [26]

Jiang et al. [64] studied selective gas reduction-oxidation and melting separation of the electrode materials of a Ni-MH battery. The materials were treated with H_2 at 800 ^{o}C and 900 ^{o}C in a selective redox-process. Active elements such as REEs in the electrode powder were oxidized. Silica and alumina were added as fluxes and melted at 1550 ^{o}C to produce Ni-Co alloy and a slag containing the REE oxides. The REO content of the slag was high, almost 50 w-%, which is concentrated enough that extraction of REE oxides is possible. [64]

Tang et al. [55] used a high temperature slagging treatment to recover REEs from the inner part of a used Ni-MH battery. The REOs were absorbed by waste metallurgical slags that mainly consisted of SiO_2 and CaO. The smelting was done in 1700 ^{o}C in an inert atmosphere. After the slagging treatment almost all REE oxides remained in the molten slags. The REE oxides precipitated selectively as solid x $SiO_2 \cdot yCaO \cdot zRe_2O_3$. The

matrix of the slag phase was deficient of Re_2O_3 which is a positive sign for concentrating Re_2O_3 oxides in slags. Precipitation and filtration can be used to selectively enrich the REE oxides from the slag. [55]

Korkmaz et al. [62] separated REEs from the other elements present in the Ni-MH battery into leachate which was suitable for further processing to extract the REEs. All the elements in the active material were transformed into their sulfate form by mixing them with sulfuric acid. The mixture was then dried and roasted, which resulted in REE sulfates and oxides of the other elements. This solid phase was then leached in water which dissolved the REE sulfates and left the oxides in the leach residue. REE sulfates in the leach liquor could be separated from the solid oxides by filtration. Total recovery of REEs was 96 % and there was negligible contamination of the REE stream. [62]

Müller and Friedrich [50] also developed a treatment process for Ni-MH batteries which combined pyrometallurgical and hydrometallurgical processing. The batteries were first dismantled to separate the valuable materials which were then melted in an electric arc furnace. This produced a Ni-Co alloy and a slag which was highly enriched in REE oxides. The slag containing REEs was deemed concentrated enough to be used as a raw material in the chemical industry. [50]

There are many different possible methods for pyrometallurgical treatment of Ni-MH batteries to recover REEs. The methods combine different pyrometallurgical processing steps to separate the valuables to different phases and are often used together with hydrometallurgical treatment methods to recover the valuable elements. The studies detailing the investigations on pyrometallurgical recovery of REEs from spent Ni-MH batteries are gathered in Table 7.

Table 7 Pyrometallurgical recovery of REEs from spent Ni-MH batteries.

Ref	Process	Temperature °C	REE phase	REE recovery	REE content
[26]	Thermal isolation, redox	1000, 1550	oxide	-	87/64 %
[64]	Redox, melting separation	1550	slag	-	50 %
[55]	High temperature slagging	1700	slag	70 %	50/70 %
[62]	Roasting, leaching	850	-	96 %	-
[50]	Melting in EAF	1600/1700	slag	80 %	50-60 %

Some industrial processes containing pyrometallurgical steps have been designed and used to recover also REEs from spent batteries. The Umicore process combines pyrometallurgical and hydrometallurgical steps to better separate all valuable materials in spent Ni-MH batteries, including the REEs. The batteries are fed into a vertical furnace along with coke, air and a slag former. An alloy of base metals and a slag containing among others the REEs are formed. The slag is then treated to form a REE concentrate which is sent to the Solvay separation plant in France to be treated to recover the REEs. [44]

There are benefits and disadvantages associated with pyrometallurgical processing of Ni-MH battery scrap. Pyrometallurgical processes produce less wastewaters and use less chemicals than hydrometallurgical processes. The technology used for pyrometallurgical processing is well developed and established. The same processing steps may be used to extract REEs from slags as are used to extract them from

primary ores. Plastic casings and other organic components can be used for their energy value as fuel in the process.

Disadvantages of pyrometallurgical processing of battery scrap include high investment cost for the furnace. REEs oxidize during smelting and report to the slag phase and must thus be extracted if they are to be recovered. The REEs are also recovered as mixtures and must thus be separated with further processing if pure metals are needed. [32]

Recycling Ni-MH batteries in a way that aims to recover all valuable elements is a relatively new development. Feeding the EoL Ni-MH batteries to primary processes has been the traditional way of recycling the REE containing batteries. The recycling of REEs, however, has not been functional as they are lost to slag and are not recovered. The slag is used as material for construction.

One way to recycle used Ni-MH batteries has been to use the batteries as a cheap source of Ni in stainless steel production but the issue with this is that only nickel is functionally recycled. Cobalt is not paid for as it is not necessary in the process. It acts like nickel and remains in the metal but unlike nickel it is not treated as a valuable. The REEs report to slag and are thus lost. [20]

WEEE which contains REEs in e.g. portable batteries and permanent magnets are often recycled by feeding them into the copper smelting process. This has the same issue of mainly recovering base metals while valuable trace elements are oxidized into the slag and lost. [35] REEs can be recovered from the slag with hydrometallurgical processing or bioleaching.

Currently the slag containing REEs after the smelting process has market value as building or construction material. This value would be lost if the REEs would be extracted from the slag by treating it with chemicals to leach out the metals. The treatment of the slags to recover REEs might also generate large quantities of new waste that has to be dealt with. [32] The value of treating slags to recover REEs is thus questionable.

The recovery of REEs used as secondary feeds to primary copper matte smelting processes has not been extensively studied. The distribution coefficients of Ni-MH battery elements at 1200-1275 ^{o}C in copper converting were investigated by Tirronen et al. [2]. Nd was used in the study to represent the REEs present in the batteries since they have almost identical chemical behaviours. Nd distributed strongly into the liquid iron silicate slag. The concentrations of Nd in metallic copper and copper sulphide matte were negligibly small. The concentration in solid primary magnetite was larger than in metal or matte but small compared to the concentration in slag. Nd oxidizes in converting and prefers the slag over the metal phase. [2]

Some advantages and disadvantages exist for the recycling of spent Ni-MH batteries as secondary raw materials in primary smelting processes. Many of them are the same as they are for pyrometallurgical processes designed for the recovery of valuable materials from spent batteries. Compared to hydrometallurgical processing they share the benefits of less production of wastewater and less chemicals used. Compared to recycling processes made specifically for spent batteries, there are no investments costs, which can be high for the furnaces. The technology and plants for copper smelting are well established and developed. The plastic and organic fractions of the battery need not go to waste as the fuel value they contain can in certain processes be recovered when they burn in the furnace and develop heat.

REEs do report to the slag phase but they can be extracted from the slag using the same process steps as are used when they are extracted from primary ore. Unlike hydrometallurgical processing, pyrometallurgical processing cannot obtain REEs as separate pure metals and mixtures of REEs are produced when they are extracted from the slag. The economic recovery of the REEs from the slag phase may, however, be difficult since the concentrations are usually low [32].

4.4 Recycling rate

Recycling rate refers to the amount of material that is collected at its EoL stage, recovered from the end-product and functionally recycled back into one of its

applications. The recycling of REEs from end-products is very minimal. In the recent years the percentage of REEs recovered from end-products has been less than one. [20, 32]

The small amount of functional recycling of REEs that does happen is mostly the recycling of new scrap. Old scrap is more difficult to recycle due to its complexity and the dispersed nature of the REE elements in the products [35]. Even the little that is recycled mostly comes from REE permanent magnets and REEs used as catalysts in the chemical industry [11]. Also the historically relatively low prices of REEs have not given incentive to develop methods for functional recycling of REEs from EoL consumer products [29].

None of the 74 tons of Nd metal that was discarded in used Ni-MH batteries in the EU in 2010 was recycled. Most of it went to the landfill and the rest to dispersion in cement factories. [7] Du and Graedel [38] reported in 2011 that there was no post-consumer recycling of La and all discarded La was therefore lost [38]. Also more recently in 2017 the end-of-life recycling rates for La and Ce was less than 1 % [36]. The recycling rates of all REEs were less than 1 %. The average recycled content or the fraction of scrap used compared to the total input to production was less than 1 % for most heavy REEs and yttrium and between 1-10 % for light REEs. [41]

Eurostat statistics indicated that in 2016 the end-of-life recycling input rate, which means the share of the input to a production process that comes from EoL consumer goods, varied between 0 and 31.4 % for different REEs. Dysprosium had the smallest EoL recycling input rate with 0 whereas yttrium topped the charts with 31.4 %. The EoL recycling input rate of neodymium was 1.3 and for praseodymium 10 %. [65] The stark difference between different REEs may be due to their use in different amounts and in different types of applications. Dysprosium is often used in only trace amounts and is therefore difficult to recover. Other applications which use larger amounts have long lifetimes which limit the amount of scrap that is available for recycling.

There are several reasons for the low recycling rates of REEs. Technological problems are standing in the way, collection of REE containing post-consumer products is also ineffective and there is not enough incentive, financial or otherwise, to recycle REEs.

Low recycling rates can be in part attributed to the complexity of the products in which REEs are found. The REEs are dispersed and intricately embedded in the products. This presents a distinct challenge for the recycling as the technological solutions and processes required to separate the REEs from the scrap are increasingly complicated.

Efficient collection infrastructure is needed to increase the recycling rate of REEs from the products that contain them [40]. Many products containing REEs are not effectively collected and, thus, they disperse into the environment or end up at landfills. [35] Another factor influencing specifically the recycling rate of batteries is the tendency of consumers to hoard EoL batteries and electronic products in their homes rather than recycling them. It may be several years after the product entered the EoL phase before it is recycled. [41, 40]

One more factor affecting the recycling rates of REEs is their low price which does not give enough incentive to recycle and recover them from EoL products. [3] The incentive to recycle REEs is especially low when it comes to the light REEs such as cerium and lanthanum which are overproduced because of the balance problem.

Legislation may also be required or helpful in making sure that valuable materials are not discarded and landfilled even if the collection and recycling of them is not currently lucrative. Some countries already have legislation in place which encourages the recycling of spent batteries by making it free to the consumer and making manufacturers responsible for the costs. EU regulations require that all member states to collect minimum 15-25 % of spent batteries and recycle at least 45-50 % of them. Germany is one example of a country where the producers and importers of batteries are responsible for the cost of collecting, processing and disposing of them. [40]

These legislations have little effect, however, on the recycling rate of REEs in the battery scrap as the recycling of Ni-MH batteries is usually only functional for the nickel they contain. Other valuable elements are considered impurities and not payed for or end up in the slag phase from which they are not recovered. To truly increase the recycling rate of REEs, legislation that dictates how the batteries should be recycled may be necessary if the incentive to recover REEs does not come from elsewhere.

5 Distribution of elements in copper matte smelting

The thermodynamic factors determine the behaviour of elements in any system. Knowledge of the factors provide information and explain the observed phenomena in a matte-slag system.

Three phases are formed during the copper matte smelting operations. The phases are the liquid sulfidic copper matte and the iron silicate slag, as well as the gaseous offgas. If all gangue materials and trace elements are disregarded, the system in copper matte smelting consists of five components: Cu, Fe, S, O and Si

Copper and iron sulphides forms the matte while most trace elements and impurities are oxidized and report to the slag. Some of the iron is oxidized, forming the slag with silica flux. The copper grade of the matte is thus largely dependent on the degree of oxidation of the iron sulphide. The sum reaction of concentrate behaviour during copper matte smelting is given in reaction equation 4.

$$\mathrm{CuFeS_2 + O_2 + SiO_2 \rightarrow (Cu, Fe, S)(matte) + FeO \cdot SiO(slag) + SO_2} \qquad (4)$$

The reactions of the elements in the flash smelting furnace depend highly on several factors. Important ones are the partial pressures of oxygen and sulfur in the system. In addition the temperature, activity of volatile elements and matte grade have an effect on the reactions that the elements are likely to partake in the furnace.

The distribution of elements during copper matte smelting is dependent on the composition of the slag as well as temperature and oxygen partial pressure. The distribution of a trace element M between matte and slag can be described by reaction equation 5 and 6. [66]

$$\mathrm{M} + \frac{v}{2}\mathrm{O_2(g)} \rightarrow \mathrm{MO_v} \qquad (5)$$

$$M + \frac{v}{2}S_2 \rightarrow MS_v \qquad (6)$$

The equilibrium constant K of the reaction can be expressed by the activities of the components and the partial pressure of oxygen according to equation 7. [67]

$$K = \frac{a_{MO_v}}{a_M \cdot pO_2^{v/2}} \tag{7}$$

If the metal oxides are expressed in their monocation form then the activities can also be written using the concentrations of the species in their respective phases and their activity coefficients in those phases according to equations 8 and 9. [67]

$$a_{MO} = \gamma_{MO} N_{MO} = \gamma_{MO} \frac{n_M}{n_T} = \gamma_{MO} \frac{\%M}{M_M n_T} = \frac{\gamma_{MO} \%M}{M_M n_T} \tag{8}$$

$$a_M = \gamma_M N_M = \gamma_M \frac{n_M}{n_T} = \gamma_M \frac{\%M}{M_M n_T} = \frac{\gamma_M \%M}{M_M n_T} \tag{9}$$

These can be substituted into equation 7 which gives equation 10. [67]

$$K = \frac{[n_T](\gamma_{MO_v})(\%M)}{(n_T)[\gamma_M][\%M] pO_2^{v/2}} \tag{10}$$

The distribution of metal M between matte and slag can be defined according to equation 11.

$$L_M^{m/s} = \frac{[\%M]}{(\%M)} = \frac{[n_T](\gamma_{MO_v})}{K(n_T)[\gamma_M] pO_2^{v/2}} \tag{11}$$

In the equations 7-11,

$\%M = mass\ percent\ of\ the\ metal\ M$

$M_M = molar\ mass\ of\ metal\ M$

$N_M = mole\ fraction\ of\ metal\ M$

$( ) = value\ of\ slag\ phase$

$[ ] = value\ of\ matte\ phase$

$n_T = total\ mole\ fraction\ of\ monocation\ components\ in\ 100\ g\ of\ each\ phase$

$\gamma = activity\ coefficient$

$pO_2 = partial\ pressure\ of\ oxygen$

The distribution coefficient $L_M^{m/s}$ is dependent on the equilibrium coefficient K which in turn depends on the temperature and is calculated based on the standard Gibbs free energy change of the oxide forming reaction. The equilibrium coefficient can be calculated according to equation 12. [67]

$$K = e^{(\frac{-\Delta G^\circ_{MO_v}}{RT})} \tag{12}$$

The value of v which can be seen in equations X, X can be determined by drawing values of $\log L_M^{m/s}$ as a function of $\log pO_2$. The value of –v/2 is the value of the slope in equation 13. This value can be used to determine the oxidation number of the metal in slag. [67]

$$\log L_M^{m/s} = -\frac{v}{2}\log pO_2 + \log A \tag{13}$$

In equilibrium the activities of the elements are the same in the matte and the slag. The distribution is thus dependent on the value of the activity coefficients of the elements in the different phases. The activity of a metal oxide in the slag depends on the interactions of all components present in the slag and is thus dependent on the slag composition. The activities of basic metal oxides will be greater than unity in basic slags and much smaller in acidic slags. E.g. silica slag is an acidic slag and thus attracts basic oxides and therefore the activity coefficients of basic oxides in silica

slag are low. [67] REE oxides La_2O_3 and Nd_2O_3 are both strongly basic oxides [9]. Therefore, they have low activities in acidic slags such as silica slags.

Behaviour of elements in the matte-slag system may be divided into different categories such as sulfidic, oxidic, monatomic, molecular and halidic dissolution. They describe the type of component that the elements form under a certain oxygen partial pressure. The most usual ones when it comes to reactions in the flash smelter are oxidic and sulfidic dissolution, which refer to elements that form stable oxidic and sulfidic components, respectively, at a certain oxygen partial pressure. The oxygen and sulfur partial pressures affect in which form the elements can dissolve.

The distribution and behaviour of elements in a copper matte-slag system has been investigated in detail. Guntoro et al. [1] studied the separation of copper matte and slag in matte smelting. They used a mixture of synthetic slag and chalcopyrite concentrate which were contacted in air and argon atmospheres. Based on the results they outlined the occurring sequential reactions and separation processes. First the chalcopyrite is rapidly oxidized by available oxygen into matte and SO_2. In an inert atmosphere the oxygen is released from the oxidizing fayalite slag. In air atmosphere the important factors for chalcopyrite oxidation are the oxygen partial pressure and gas diffusion, while under an inert atmosphere the key factors are oxygen potential of slag and mass transport in it. [1]

In air atmosphere the oxidation of chalcopyrite is followed by magnetite formation, deironization of matte and slag formation, while in an inert atmosphere magnetite formation is limited. Iron silicate slag is formed through iron oxides' reactions with silica. Density differences separate the matte and slag as matte droplets coagulate together and separate from the slag. Lastly, in air atmosphere, due to the abundance of available oxygen, copper sulphide in the matte could be oxidized into cuprous oxide, and subsequently react with iron and copper sulphide to produce metallic copper. [1]

Wan et al. [68] investigated the behaviour of metallic elements in WEEE in flash furnace smelting. The experiments were conducted in both air and inert atmospheres. They found that the minor and precious metals in printed circuit boards (PCB) dissolve to the matte phase or form their own metallic phase. Even with higher PCB ratios no PCB metals were found in the slag and thus loss of the metals to slag can be contributed to mechanically entrained matte in slag. The change in Cu, Fe and S concentrations in the matte is given in Figure 3. [68]

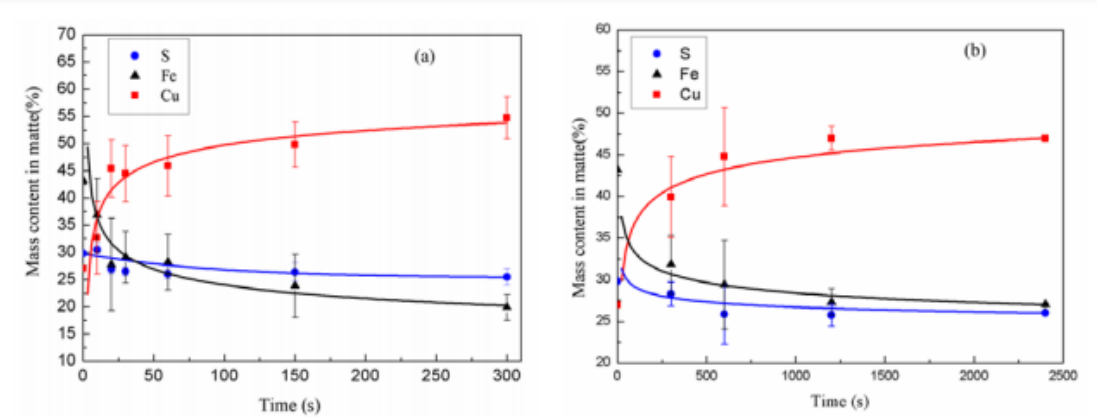

Figure 3 Changes in Cu, Fe and S concentrations in matte phase in (a) air atmosphere and (b) argon atmosphere [68].

The distribution of REEs in different systems has been investigated and reported and it is known that the REEs report to the oxide or slag phase [64, 26, 50, 55, 2]. REEs exhibit high oxygen affinities compared to transition elements such as iron or nickel.

The most relevant thermodynamic study of the equilibrium behaviour of REEs in copper matte smelting was done by Tirronen et al. [2] who measured the distribution coefficients of Li-ion and Ni-MH battery elements in copper converting. Nd was used in the study to represent the REEs present in the batteries, since they have almost identical chemical behaviours. [2]

The experiments were performed by equilibrating the samples at 1200, 1225, 1250 and 1275 °C which was followed by rapid quenching. The rapid quenching retains the high temperature equilibrium composition unchanged. The equilibration times were 4 h at 1200 °C, 2 h at 1225 °C, 1 h at 1250 °C and 45 min at 1275 °C. The composition

of the samples was analyzed using Electron Probe X-Ray Microanalysis (EPMA) and Laser Ablation - Inductively Coupled Plasma - Mass Spectrometry (LA-ICP-MS). [2]

The study used a silica saturated iron silica slag. The synthetic slag was produced by equilibrating 40 wt-% SiO_2 and 60 wt-% Fe_2O_3 in a pure silica crucible. The composition of the final slag was determined by SEM-EDS analysis to be 51 wt-% Fe and 34.2 wt-% SiO_2 as well as homogenous in nature. [2] The same type of fayalite slag is used in industrial copper matte smelting processes.

Nd distributed strongly into the liquid iron silicate slag. The concentrations of Nd in metallic copper and copper sulphide matte were negligibly small; considerably below the detection limit of the analytical technique (EPMA) used. The concentration in solid primary magnetite was higher than in metal or matte but low compared to the concentration in slag. Nd oxidizes in converting and prefers the slag over the metal phase. [2]

6 Materials and methods

6.1 Raw materials

The raw materials used in this study were copper concentrate, synthetic fayalite slag and neodymium and lanthanum oxides. Quartz was used as the crucible material.

The synthetic slag was prepared from hematite powder (Alfa Aesar, 99.99 % purity) and silica powder (Umicore, 99.99 % purity). The mixture was prepared using a mass ratio of 65 wt-% Fe_2O_3 and 35 % SiO_2 and ground in a mortar until fine and homogeneous. The mixture was then heated in a furnace in air atmosphere for 8 hours at 1300 °C. After smelting and quenching the slag was composed of solid iron oxide and silica. During the experiments this solid synthetic slag would form a liquid fayalite slag when in contact with the sulphide phase.

The industrial copper concentrate powder used in the experiments was acquired from Boliden Harjavalta (originally from Pyhäsalmi mine). Elemental composition results from X-Ray Fluorescence (XRF) spectrometry analysis, performed with two different analytical procedures, are shown in Table 8. The equipment used was Panalytical Axios Max wavelength dispersive XRF (Malvern Panalytical). The sample was prepared by grinding 20 g of the concentrate and 1 g of binder (Herzog PE-190) into a homogeneous mixture, followed by pressing the mixture into a button. The XRF voltage was set to 25, 50 or 60 kV depending on the element analysed, and the current to 160, 80 or 66 mA. Chemically analysed standard materials (optimized for copper sulphide analyses) were used for calibration in the classical calibration procedure. In the semiquantitative analyses, the calibration was performed with Omnian set-up samples. In general, correctly optimised classical calibration provides more accurate results, but as seen from Table 8, the results from the two procedures are relatively close to each other.

Table 8 Elemental composition of the concentrate.

Boliden Harjavalta XRF						
S	Fe	Cu	Zn	SiO2	Pb	CaO
33.17	27.36	27.34	3.77	2.53	0.13	0.09
Cr	Ni	Bi	Cl	Sb	As	
0.012	0.004	0	0	0	0.026	
Boliden Harjavalta Semiquantitative						
S	Cu	Fe	O	Zn	Si	Mg
33.426	28.625	27.472	4.935	4.166	0.657	0.347
Ca	Al	Ba	Ag	Mn	Cd	As
0.065	0.053	0.051	0.025	0.018	0.016	0.014
P	Se	K	Ni	Pb		
0.004	0.004	0	0.013	0.107		

Lanthanum and neodymium oxides, La_2O_3 (Alfa Aesar, 99.9 %) and Nd_2O_3 (Sigma-Aldrich, 99.99%), respectively, were used as the source of REEs in the kinetic experiments. Several REEs can be found in Ni-MH batteries, but only two were chosen since the behaviour of these elements should be very similar due to the high stability of their oxides [2]. Lanthanum was chosen based on the amount of La in the batteries; it represents most of the REEs contained in Ni-MH batteries [51]. Neodymium was chosen because of its widespread use in different applications. In addition to Ni-MH batteries, it is also used in permanent magnets and printed circuit boards, some of which, when scrapped, are recycled in the copper smelting process. [4]

The experiments were conducted in air and argon atmospheres. No gas flow was used for the experiments conducted in air atmosphere. Instead the work tube was filled with air from the surrounding atmosphere since the lower end of the working tube was left unplugged. For the experiments conducted in argon atmosphere, the work tube was plugged and a flow of 400-500 mL/min argon (AGA Linde, 99.999 % purity) was used.

6.2 Sample preparation

The slag/concentrate mixing ratio was set at 1.116 based on previous studies. However, the concentrate used in this work was slightly different from the one used in previous studies. The feed mixture was prepared so that the SiO_2/Fe ratio would be similar to that used in industrial flash smelting furnaces. The SiO_2/Fe flux ratio with this mixing ratio is 0.533 or 0.517, depending on which analysis results from Table 8 are used.

The mixing ratio of the slag and concentrate was chosen based on previous studies so that the silica would be oversaturated. Oversaturation of silica is desired to ensure good fayalite formation so that the matte and slag phases could be separated during contacting at high temperatures. The use of a silica crucible helped ensure that the system would be oversaturated with silica as the crucible could also react with the sample. In industry, overfeeding of silica is avoided since it causes difficulties in slag handling due to silica polymerizing as it melts [69].

The amount of La and Nd oxides added to the mixture was 5 % of the concentrate mass. In total, the amount of REOs added was 10 % of the concentrate mass. The high amount of REEs was chosen to ensure that detection of them would be possible with the used methods.

The powders were mixed thoroughly and ground in a mortar until homogenous. The mixture was then divided into cone shaped silica crucibles (Finnish Special Glass, Finland) with a sample size of 0.5 g.

6.3 Equipment

The furnace that the experiments were performed in was a Lenton LTF 16/450 (Lenton, UK) single phase vertical tube furnace. The furnace was equipped with four silicon carbide heating elements, which were positioned near the alumina working tube (Frialit AL23, Friatec AG, Germany) with an inner diameter of 35 mm. The working tube of the furnace extended through the entire height of the furnace. Enveloped by the working tube was the alumina inner tube with an inner diameter

of 22 mm. The inner tube was located between the top of the furnace and 20 mm above the geometrical centerline of the furnace. The bottom of the inner tube was located in the hot zone of the furnace. A schematic illustration of the furnace and the crucible position is shown in Figure 4.

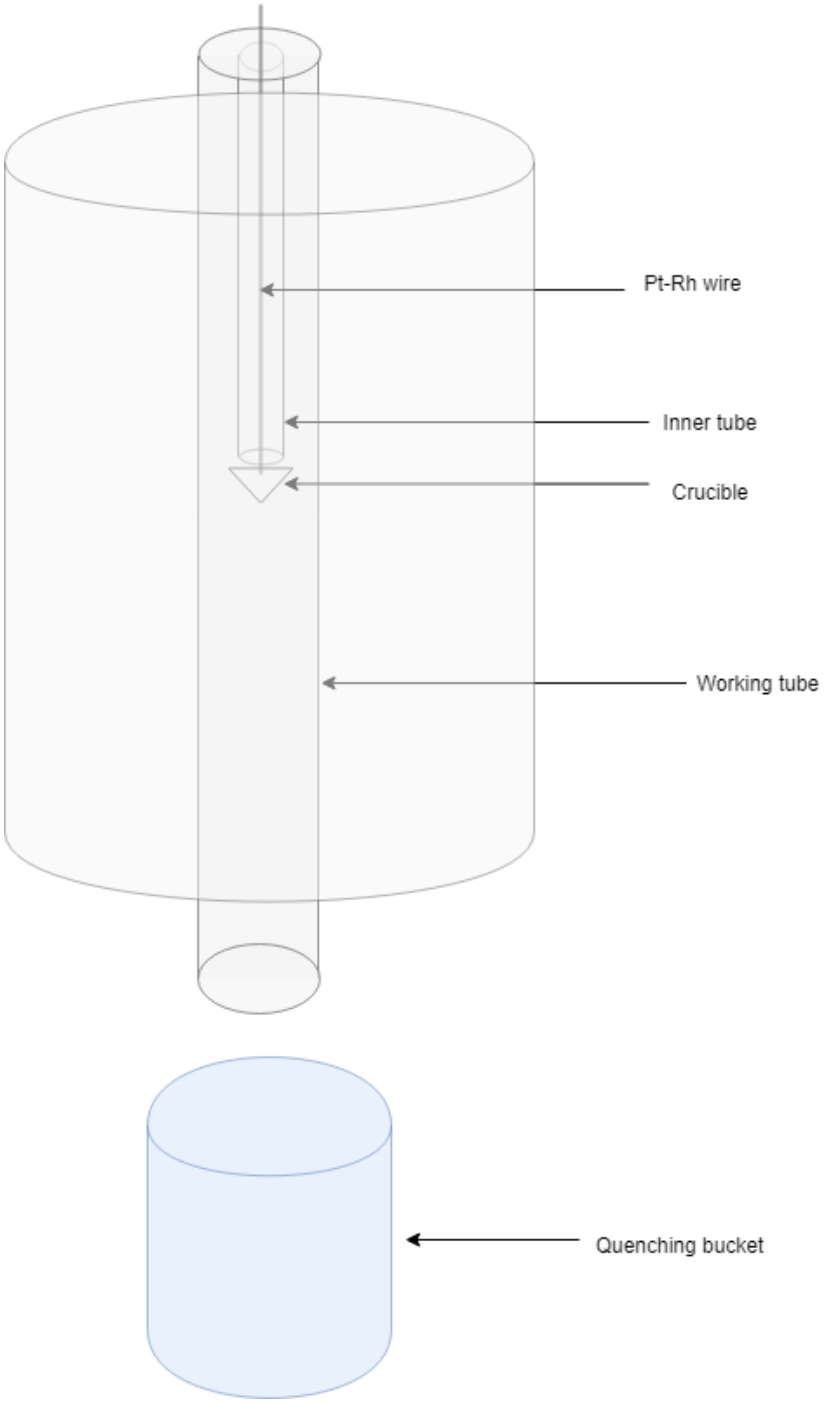

Figure 4 Schematic illustration of the furnace setup and the crucible position in the furnace.

The hot zone temperature was held at the experimental temperature, 1300 °C. A calibrated S-type Pt/Pt-10Rh thermocouple (Johnson Matthey Noble Metals, UK) connected to a Keithley 2700 multimeter (Keithley, USA) was used to measure the temperature of the hot zone. The furnace temperature was controlled by a Eurotherm 3216 PID controller. The cold junction temperature was measured with a Pt100 resistance thermometer connected to a Keithley 2000 DMM multimeter (Keithley, USA). Temperature data was logged with LabVIEW software.

6.4 Procedure

Experiments were conducted in both air and inert argon atmospheres. Experiments in air were conducted for 10, 20, 30, 60, 150 and 300 second contact times. Each experiment was repeated three times. Experiments in argon atmosphere were conducted for 5, 10, 20 and 40 minute contact times and each experiment was repeated twice.

The main difference between the experiments conducted in air and inert argon atmospheres was the presence or absence of oxygen in the atmosphere. The oxidizing reactions that took place in the inert atmosphere were limited in the amount of oxygen since all oxygen available for the reactions came from the sample itself, namely the fayalite slag. An air atmosphere on the other hand provided the system with a constant supply of oxygen.

The experiments in air were carried out to study the distribution and behaviour of REEs with enough oxygen to potentially correspond to the conditions in the shaft of a flash smelting furnace. During the settling process at the bottom of the furnace the amount of available oxygen is low. The experiments conducted in argon atmosphere were carried out to study the distributions and behaviour of REEs in the settler area.

The sample was fitted into a sample holding basket made of platinum wire. The basket was hooked onto a platinum-rhodium sample holding wire which was used to raise the sample into the furnace hot zone. In the case of experiments conducted in argon atmosphere, the sample was first lifted to the furnace cool zone, after which

the working tube was plugged. The furnace was flushed with argon for 20 minutes to ensure an inert atmosphere inside the working tube. The experiment was initiated by raising the crucible to the hot zone of the furnace. The hot zone of the furnace was located just below the inner tube and the outer diameter of the sample holding basket was larger than the diameter of the inner tube. Therefore, it was possible to prevent the crucible from moving any higher than the hot zone of the furnace and ensure its fixed position. In the case of experiments conducted in air, the sample was raised to the furnace hot zone directly without flushing the furnace first.

After the set contacting time of the experiment was reached, the sample was rapidly quenched in an ice water bath. In the case of the experiments conducted in air, this was done simply by pulling on the platinum-rhodium sample holding wire, which caused the sample-basket assembly to fall through the working tube. The volume of the ice water bath was large compared to the sample and it was located directly below the alumina working tube. In the case of the experiments conducted in an inert atmosphere, air leakage had to be prevented and therefore the plug was switched with the quenching bucket shortly before the set contacting time. The water level in the quenching bucket was kept above the level of the bottom part of the working tube.

6.5 Sample characterization

After quenching, the sample was mounted in epoxy resin, cut in half and mounted again in epoxy resin to be able to analyze the cross section of the sample-crucible assembly. The sample was then ground and polished using silicon carbide papers (P120, P240, P400, P800, P1200, P2400) and diamond polishing (3 μm and 1 μm). The polished samples were carbon coated in preparation for sample characterization using SEM and EPMA.

Microstructure and elemental analysis of the samples was performed using a Tescan MIRA3 Scanning Electron Microscope (SEM) (Tescan, Czech Republic). Composition of the samples was analyzed using UltraDry Silicon Drift Energy Dispersive X-ray Spectrometer (EDS). Thermo-Scientific NSS Spectral Imaging software (Thermo

Fischer Scientific, USA) was used for concentration quantifications. The used acceleration voltage was 15 kV and the beam current on the sample surface was 11 nA. The utilized standards were Cu Kα (Cu), Fe Kα (hematite) and O Kα (quartz), S Kα (marcasite), Si Kα (quartz). Of the standards, Cu was pure metal and the others were naturally occurring minerals. Standards were not made for La and Nd, they were analysed using only the internal standards of the NSS software since their actual concentrations were analysed using EPMA and LA-ICP-MS. Samples from experiments conducted in air with a contact time of 10 seconds were analyzed using only EDS because there was no liquid slag present yet, only solid magnetite and silica grains. For the matte phase, the major element concentrations were only analyzed with EDS in this work.

Analysis of the slag composition was done using Electron Probe Micro-Analysis (EPMA). The relevant trace elements, La and Nd, distribute predominantly to slag. Therefore, it was possible to reliably analyze the concentration of La and Nd in slag using EPMA. Two best samples out of the three experiments conducted for each contact time in air were analyzed using EPMA, as were both samples for each contact time in argon. EPMA analysis of the samples was performed at Geological Survey of Finland (GTK). The electron microprobe was a Cameca SX100 (Cameca SAS, France) equipped with five wavelength dispersive spectrometers (WDS). The used accelerating voltage was 20 kV. The beam current was 60 nA and the beam diameter was 50-100 µm depending on the size available for the beam. The analyzed elements, X-ray lines and standards used were Si Kα (quartz), Mg Kα (diopside), Fe Kα and O Kα (hematite), La Lα (monazite), Nd Lα (Nd-phosphate), Pb Lα (galena), Cu Kα (Cu), Zn Kα (sphalerite) and S Kα (pentlandite). Of the standards, Cu was 100 wt-% pure metal, Nd-phosphate a synthetic phosphate and the others were naturally occurring minerals. The detection limits of the analyzed element concentrations are given in Table 9.

Table 9 EPMA and LA-ICP-MS detection limits in ppm.

	O	Si	Mg	S	Fe	Cu	La	Pb	Zn	Nd
EPMA (slag)	1008	220	110	135	253	310	281	1008	359	146
LA-ICP-MS (matte)		8.0	0.20		1.5		0.001	0.004	0.17	0.006

The concentrations of lanthanum and neodymium in the matte phase were very low, and therefore the matte phase was analyzed with Laser Ablation-Inductively Coupled Plasma-Mass Spectrometry (LA-ICP-MS). Two best samples out of the three experiments conducted for all contact times excluding 10 s in air were analyzed using LA-ICP-MS. For argon atmosphere, all the conducted experiments were analyzed with LA-ICP-MS.

A Photon Machines Analyte Excite laser ablation system with 193 nm wavelength 4 ns ArF excimer laser (Teledyne CETAC Technologies) coupled to a NuAttoM single collector sector field ICP-MS (Nu Instruments, UK), housed at GTK, was used in this work. The laser spot size was selected as 50 µm and the laser was fired with 10 Hz frequency. The energy was set to 27.9% of 4 mJ, resulting in a fluence of 2.5 J/cm^2 on the sample surface. The analysis procedure consisted on 5 preablation pulses to remove carbon coating and possible contamination from the surface, followed by 20 second pause, 20 second gas background analysis, and 350 pulses of sample analysis.

USGS GSD-2G glass [70] was used as the external standard material for matte analyses. It is a silicate glass, and therefore not the best matrix-matched standard for sulphides. However, since the elements of interest in this work were lanthanum and neodymium, which are not found in sulphide reference materials, this silicate was selected. USGS GSE-2G [70] as well as USGS MASS-1 [71] reference materials were analyzed as unknowns for monitoring the hardware conditions and analysis quality. ^{59}Co isotope was analyzed throughout the series for checking how well the GSD silicate glass reproduces the concentration values in MASS-1 sulphide. The obtained concentration of cobalt was consistently very close to the reported one [71], which

indicates that the GSD glass can be used as an external standard for sulphide analyses. ^{57}Fe was used as the internal standard with concentration values obtained from EDS.

The mass spectrometer was operated in FastScan mode with low resolution (ΔM/M = 300) for maximum sensitivity. Data reduction was performed with Glitter software [72]. For lanthanum, the only stable isotope ^{139}La was analyzed, and for neodymium, isotopes ^{143,145,146}Nd were analyzed. All of these isotopes should be interference-free with the used standard materials and sample matrix, and therefore any of the Nd isotopes can be used for concentration quantifications. The obtained detection limits are collected in Table 9.

The time-resolved analysis signals obtained from LA-ICP-MS showed homogeneous distribution of La and Nd in some samples, and fairly inhomogeneous in others. In general, the distributions in the ablated areas became more homogeneous as the contact time in the furnace increased. Two examples of these signals are shown in Figure 5. These signals illustrate the heterogeneity after 20 seconds, as well as the decrease in the concentration of neodymium in the matte phase as time was increased. Two SEM images of the laser ablation pits in the matte phase are shown in Figure 6.

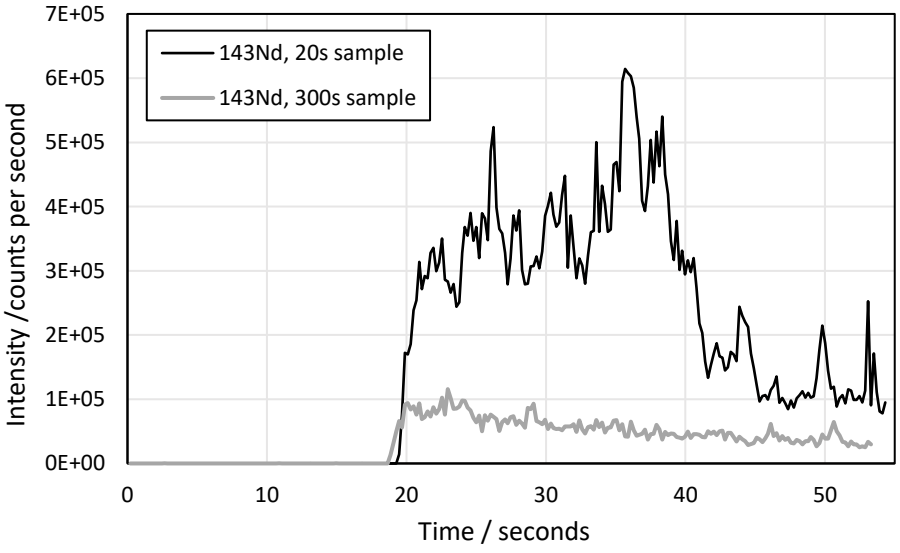

Figure 5 Time-resolved analysis signals from two samples (20s and 300s).

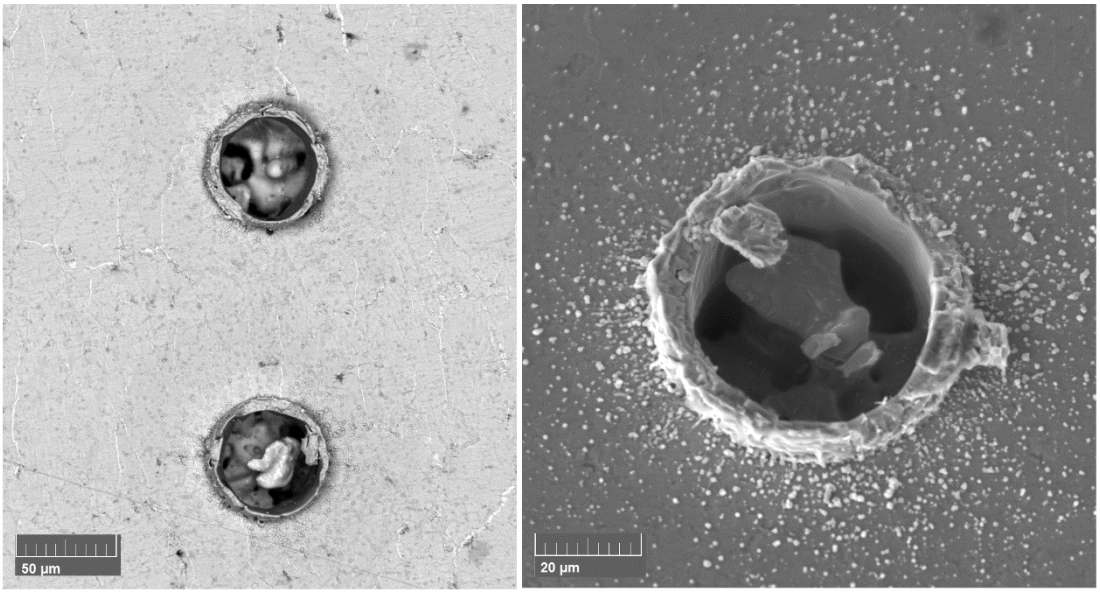

Figure 6 Left side: SEM-BSE image of laser ablation pits in the matte phase. Right side: SEM-SE image of a single ablation pit. The rim around the pit is formed as the four-nanosecond laser pulses are long enough to melt part of the material, which is not desired.

7 Results

This chapter discusses the results of optical and chemical analysis of the samples. The SEM-images in this chapter are from typical areas in the samples and additional SEM micrographs of all samples are provided in the appendices.

7.1 SEM results

7.1.1 Air

After 10 s contacting time, the structure of the sample is very heterogeneous. The matte and slag phases are not fully formed yet and they are randomly distributed in the structure. The time is not enough for fayalite slag to form and instead separate areas of iron oxide and unmelted silica can be observed. The concentrate appears to have begun melting. A SEM micrograph of a polished cross section of a sample after 10 s contacting time is shown in Figure 7.

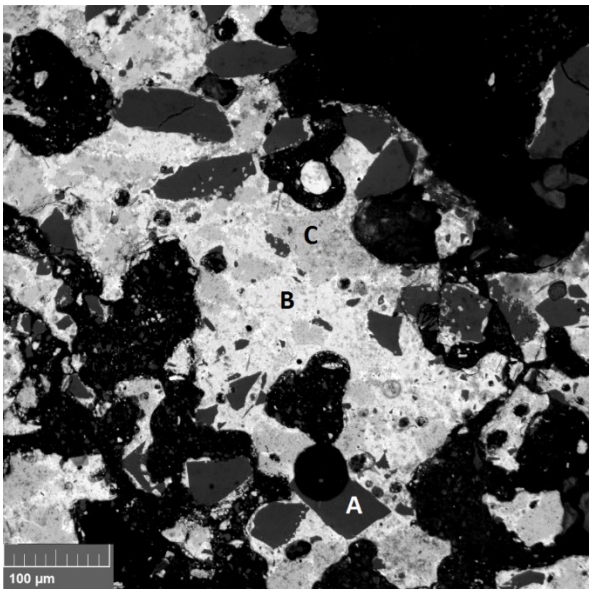

Figure 7 Micrograph of sample 19 after 10 s contacting time in air atmosphere showing phases of (A) silica, (B) copper matte and (C) iron oxide.

After 20 s contacting time, the structure of the sample is already more defined. Separate areas of matte and forming slag were observed but the distribution of them in the sample was still quite random and the settling process was not finished. The

slag phase is still forming, and large grains of silica were observed. Droplets of matte were found in the slag phase. Segregated iron oxide was observed in the matte phase. A SEM micrograph of a sample after 20 s contacting time is shown in Figure 8.

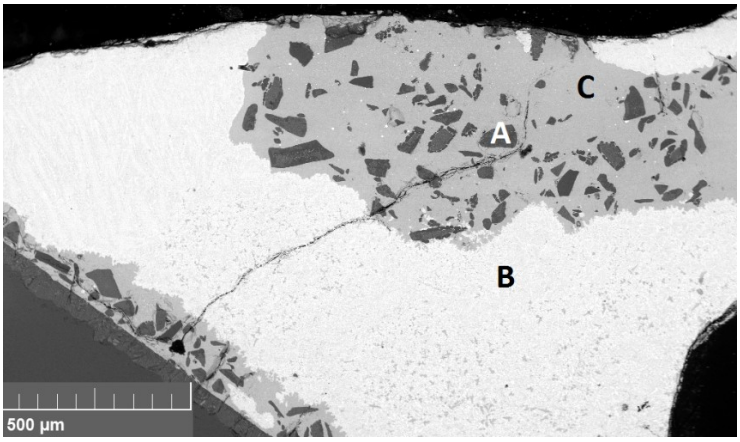

Figure 8 Micrograph of sample 5 after 20 s contacting time in air atmosphere showing phases of (A) silica, (B) copper matte and (C) forming fayalite slag.

After 30 s contacting time, the separation of matte and slag phases has progressed significantly. The slag is not fully formed yet, but the amount of primary silica grains has decreased. Matte droplets were observed entrained in the slag. Some veins of high copper content could be seen in the matte phase. Segregated iron oxide was observed in the matte phase. A SEM micrograph of a sample after 30 s contacting time is shown in Figure 9.

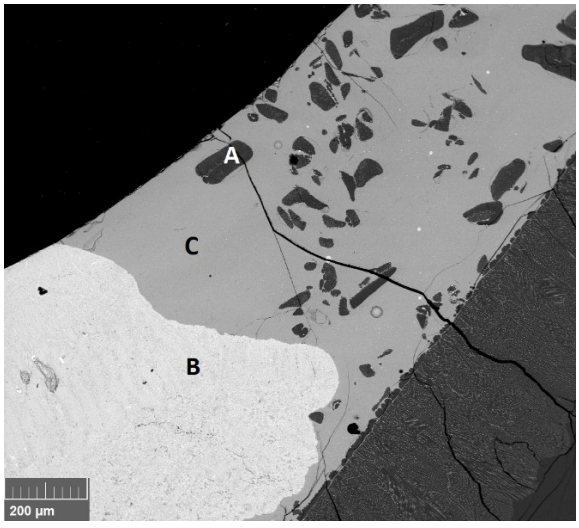

Figure 9 Micrograph of sample 4 after 30 s contacting time in air atmosphere showing phases of (A) silica, (B) copper matte and (C) forming fayalite slag.

After 60 s contacting time, the copper matte and fayalite slags are already well separated. Some veins of copper could be seen in the matte phase. Droplets of matte were still observed in the slag. Segregated iron oxide was observed in the matte phase. Only small amounts of unmelted silica remained in the slag phase. Silica from the crucible was observed reacting with the slag phase. A SEM micrograph of a sample after 60 s contacting time is shown in Figure 10.

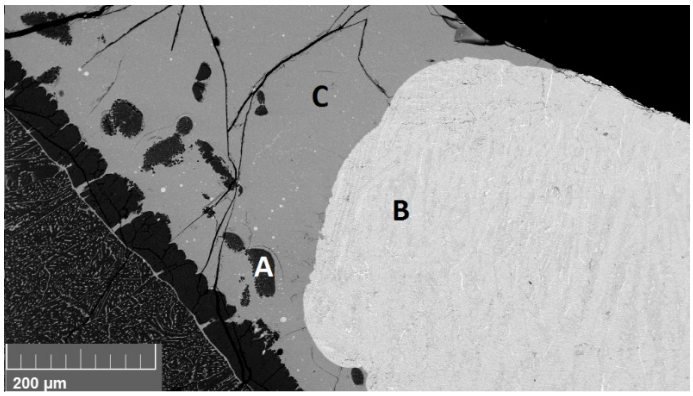

Figure 10 Micrograph of sample 1 after 60 s contacting time in air atmosphere showing phases of (A) silica, (B) copper matte and (C) fayalite slag.

After 150 s contacting time, the copper matte and fayalite slag phases are well separated and the settling of the phases has progressed. Small matte droplets could still be observed in the slag phase. Some veins of copper could be seen in the matte phase. Segregated iron oxide was observed in the matte phase. Silica from the crucible is still reacting with the slag phase. A SEM micrograph of a sample after 150 s contacting time is shown in Figure 11.

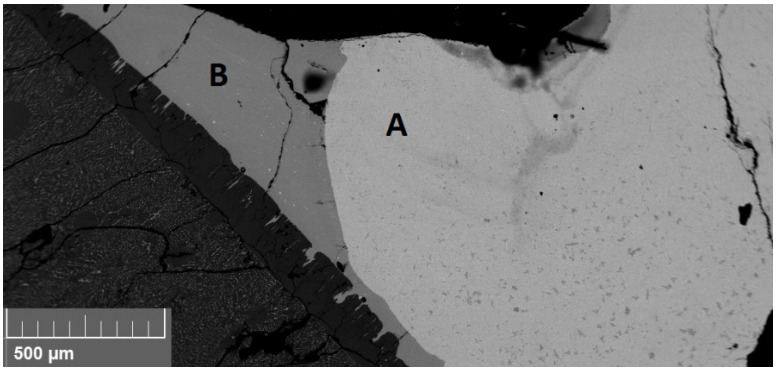

Figure 11 Micrograph of sample 16 after 150 s contacting time in air atmosphere showing phases of (A) copper matte and (B) fayalite slag.

After 300 s contacting time, the copper matte and fayalite slag phases are well separated and settled. The amount of matte droplets in the fayalite slag had decreased. Some veins of copper could be seen in the matte phase. Segregated iron oxide was still observed in the matte phase. Silica from the crucible is still reacting with the slag phase. A SEM micrograph of a sample after 300 s contacting time is shown in Figure 12.

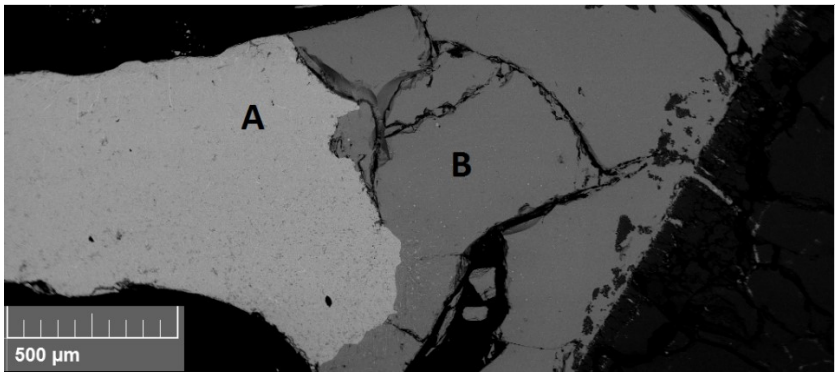

Figure 12 Micrograph of sample 8 after 300 s contacting time in air atmosphere showing phases of (A) copper matte and (B) fayalite slag.

The change in Cu, Fe and S content in the matte was analyzed using SEM-EDS. The results are given in Figure 13. The concentration of copper in the matte started increasing soon after the start of the experiment. It increased steadily until 150 s contacting time, after which it appears to level out. The concentration of iron in the matte changed slowly at first but decreased between 60 s and 150 s contacting times before leveling. The concentration of sulfur in the matte decreased at the beginning with shorter contacting times but soon leveled after 30 s contacting time. The deviation between measured copper and iron values for different samples with same contacting times seems to increase with increasing contacting time, which is unexpected, as the phases become more homogeneous as the time increases, according to SEM images. The deviation in values within the sample is small. The error bars in Figure 13 represent the standard deviations (1σ) of the results.

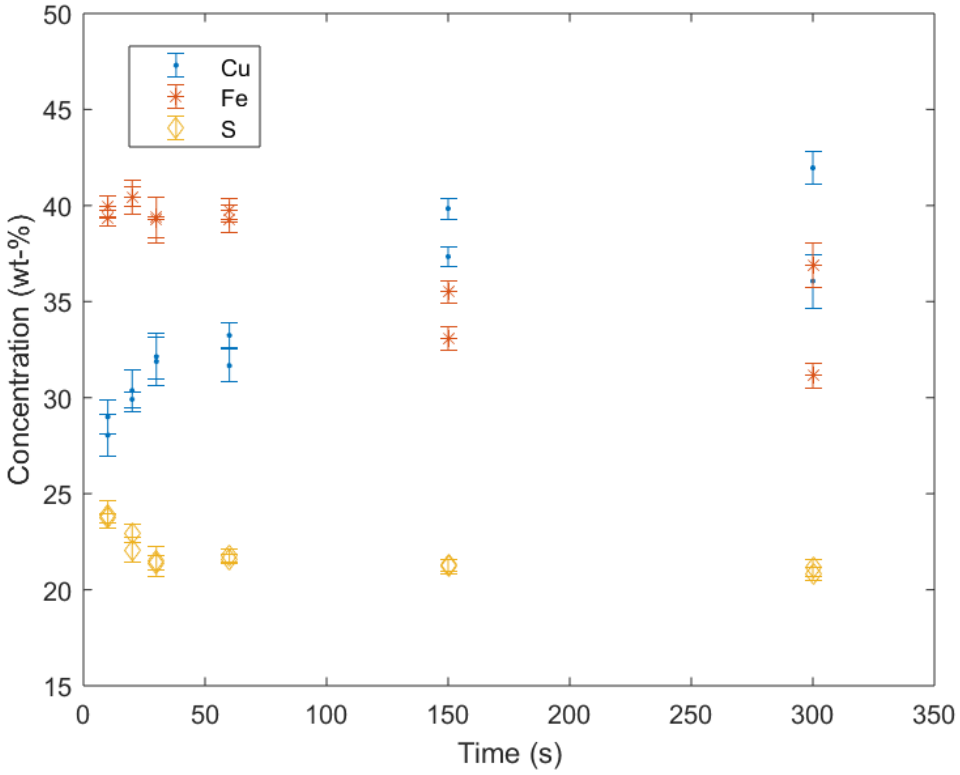

Figure 13 SEM-EDS results for Cu, Fe and S content in matte phase after contacting in air atmosphere.

7.1.2 Argon

The microstructures of all samples in argon atmosphere, regardless of contacting time, were similar. Both copper matte and fayalite slag phases were clearly observed with all contact times. Undissolved silica was also detected in the slag phase at all contacting times. Silica from the crucible was observed dissolving into the slag phase. Small droplets of copper matte could be seen in the slag phase. Veins of higher copper content were visible in the copper matte phase. Micrographs of samples of all contacting times showing the typical structure are shown in Figure 14. A micrograph showing a closer look at the typical microstructure of a sample after 40 min contacting time in argon atmosphere is shown in Figure 15.

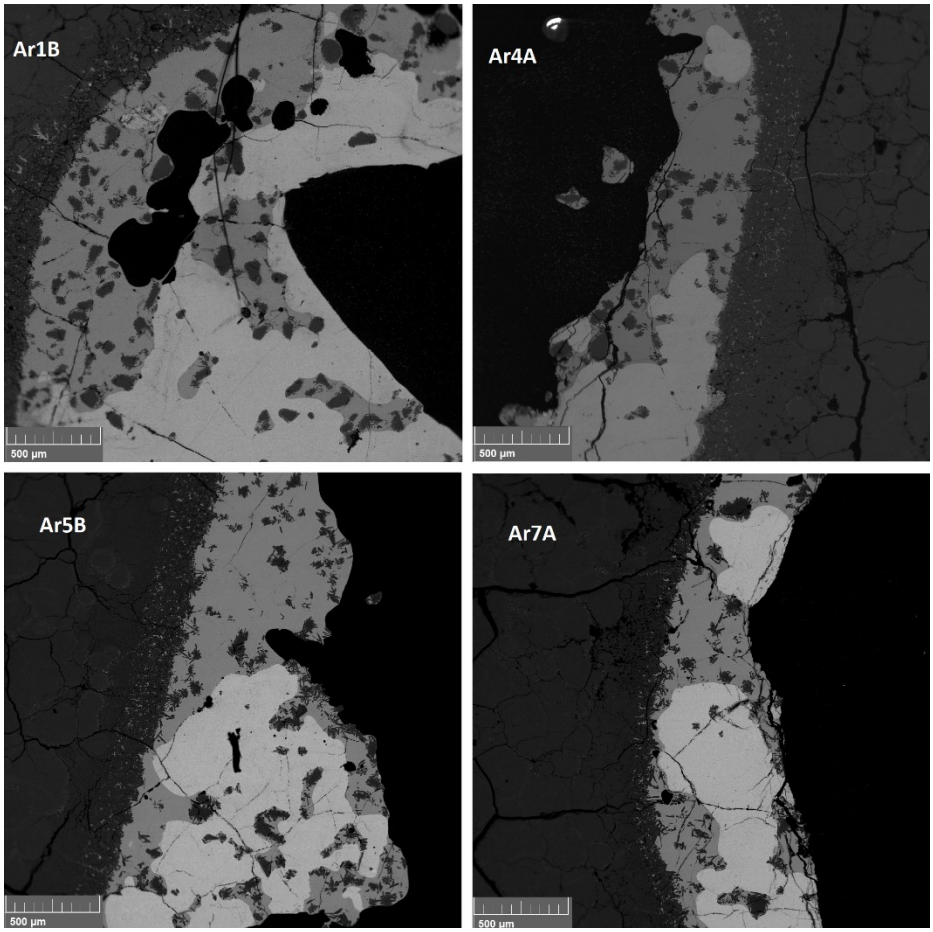

Figure 14 Micrographs of samples 1, 4, 5 and 7 with 5, 10, 20 and 40 minute contacting times, respectively, in argon atmosphere.

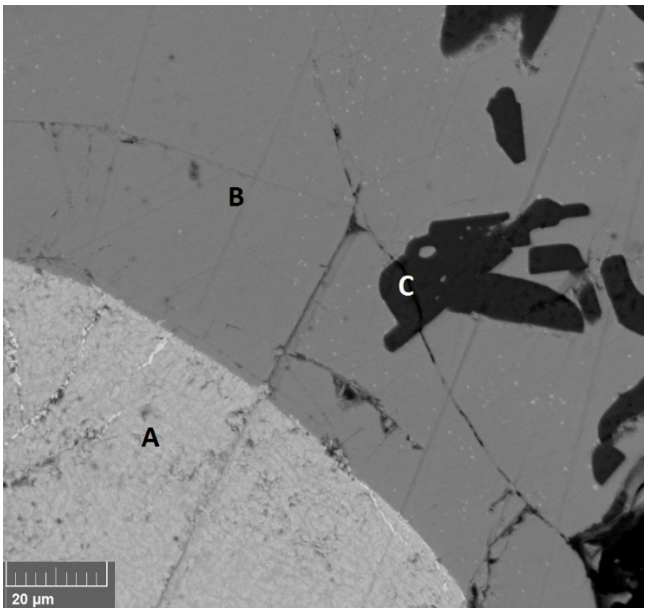

Figure 15 Micrograph of sample 7 after 40 min contacting time in argon atmosphere showing phases of (A) copper matte, (B) fayalite slag and (C) silica.

The change in Cu, Fe and S concentrations in the matte was analyzed using SEM-EDS. The results are given in Figure 16. The concentrations of all three elements remained fairly steady throughout all contacting times. Copper concentration increased very slightly. The concentration of iron remained steady throughout. The concentration of sulfur decreased ever so slightly. Both the deviation within the sample and the deviation between the samples seems to increase with longer contacting times, similarly as with the air atmosphere samples.

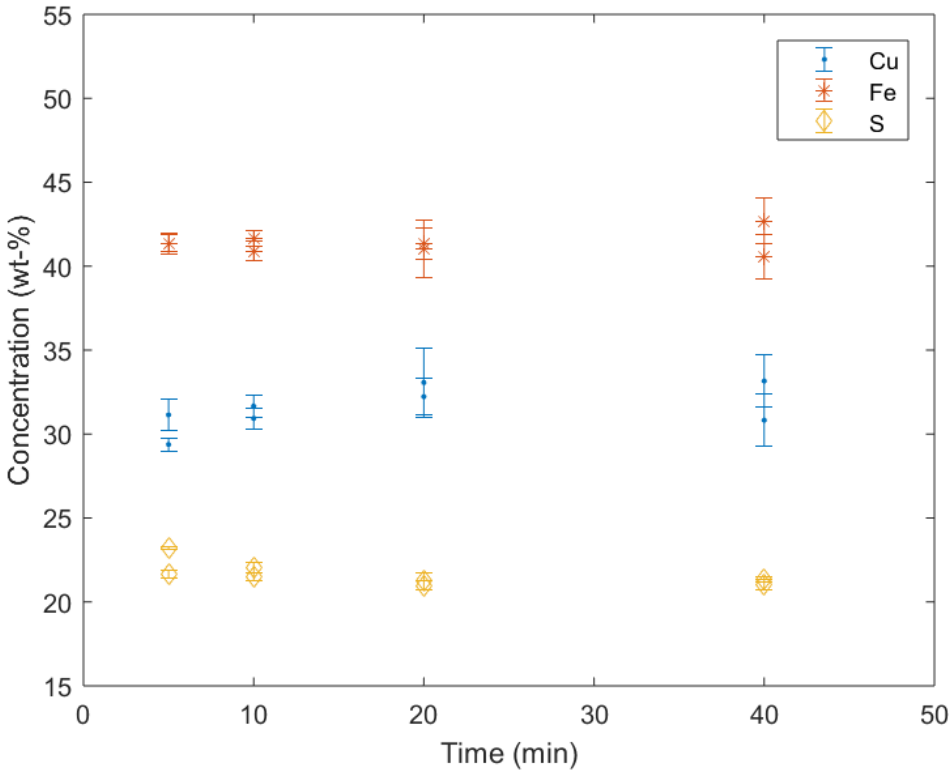

Figure 16 SEM-EDS results for Cu, Fe and S content in matte phase after contacting in argon atmosphere.

7.2 LA-ICP-MS results

The change in REE concentrations in the matte was analyzed using LA-ICP-MS. Two samples were analyzed for each contacting time in both air and argon atmospheres. The samples that were contacted for 10 s in air were excluded, since clear phases were not found during SEM analysis. The error bars represent standard deviations (1σ) of the results.

The results for experiments conducted in air atmosphere show the weight percent of La and Nd in the matte decreasing with increasing contacting time. The LA-ICP-MS results for La and Nd content in the matte are given in Figures 17 and 18, respectively. The deviation between measurements of the same sample seems to decrease with increasing contacting times, which was expected based on the time-resolved analysis signals, as showed and explained in Figure 5. The deviation between different samples with the same contacting times, however, seems to increase with longer contacting times. The decrease in deviation within the sample is logical given that the homogeneity of the phases should increase over time.

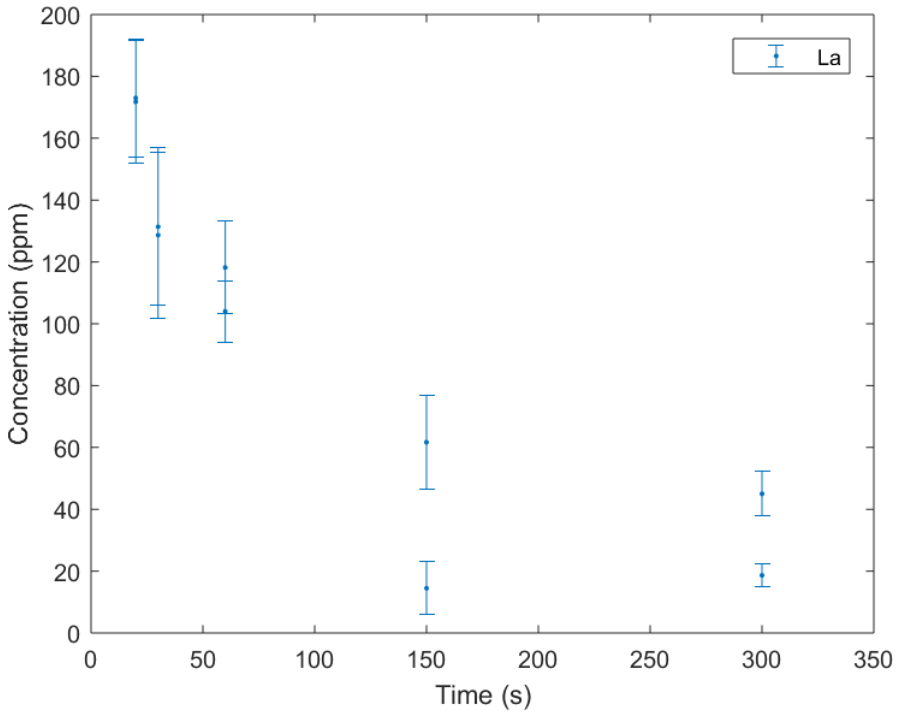

Figure 17 LA-ICP-MS results for La concentration in matte after contacting in air atmosphere.

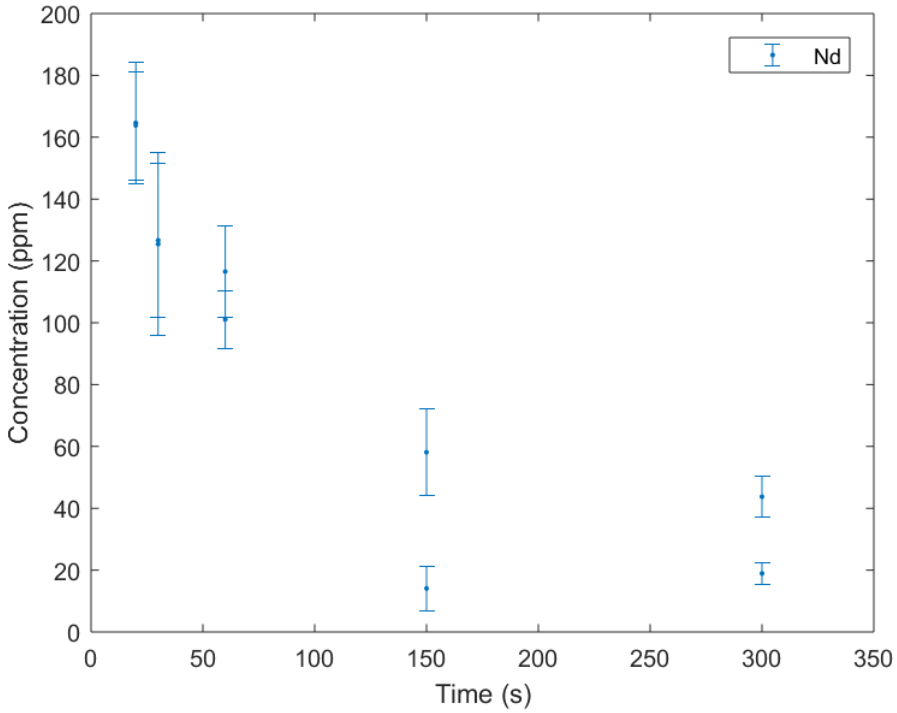

Figure 18 LA-ICP-MS results for Nd concentration in matte after contacting in air atmosphere.

The results for experiments conducted in argon atmosphere also show the weight percent of La and Nd in the matte decreasing with increasing contacting time. The LA-ICP-MS results for La and Nd concentrations in the matte are given in Figures 19 and 20, respectively. The deviation between the samples remains small for all contacting times. The deviation within the samples does not exhibit a clear trend but most are small compared to those of the air atmosphere results. It can be concluded that the samples contacted in argon were more homogeneous than the ones contacted in air.

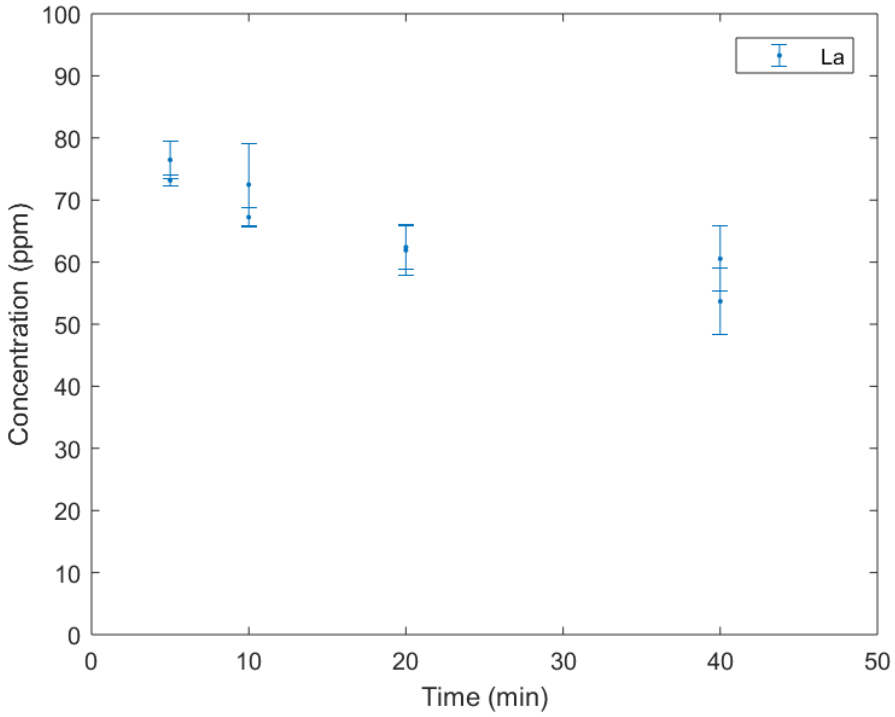

Figure 19 LA-ICP-MS result for La concentration in matte after contacting in argon atmosphere.

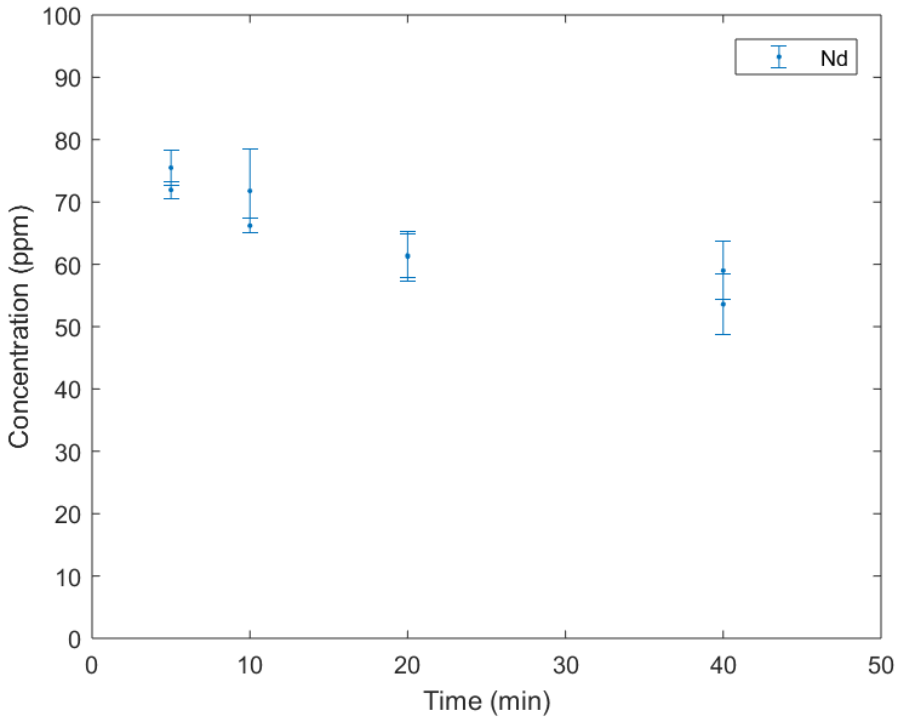

Figure 20 LA-ICP-MS result for Nd concentration in matte after contacting in argon atmosphere.

7.3 EPMA results

The change in REE concentrations in the slag phase were analyzed using EPMA. Two samples were analyzed for each contacting time in both air and argon atmospheres. The samples that were contacted for 10 s in air were excluded since clear phases were not found during SEM analysis. The error bars represent standard deviations (1σ) of the results.

The EPMA results for La and Nd concentrations in the slag in experiments conducted in air atmosphere are given in Figures 21 and 22, respectively. The weight percent of La and Nd in the slag decreases with increasing contacting time. This can most likely be attributed to the increasing slag volume; when the same amount of trace elements is diluted in a larger volume, the concentration decreases. The deviation between measurements of the same sample seems to decrease with increasing contacting times, which is logical given that the homogeneity of the phases increases over time. The deviation between different samples with the same contacting times, however, seems to increase with longer contacting times, which is, again, unexpected.

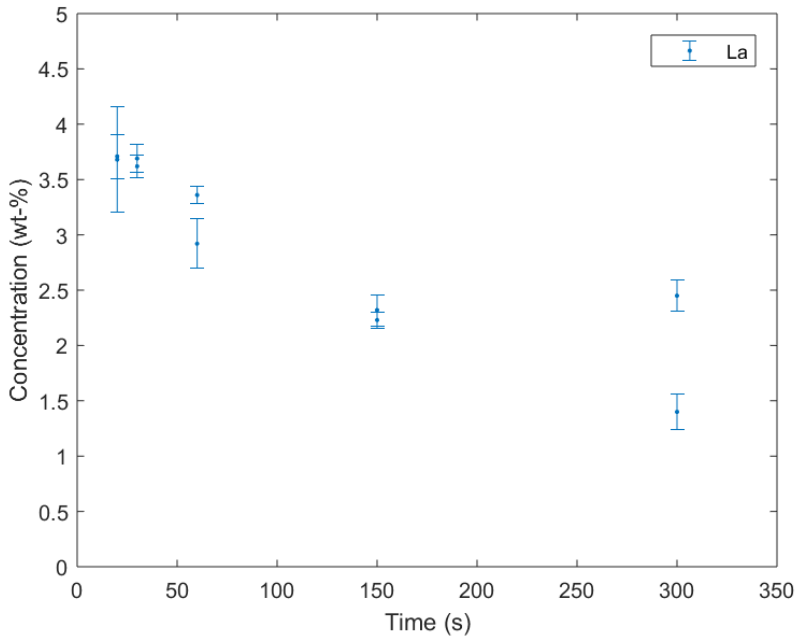

Figure 21 EPMA results for La concentration in slag phase after contacting in air atmosphere.

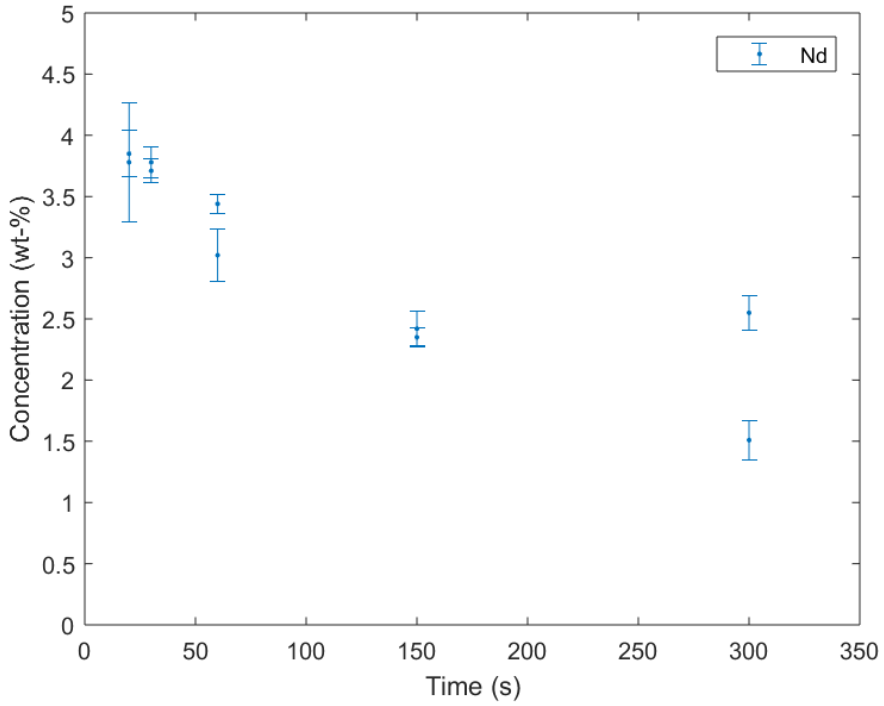

Figure 22 EPMA results for Nd concentration in slag phase after contacting in air atmosphere.

The EPMA results for Fe and Si concentrations in the slag in experiments conducted in air atmosphere are given in Figures 23 and 24, respectively. The concentration of Fe in samples contacted for 20 s is higher than in the other samples. For the other samples, the concentration of iron increases with increasing contacting time. The Si concentration in the slag phase remains stable except for the samples contacted for 20 s, the result for which is lower than for the other samples.

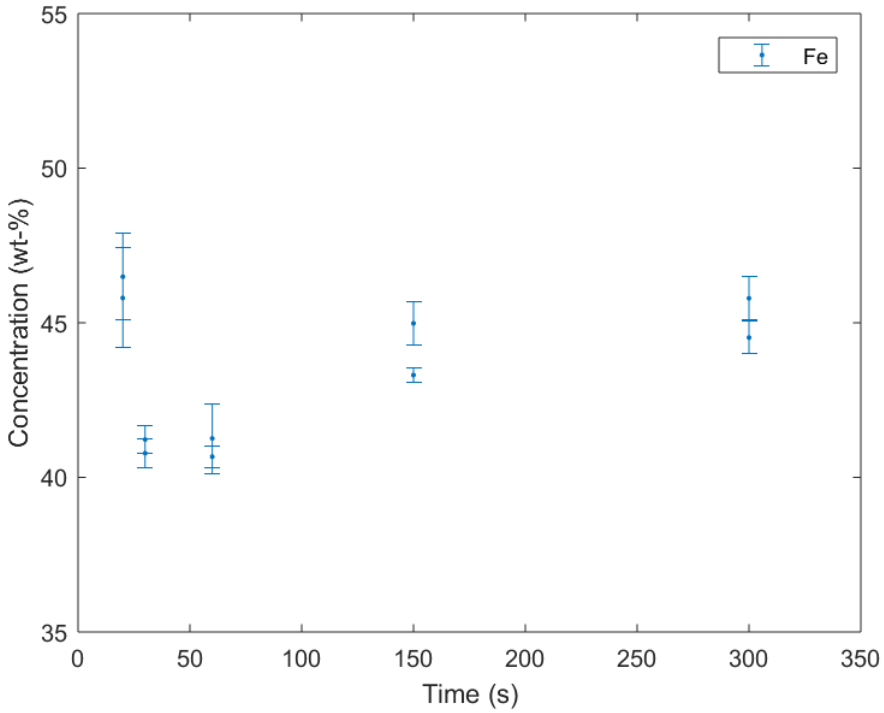

Figure 23 EPMA results for Fe concentration in slag phase after contacting in air atmosphere.

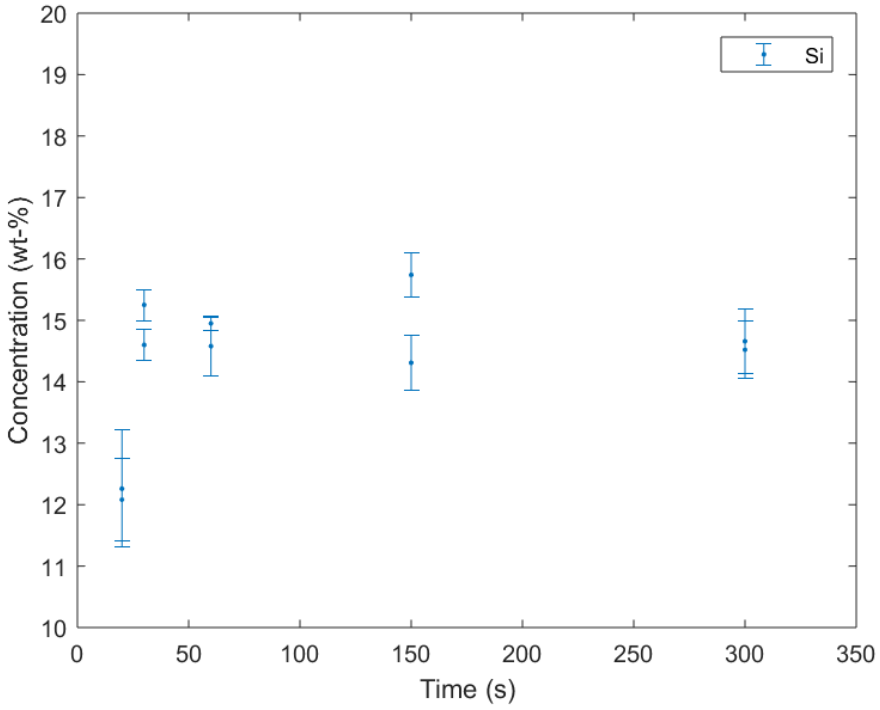

Figure 24 EPMA results for Si concentration in slag phase after contacting in air atmosphere.

The EPMA results for La and Nd concentrations in the slag in experiments conducted in argon atmosphere are given in Figures 25 and 26, respectively. The behaviour of La and Nd is extremely similar. Contrary to air experiments, no clear trend in changing weight percent with time can be determined from the results. In argon experiments, the volume of slag does not change significantly as a function of time, based on the microstructural observations. Therefore, it is logical that the La and Nd concentrations do not decrease as a function of time. The standard deviations in EPMA measurements are very small, except for both 10 min samples and one 5 min sample.

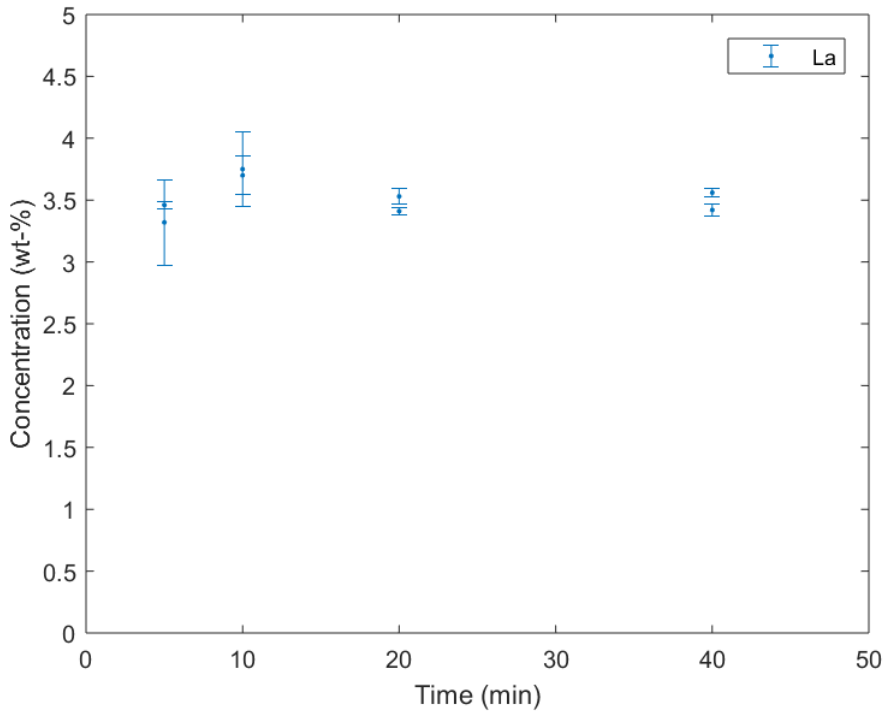

Figure 25 EPMA results for La concentration in slag after contacting in argon atmosphere.

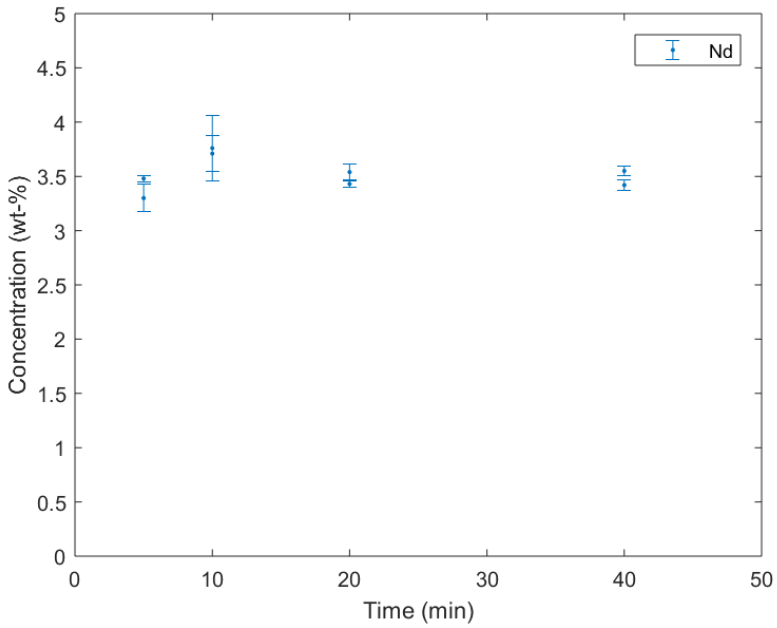

Figure 26 EPMA results for Nd concentration in slag after contacting in argon atmosphere.

The EPMA results for Fe and Si concentrations in the slag in experiments conducted in air atmosphere are given in Figures 27 and 28, respectively. The concentration of Fe and Si shows almost no change with changing contacting time.

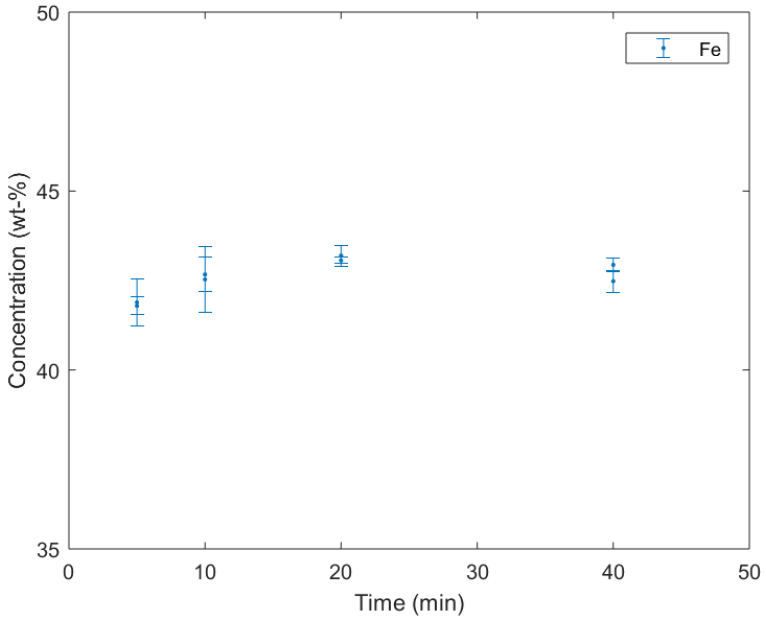

Figure 27 EPMA results for Fe concentration in slag after contacting in argon atmosphere.

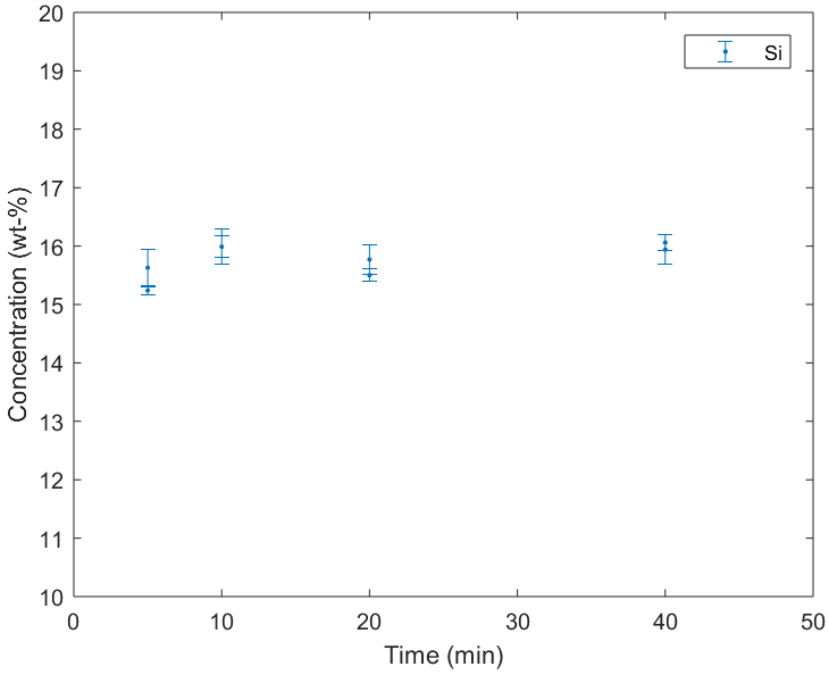

Figure 28 EPMA results for Si concentration in slag after contacting in argon atmosphere.

7.4 Distribution coefficients of La and Nd

The distribution coefficients between matte and slag for La and Nd in air atmosphere are presented in Figures 29 and 30, respectively. The distribution coefficients of both La and Nd are very small, which shows that they distribute strongly into the slag phase. The distribution coefficients also decrease with increasing contacting time, which suggests that the REEs continue to distribute increasingly from the matte phase into the slag phase as time goes on. The large deviation between 150 s samples is strange, and no obvious explanation can be given.

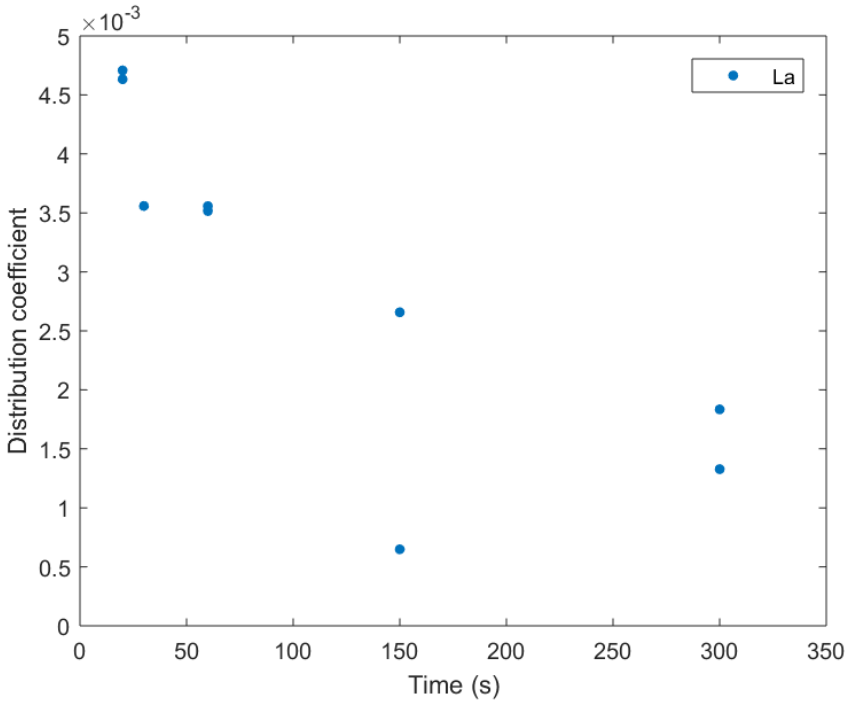

Figure 29 Distribution coefficient of La between matte and slag, after contacting in air atmosphere.

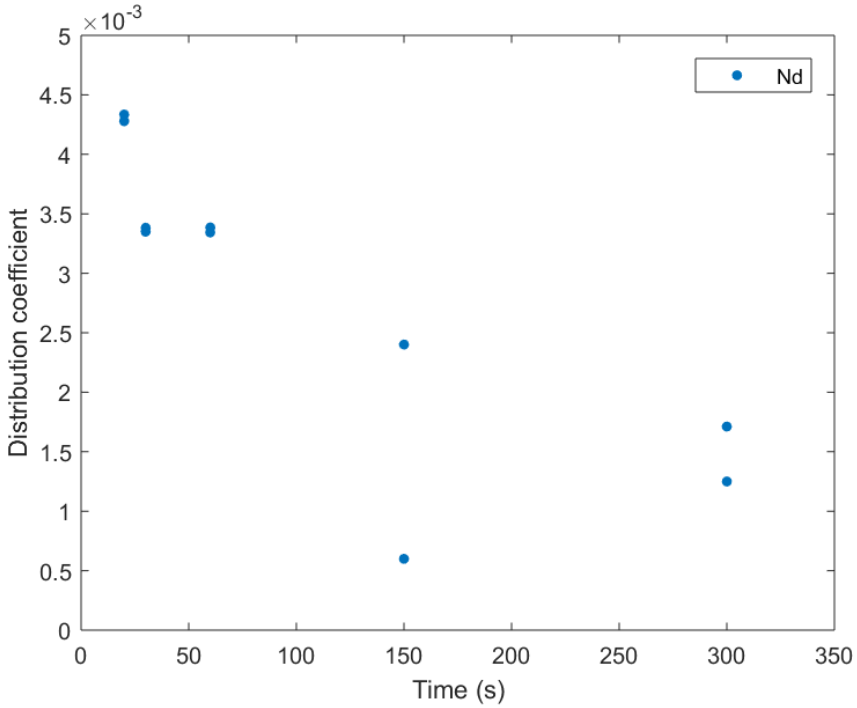

Figure 30 Distribution coefficient of Nd after contacting in air atmosphere.

Distribution coefficients for La and Nd in argon atmosphere are presented in Figures 31 and 32, respectively. The distribution coefficients of both La and Nd are small,

which shows that they distribute strongly into the slag phase in argon atmosphere as well. The distribution coefficients also decrease with increasing contacting time, which suggests that the REEs continue to distribute from the matte phase into the slag phase as time goes on.

The distribution coefficient of Nd in argon atmosphere is compared to results from an equilibration study [2] between copper, matte, slag and magnetite phases. The reference values were chosen from results where the temperature (1275 °C) was closest to the temperature used in this work (1300 °C). t_e in Figure 32 refers to the equilibration time in the reference (45 minutes). The concentration of Nd in matte was well below the detection limit of the analytical technique (EPMA), so the reference value should be regarded as an approximate.

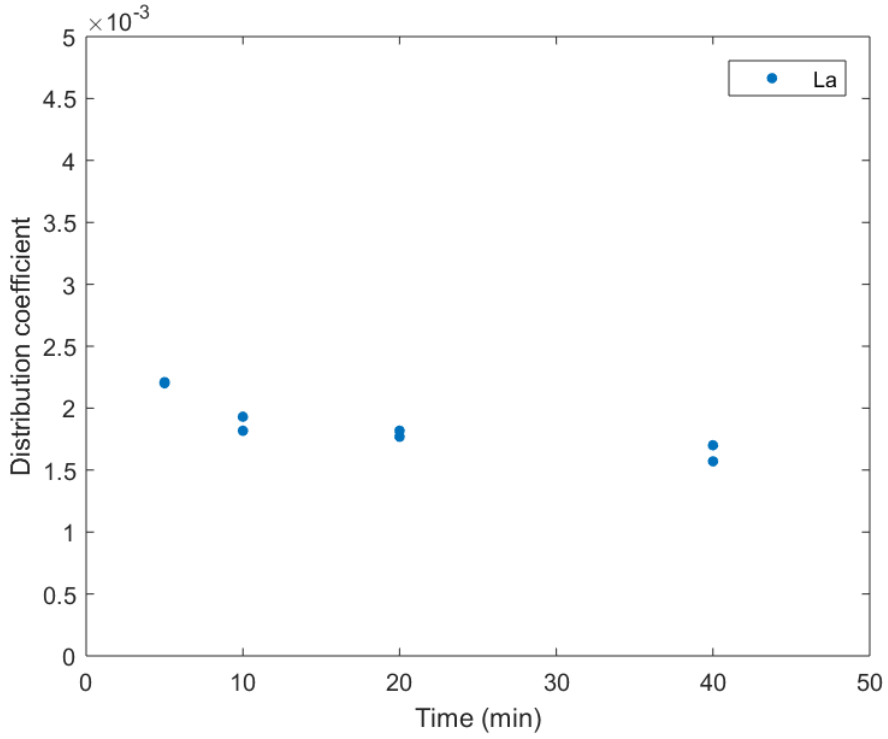

Figure 31 Distribution coefficient of La after contacting in argon atmosphere.

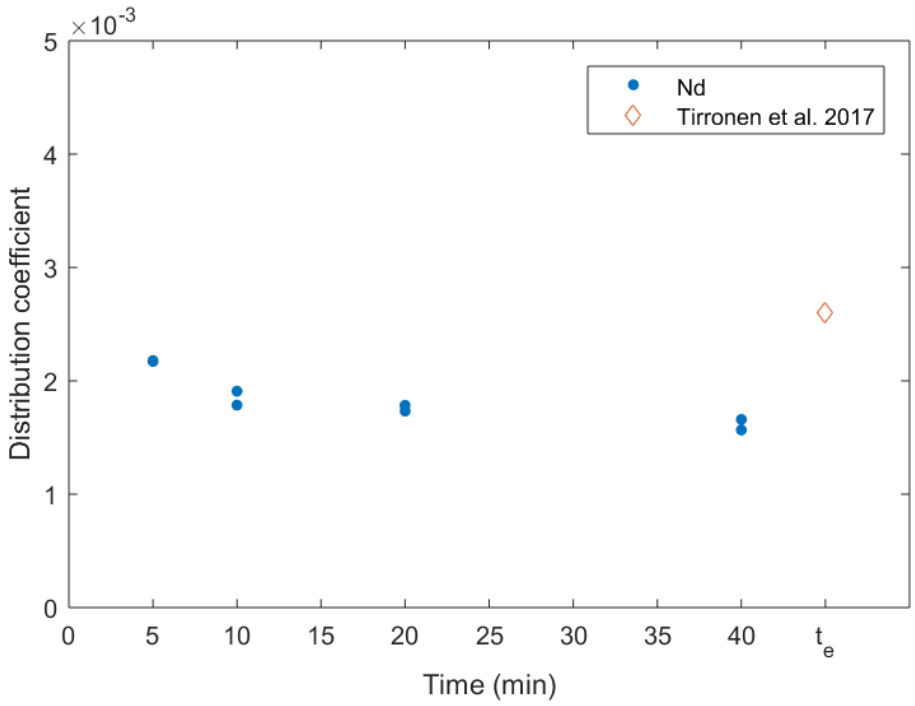

Figure 32 Distribution coefficient of Nd after contacting in argon atmosphere, t_e refers to the equilibration time in the reference.

8 Discussion

8.1 Microstructure

The progression of changes in the microstructure of the samples contacted in air atmosphere can be estimated based on the SEM analyses. The changes follow the reactions described by Guntoro et al. [1]. The sulphides present in the concentrate are unstable in air atmosphere and some of them will thus be oxidized. This is followed by the slag forming stage, during which the fayalite slag is formed and once the volume of slag is considerable, the matte and slag will start to separate. [1]

Segregated iron oxide was observed in the matte. According to Guntoro et al. [1] magnetite is insoluble in solid matte and is thus thought to precipitate. Copper rich veins were also observed in the matte. According to Guntoro et al. [1] they are formed during quenching and are associated with cracks in the structure.

The progression of changes in the structure of the samples contacted in argon atmosphere can also be estimated based on the SEM analyses. Apart from reactions requiring oxygen, the changes mainly follow the same reactions as took place in air atmosphere. Matte formation was similarly rapid. Like in samples contacted in air atmosphere, copper rich veins were found in the matte phase.

Unlike in air atmosphere, segregated magnetite was not observed in the matte phase after contacting in argon atmosphere. According to Guntoro et al. [1] this is likely because magnetite formation was limited by the low availability of oxygen. Oxidation reactions in an inert atmosphere are expected to be limited as there is no gaseous oxygen in the system and oxygen needed by reactions is provided solely by the slag phase. [1]

A clear progression in the settling phenomenon could be seen with increasing contacting time in samples contacted in both atmospheres. The progression can be seen in the micrographs in Appendices I and II showing the whole cross sections of the crucibles. No separation has happened after 10 s contacting time in air atmosphere. The separation has started after 20 s contacting time, but the phases

are still quite randomly distributed in the crucible. With increasing contacting time, the separation of matte and slag phases becomes more defined. For the samples contacted in argon atmosphere, with shorter contacting times the matte and slag phases are more randomly distributed within the crucible. With increasing contacting times, the phases appear to separate further with the matte settling on the bottom of the crucible with slag on top of it and along the sides of the crucible.

8.2 Distributions

The changes in Cu, Fe and S concentrations in matte in experiments conducted in air atmosphere follow a similar trend to those found in previous studies. Similar experiments have been performed by Kleemola [73]. The results of her study showed large scatter in the results of experiments contacted for 300 s in air atmosphere. The final matte grade is thus hard to determine, but the trend in the results is similar to those found in this work. In both studies, the copper concentration began to increase soon after the system reached high temperatures, while the iron concentration correspondingly began decreasing. In this work, the copper content stabilized at approximately 40 wt-% while the Fe content leveled at around 35 wt-%. In the results of the previous study [73], the final Cu and Fe concentrations were above 35 wt-% and below 30 wt-%, respectively. Similar experiments were also performed by Wan et al. [68], the results of which were shown in Figure 3 in Chapter 5. The matte grade (wt-% Cu) reached in these experiments was much higher. These experiments used a different concentrate than the experiments performed by Kleemola and in this work, which might help in explaining the difference. No experiments have been conducted so far with the same concentrate used in this work, without any added trace elements.

In the experiments conducted in argon atmosphere, the changes in Cu, Fe and S concentrations in matte are similar to the results in previous studies. The current and previous results showed almost no change in the concentrations of Cu, Fe and S. The previous results of Kleemola [73] showed that the samples with the longest contacting times contained around 30 wt-% Cu, around 35 wt-% Fe and around 25

wt-% S. The results of this work show a concentration of more than 40 wt-% Fe, around 33 wt-% Cu and around 21 wt-% S. The trends are similar even though the concentration of iron is higher in the current work. In the experiments by Kleemola, precious metals in the system distributed into the matte, thus reducing the concentrations of iron and copper, which might explain the difference.

The concentration of Fe in most samples contacted in air atmosphere increases with increasing contacting time. This is expected as the de-ironisation of matte progresses. Samples contacted for 20 s are the exception to this and they have a concentration higher than in the other samples, which is unexpected. The same samples have a significantly lower Si concentration compared to other samples contacted in air atmosphere. The Si concentration in other samples does not significantly change with contacting time. In argon atmosphere the concentration of both Fe and Si remains relatively stable regardless of contacting time.

REEs deport quickly to the slag phase during copper matte smelting. In both experiments conducted in air and argon atmospheres, the concentrations of REEs in the matte were low in all experiments and continued to decrease with increasing contacting times.

The REE concentrations in the matte phase were much higher in the beginning of the experiments conducted in air atmosphere. The measured changes in concentrations were much smaller in experiments conducted in argon atmosphere. The lowest concentrations reached with the longest contacting time are very similar in both atmospheres.

According to the results for the experiments conducted in air atmosphere, the concentration of REEs in the slag phase decreases with increasing contacting time. This is likely due to the volume of the slag phase increasing, rather than the mass of REEs decreasing in the slag phase. In the experiments conducted in argon atmosphere, the concentration of REEs remained somewhat stable at a value similar to those found in the beginning of the experiments conducted in air. This is logical, as the slag volume change was far less significant in argon atmosphere.

The values of the distribution coefficients calculated from the experiments conducted in air atmosphere decreased with increasing contacting time. The concentration of REEs also decreased with increasing contacting time in air in both matte and slag phases. The volume of the slag changes over time since longer contacting times lead to increased formation of slag. Since the value of the distribution coefficient decreases, the concentrations of REEs in matte decrease more compared to the concentrations in slag. It can be concluded that the low concentrations of REEs from the matte are increasingly deporting to the slag phase over time. The change is fairly small, since the REEs distribute mostly to the slag phase rapidly at the beginning of the experiment.

The values of the distribution coefficients calculated from the experiments conducted in argon atmosphere also decreased with increasing contacting time. The concentration of REEs decreased with increasing contacting time in the matte phase. The concentration of REEs in the slag phase varied somewhat but remained relatively stable. Thus, a similar conclusion can be drawn as for the experiments conducted in air.

The distribution coefficient of Nd in argon was compared to a reference value taken from an equilibration study [2]. The concentration of Nd in the matte phase in the equilibration study was below the detection limit of the analytical technique used (EPMA), so the distribution coefficient should only be regarded as an approximate. The distribution coefficient at the equilibration time is in the same range but slightly higher than the distribution coefficients calculated in this work. It is probably likely that the distribution coefficients of REEs approached their equilibrium values already with the longest contacting times used in this work.

The distribution coefficient in the beginning of the experiments conducted in air atmosphere is higher than the one in the beginning of the experiments conducted in argon. The distribution coefficient calculated from the longest contacting times in air has a similar value to those calculated from argon results. In other words, regardless

of whether the contacting is done in air or argon atmosphere, REEs distribute almost entirely to the slag phase, leaving a negligible concentration in the matte phase.

All results support the fact that REEs behave extremely similarly. Results from experiments in both air and argon atmospheres were nearly identical for La and Nd.

8.3 Recycling

REEs report to the slag phase during matte smelting. They are thus lost in regard to recycling, unless recovered from the slag using another process. This makes the recycling of REEs using matte smelting processes more complicated but not impossible.

Practically all the REEs used in the experiments reported to the slag phase as oxides. The concentrations of REEs found in the matte phase were negligible compared to the concentrations in the slag phase. The deportment was almost instantaneous, and even with short contacting times, the concentrations of REEs found in the matte were small. With increasing contacting time, the REEs distributed even more strongly to the slag phase.

The behaviour of REEs in a copper matte-slag system might support the recycling of REE containing scrap using pyrometallurgical processes. Since the REEs report to the slag phase their recovery is not as straightforward as of those elements that distribute to the matte phase and are thus more easily recovered. However, nearly all of the REEs distribute to the slag phase, making their possible recovery rate high as long as there is a suitable process that can be used in addition to the copper smelting.

Once the copper matte-slag system reaches high temperatures, the distribution of REOs to the slag phase seems to be almost instantaneous. The same applies whether the system is in air or inert atmosphere. This also supports using REE containing scrap in copper smelting processes as it helps ensure that all REEs will end up in the slag phase during the smelting process.

It is possible to extract REEs from fayalite slags used in matte smelting but not much research has been done on the subject. Mikoda et al. [74] studied the use of bioleaching to recover REEs, among other elements, from different copper slags. One of the slags was a granulated slag formed after copper is removed from flash furnace slags using an electric arc furnace. The study used a gram-negative *Acidithiobacillus thiooxidans* strain and under optimal conditions up to 99 % of REEs could be extracted from the granulated slag. [74]

The recovery of REEs from matte smelting slags is at the moment likely uneconomical. Mikoda et al. [74] calculated that the value of the metals extracted from the slag is well below the cost of the operation [74]. Using the same method for calculations used in [74] the change in profitability is very small even when using the highest prices for REEs during the crisis. The value of REEs only rose from covering about 0.0057 % of the cost of operation to covering about 0.17 %. For the recovery of REEs from copper smelting slags to be economical the price of REEs would have to rice significantly or more efficient and economical processes need to be developed.

9 Conclusions and recommendations for future work

The time-dependent behaviour of REEs in a copper matte-slag system was experimentally studied. The conditions were simulated to represent those of copper concentrate flash smelting conditions. The experiments were conducted in air and argon atmospheres at 1300 °C. The contacting times in air were between 10 and 300 seconds, while the contacting times in argon were between 5 and 40 minutes. Metallographic sample preparation methods were used to prepare the samples for analysis. SEM-EDS was used for visual and compositional analysis, while LA-ICP-MS and EPMA were used to acquire more accurate data on the composition of matte and slag phases, respectively, focusing on the concentrations of La and Nd.

The thermodynamic and kinetic behaviour of REEs in copper matte-slag system was investigated experimentally and using a literature review. With little kinetic data available on REEs in copper matte-slag system, the results were compared to equilibration distribution values.

REEs strongly prefer the slag phase over the matte phase, which was also evident in the results of this work. The results of this work also indicate that REEs distribute to the slag phase almost instantly when the system reaches high temperatures in copper matte smelting conditions. The concentrations of REEs remaining in the matte phase after the longest contacting times in both air and argon atmospheres were negligible compared to the concentrations in the slag phase. Distribution coefficient values indicate that with increasing contacting times, REEs distribute increasingly strongly into the slag phase. Distribution coefficient values calculated from samples contacted in argon atmosphere were compared to equilibration distribution values. The comparison indicates that the distribution of REEs likely approached or reached equilibrium values even with the relatively short experimental times used in this study.

The use of pyrometallurgical processing for the recycling of REE containing scrap is supported by the fact that REEs distribute almost completely to the slag phase and

the distribution is almost instantaneous. However, distribution to the slag phase over the matte phase complicates the recycling as another process is required to recover the REEs from the slag. It is possible but currently not cost-efficient.

There was large scatter in the SEM-EDS, LA-ICP-MS and EPMA results for samples contacted in air for 300 s. There was also significant scatter in the LA-ICP-MS results for samples contacted in air atmosphere for 150 s. Additional experiments around the 150 s and 300 s contacting times are suggested to see if the scatter in the results is repeatable.

To better evaluate and compare the results of these and similar experiments, it would be beneficial to perform the same experiments using only concentrate and slag without the addition of trace elements.

For more insights regarding the distribution kinetics, the samples could also be characterized more comprehensively; it is not evident that the concentrations of La and Nd remain the same in both phases for example near the phase boundaries compared to further from these areas. This would of course increase the analysis costs notably.

Bibliography

[1] P. I. Guntoro, A. Jokilaakso, N. Hellstén and P. Taskinen, "Copper matte-slag reaction sequences and separation processes in matte smelting," *Journal of Mining and Metallurgy, Section B: Metallurgy,* vol. 54, no. 3, pp. 301-311, 2018.

[2] T. Tirronen, D. Sukhomlinov, H. O'Brien, P. Taskinen and M. Lundström, "Distributions of lithium-ion and nickel-metal hydride battery elements in copper converting," *Journal of Cleaner Production,* vol. 168, pp. 399-409, 2017.

[3] F. G. G. (. Wall, "Rare earth elements," in *Critical Metals Handbook (1st ed.)*, John Wiley & Sons, Ltd., 2014, pp. 312-337.

[4] P. Meshram, B. Pandey and B. Abhilash, "Perspective of availability and sustainable recycling prospects of metals in rechargeable batteries – A resource overview," *Resources Policy,* vol. 60, pp. 9-22, 2019.

[5] C. Gupta and N. Krishnamurthy, Extractive Metallurgy of Rare Earths, CRC Press, 2005.

[6] U.S. Geological Survey, "Mineral Commodity Summaries 2018," 2018.

[7] D. Guyonnet, M. Planchon, A. Rollat, V. Escalon, J. Tuduri, N. Charles, S. Vaxelaire, D. Dubois and H. Fargier, "Material flow analysis applied to rare earth elements in Europe," *Journal of Cleaner Production,* vol. 107, pp. 215-228, 2015.

[8] O. Takeda and T. Okabe, "Current Status on Resource and Recycling Technology for Rare Earths," *Metallurgical and Materials Transactions E,* vol. 1, pp. 160-173, 2014.

[9] N. E. A. Greenwood, Chemistry of the Elements, 2nd ed., Elsevier, 1997, pp. 218, 1229.

[10] R. Eggert, C. Wadia, C. Anderson, D. Bauer, F. Fields, L. Meinert and P. Taylor, "Rare Earths: Market Disruption, Innovation, and Global Supply Chains," *Annual Review of Environment and Resources ,* vol. 41, pp. 199-222, 2016.

[11] R. Eggert, C. Wadia, C. Anderson, D. Bauer, F. Fields, L. Meinert and P. Taylor, "Rare Earths: Market Disruption, Innovation, and Global Supply Chains," *Annual Review of Environment and Resources,* vol. 41, pp. 199-222, 2016.

[12] K. Binnemans, P. T. Jones, T. Müller and L. Yurramendi, "Rare Earths and the Balance Problem: How to Deal with Changing Markets?," *Journal of Sustainable Metallurgy,* vol. 4, pp. 126-146, 2018.

[13] Bureau of Mines, "Minerals yearbook 1990," 1990.

[14] J. B. Hendrick, "Minerals Yearbook 1995 - Rare Earths," U.S. Geological Survey.

[15] J. B. Hendrick, "Minerals Yearbook 2000 - Rare Earths," U.S. Geological Survey.

[16] J. B. Hendrick, "Minerals Yearbook 2005 - Rare Earths," U.S. Geological Survey, 2006.

[17] J. Gambogi and D. J. Cordier, "Minerals Yearbook 2010 - Rare Earths," U.S. Geological Survey, 2012.

[18] J. Gambogi, "Minerals Yearbook 2015 - Rare Earths," U.S. Geological Survey, 2018.

[19] R. S. Pell, F. Wall, X. Yan and G. Bailey, "Applying and advancing the economic resource scarcity potential (ESP) method for rare earth elements," *Resources Policy,* 2018.

[20] S. M. Jowitt, T. T. Werner, Z. Weng and G. M. Mudd, "Recycling of the rare earth elements," *Current Opinion in Green and Sustainable Chemistry,* vol. 13, pp. 1-7, 2018.

[21] T. Dutta, K.-H. Kim, M. Uchimiya, E. E. Kwon, B.-H. Jeon, A. Deep and S.-T. Yun, "Global demand for rare earth resources and strategies for green mining," *Environmental Research,* vol. 150, pp. 182-190, 2016.

[22] Chatham House, "Resource Trade .Earth," Chatham House, [Online]. Available: https://resourcetrade.earth/data?year=2017&category=187&units=weight. [Accessed 18 February 2019].

[23] G. Barakos, J. Gutzmer and H. Mischo, "Strategic evaluations and mining process optimization towards a strong global REE supply chain," *Journal of Sustainable Mining,* vol. 15, pp. 26-35, 2016.

[24] N. T. Nassar, X. Du and T. E. Graedel, "Criticality of the Rare Earth Elements," *Journal of Industrial Ecology,* vol. 19, pp. 1044-1054 , 2015.

[25] European Comission, "Communication on the list of critical raw materials 2017," 2017. [Online]. Available: https://eur-lex.europa.eu/legal-content/EN/TXT/PDF/?uri=CELEX:52017DC0490&from=EN. [Accessed 6 February 2019].

[26] S. Maroufi, R. Nekouei, R. Hossain, M. Assefi and V. Sahajwalla, "Recovery of Rare Earth (i.e., La, Ce, Nd, and Pr) Oxides from End-of-Life Ni-MH Battery via Thermal Isolation," *Acs Sustainable Chemistry & Engineering,* vol. 6, pp. 11811-11818 , 2018.

[27] X. Du and T. Graedel, "Uncovering the end uses of the rare earth elements," *Science of the Total Environment,* Vols. 461-462, pp. 781-784, 2013.

[28] A. Rollat, D. Guyonnet, M. Planchon and J. Tuduri, "Prospective analysis of the flows of certain rare earths in Europe at the 2020 horizon," *Waste Management,* vol. 49, pp. 427-436, 2016.

[29] J. H. Rademaker, R. Kleijn and Y. Yang, "Recycling as a Strategy against Rare Earth Element Criticality: A Systemic Evaluation of the Potential Yield of NdFeB Magnet Recycling," *Environmental science & technology,* vol. 47, pp. 10129-10136, 2013.

[30] T. Fishman, R. Myers, O. Rios and T. Graedel, "Implications of Emerging Vehicle Technologies on Rare Earth Supply and Demand in the United States," *Resources,* vol. 7, 2018.

[31] U.S. Department of Energy, "Critical materials strategy (DOE/PI-0009)," 2011. [Online]. Available: http://dx.doi.org/10.3133/70140094. [Accessed 19 February 2019].

[32] K. Binnemans, P. T. Jones, B. Blanpain, T. Van Gerven, Y. Yang, A. Walton and M. Buchert, "Recycling of rare earths: a critical review," *Journal of Cleaner Production,* vol. 51, pp. 1-22, 2013.

[33] A. Danczak, I. Chojnacka, S. Matuska, K. Marcola, A. Lesniewicz, M. Welna, A. Zak, Z. Adamski and L. Rycerz, "The recycling-oriented material characterization of hard disk drives with special emphasis on NdFeB magnets," *Physicochemical Problems of Mineral Processing,* vol. 54, no. 2, pp. 363-376, 2018.

[34] T. Graedel, J. Allwood, M. Buchert, C. Hagelüken, B. Reck, S. Sibley and G. Sonnemann, "What Do We Know About Metal Recycling Rates?," *Journal of Industrial Ecology,* vol. 15, pp. 355-366, 2011.

[35] N. Haque, A. Hughes, S. Lim and C. Vernon, "Rare Earth Elements: Overview of Mining, Mineralogy, Uses, Sustainability and Environmental Impact," *Resources,* vol. 3, pp. 614-635, 2014.

[36] European Commission, "Report on critical raw materials and the circular economy," European Union, 2018.

[37] T. G. Goonan, "Rare Earth Elements—End Use and Recyclability," U.S. Geological Survey, 2011.

[38] X. Du and T. Graedel, "Uncovering the Global Life Cycles of the Rare Earth Elements," *Scientific Reports,* vol. 1, pp. 1-4, 2011.

[39] Y. Yang, A. Walton, R. Sheridan, K. Güth, R. Gauß, O. Gutfleisch, M. Buchert, P. Jones and K. Binnemans, "REE Recovery from End-of-Life NdFeB Permanent Magnet Scrap: A Critical Review," *Journal of Sustainable Metallurgy,* vol. 4, pp. 122-149, 2017.

[40] S. Al-Thyabat, T. Nakamura, E. Shibata and A. Iizuka, "Adaptation of minerals processing operations for lithium-ion (LiBs) and nickel metal hydride (NiMH) batteries recycling: Critical review," *Minerals Engineering,* vol. 45, pp. 4-17, 2013.

[41] M. Reuter, "Metal Recycling - Opportunities, Limits, Infrastructure," United Nations Environment Programme, 2013.

[42] J. Zhang, L. Zhang, H. Liu, A. Sun, R.-S. Liu and R. Liu, Electrochemical Technologies for Energy Storage and Conversion, John Wiley & Sons, Incorporated , 2012.

[43] F. Liu, C. Peng, A. Porvali, Z. Wang, B. Wilson and M. Lundström, "Synergistic recycling of nickel-metal hydride batteries and lithium-ion batteries using a sustainable process," Unpiblished work.

[44] V. Innocenzi, N. M. Ippolito, I. De Michelis, M. Prisciandaro, F. Medici and F. Vegliò, "A review of the processes and lab-scale techniques for the treatment of spent rechargeable NiMH batteries," *Journal of Power Sources,* vol. 362, pp. 202-218 , 2017.

[45] P. Sommer, V. Rotter and M. Ueberschaar, "Battery related cobalt and REE flows in WEEE treatment," *Waste Management,* vol. 45, pp. 298-305, 2015.

[46] Eurostat, "Waste statistics - recycling of batteries and accumulators," Eurostat, 6 December 2018. [Online]. Available: https://ec.europa.eu/eurostat/statistics-

explained/index.php?title=Waste_statistics_-_recycling_of_batteries_and_accumulators&stable=0. [Accessed 20 February 2019].

[47] J. Yano, T. Muroi and S.-I. Sakai, "Rare earth element recovery potentials from end-of-life hybrid electric vehicle components in 2010–2030," *The Journal of Material Cycles and Waste Management ,* vol. 18, pp. 655-664, 2016.

[48] Eurostat, "Passenger cars, by type of motor energy," Eurostat, 19 April 2018. [Online]. Available: http://appsso.eurostat.ec.europa.eu/nui/show.do. [Accessed 20 February 2019].

[49] Eurostat, "New registrations of passenger cars by type of motor energy," Eurostat, 19 April 2018. [Online]. Available: http://appsso.eurostat.ec.europa.eu/nui/show.do. [Accessed 20 February 2019].

[50] T. Müller and B. Friedrich, "Development of a recycling process for nickel-metal hydride batteries," *Journal of Power Sources,* vol. 158, pp. 1498-1509, 2006.

[51] S.-L. Lin, K.-L. Huang, I.-C. Wang, I.-C. Chou, Y.-M. Kuo, C.-H. Hung and C. Lin, "Characterization of spent nickel–metal hydride batteries and a preliminary economic evaluation of the recovery processes," *Journal of the Air & Waste Management Association,* vol. 66, no. 3, pp. 296-306, 2015.

[52] K. Tang, A. Ciftja, A. M. Martinez, C. van der Eijk, Y. Bian, S. Guo and W. Ding, "Recycling the Rare Earth Elements from Waste NiMH Batteries and Magnet Scraps by Pyrometallurgical Processes," 2014.

[53] B. Mebarki, B. Draoui, L. Rahmani and B. Allaoua, "Electric Automobile Ni-MH Battery Investigation in Diverse Situations," *Energy Procedia,* vol. 36, pp. 130-141, 2013.

[54] Y. Yang, A. Walton, R. Sheridan, K. Güth, R. Gauß, O. Gutfleisch, M. Buchert, P. Jones and K. Binnemans, "REE Recovery from End-of-Life NdFeB Permanent Magnet Scrap: A Critical Review," *Journal of Sustainable Metallurgy,* vol. 31, pp. 122-149, 2017.

[55] K. Tang, A. Ciftja, C. van Der Eijk, S. Wilson and G. Tranell, "Recycling of the rare earth oxides from spent rechargeable batteries using waste metallurgical slags," *Journal of Mining and Metallurgy. Section B: Metallurgy,* vol. 49, pp. 233-236 , 2013.

[56] P. Zhang, T. Yokoyama, O. Itabashi, Y. Wakui, T. M. Suzuki and K. Inoue, "Recovery of metal values from spent nickel–metal hydride rechargeable batteries," *Journal of Power Sources,* vol. 77, pp. 116-122, 1999.

[57] L. Li, S. Xu, Z. Ju and F. Wu, "Recovery of Ni, Co and rare earths from spent Ni-metal hydride batteries and preparation of spherical Ni(OH)2," *Hydrometallurgy,* vol. 100, no. 1, pp. 41-46, 2009.

[58] X. Yang, J. Zhang and X. Fang, "Rare earth element recycling from waste nickel-metal hydride batteries," *Journal of Hazardous Materials,* vol. 279, pp. 384-388, 2014.

[59] L. E. O. C. Rodrigues and M. B. Mansur, "Hydrometallurgical separation of rare earth elements, cobalt and nickel from spent nickel–metal–hydride batteries," *Journal of Power Sources,* vol. 195, pp. 3735-3741, 2010.

[60] L. Pietrelli, B. Bellomo, D. Fontana and M. Montereali, "Rare earths recovery from NiMH spent batteries," *Hydrometallurgy ,* vol. 66, pp. 135-139, 2002.

[61] V. Innocenzi and F. Vegliò, "Recovery of rare earths and base metals from spent nickel-metal hydride batteries by sequential sulphuric acid leaching and selective precipitations," *Journal of Power Sources,* vol. 211, pp. 184-191, 2012.

[62] K. Korkmaz, M. Alemrajabi, Å. Rasmuson and K. Forsberg, "Recoveries of Valuable Metals from Spent Nickel Metal Hydride Vehicle Batteries via Sulfation, Selective Roasting, and Water Leaching," *Journal of Sustainable Metallurgy,* vol. 4, pp. 313-325, 2018.

[63] G. Xu, J. Yano and S.-I. Sakai, "Scenario analysis for recovery of rare earth elements from end-of-life vehicles," *The Journal of Material Cycles and Waste Management ,* vol. 18, pp. 469-482, 2016.

[64] Y.-J. Jiang, Y.-C. Deng and W.-G. Bu, "Pyrometallurgical Extraction of Valuable Elements in Ni-Metal Hydride Battery Electrode Materials," *Metallurgical and Materials Transactions B,* vol. 46, p. 2153–2157, 2015.

[65] Eurostat, "Contribution of recycled materials to raw materials demand- End-of-life recycling input rates (EOL-RIR)," Eurostat, [Online]. Available: https://ec.europa.eu/eurostat/tgm/table.do?tab=table&init=1&language=en&pcode=cei_srm010&plugin=1. [Accessed 20 February 2019].

[66] K. Avarmaa, H. Johto and P. Taskinen, "Distribution of Precious Metals (Ag, Au, Pd, Pt, and Rh) Between Copper Matte and Iron Silicate Slag,"

METALLURGICAL AND MATERIALS TRANSACTIONS B, vol. 47B, pp. 244-255, 2016.

[67] A. Anindya, *Minor Elements Distribution During the Smelting of WEEE with Copper Scrap,* School of Civil, Environmental & Chemical Engineering, RMIT University, 2012.

[68] X. Wan, A. Jokilaakso, I. Iduozee, E. Hürman and P. Latostenmaa, "Experimental research on the behaviour of WEEE scrap in flash smelting settler with copper concentrate and synthetic slag," in *Proceedings of EMC 2019*, 2019.

[69] M. Schlesinger, Extractive Metallurgy of Copper, Oxford: Elsevier, 2011.

[70] K. Jochum, M. Willbold, I. Raczek, B. Stoll and K. Herwig, "Chemical Characterisation of the USGS Reference Glasses GSA-1G, GSC-1G, GSD-1G, GSE-1G, BCR-2G, BHVO-2G and BIR-1G Using EPMA, ID-TIMS, ID-ICP-MS and LA-ICP-MS," *Geostandards and Geoanalytical Research,* vol. 29, pp. 285-302, 2005.

[71] S. Wilson, W. Ridley and A. Koenig, "Development of sulfide calibration standards for the laser ablation inductively-coupled plasma mass spectrometry technique," *Journal of Analytical Atomic Spectrometry,* vol. 17, pp. 406-409, 2002.

[72] E. Van Achterberg, C. Ryan, S. Jackson. and W. Griffin, "Data reduction software for LA-ICP-MS in the Earth Sciences - Principles and applications," in *Mineralogical Association of Canada short course series*, St John, Newfoundland, 2001, pp. 239-243.

[73] L. Kleemola, *Precious metals reaction mechanisms in copper matte-slag system, Master's Thesis, Aalto University, School of Chemical Engineering, Espoo,* 2019, p. 106.

[74] B. Mikoda, A. Potysz and E. Kmiecik, "Bacterial leaching of critical metal values from Polish copper metallurgical slags using Acidithiobacillus thiooxidans," *Journal of Environmental Management,* vol. 236, pp. 436-445, 2019.

Appendix I Cross sections of samples contacted in air atmosphere

10 s:

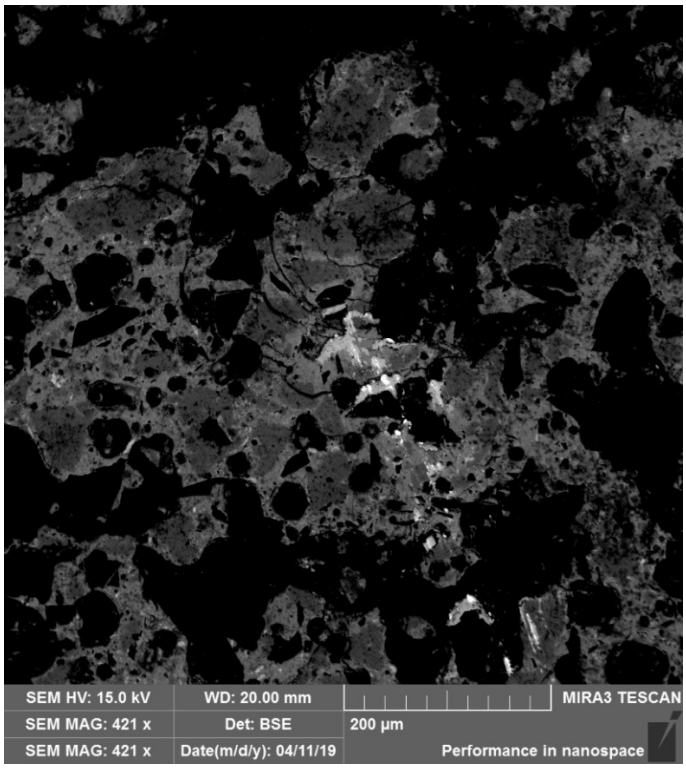

Sample 19 in air, 10 s.

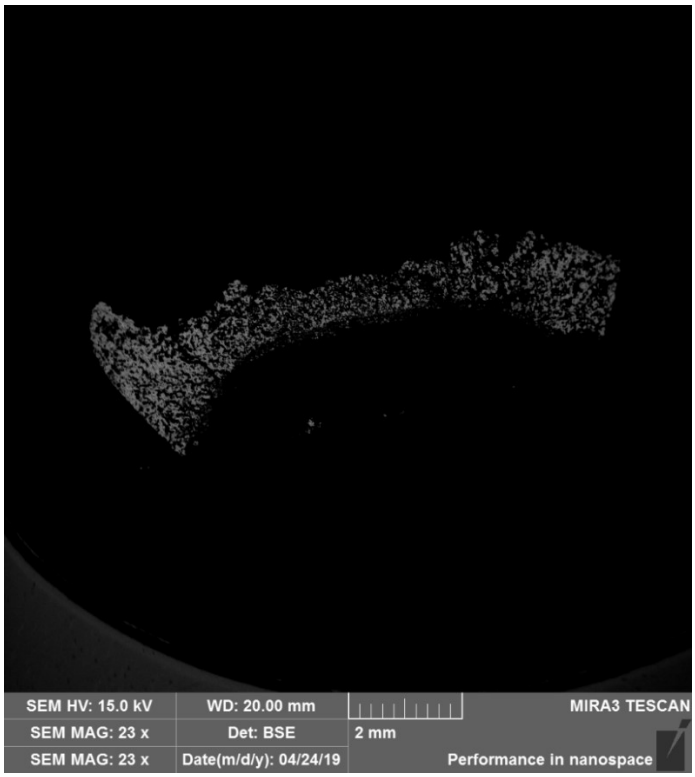

Sample 20 in air, 10 s.

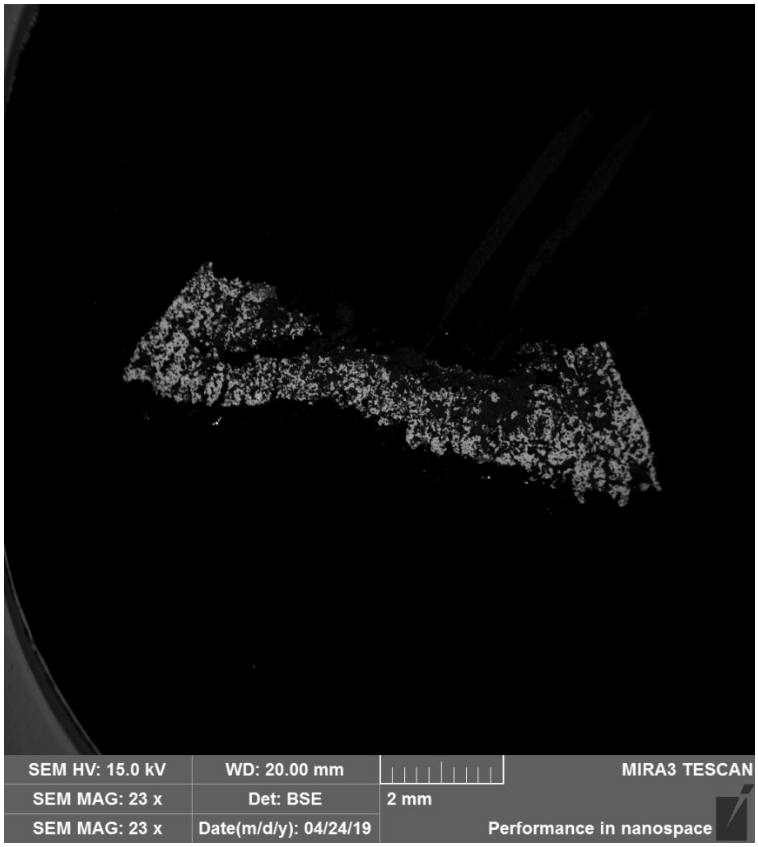

Sample 21 in air, 10 s.

20 s:

Sample 5 in air, 20 s.

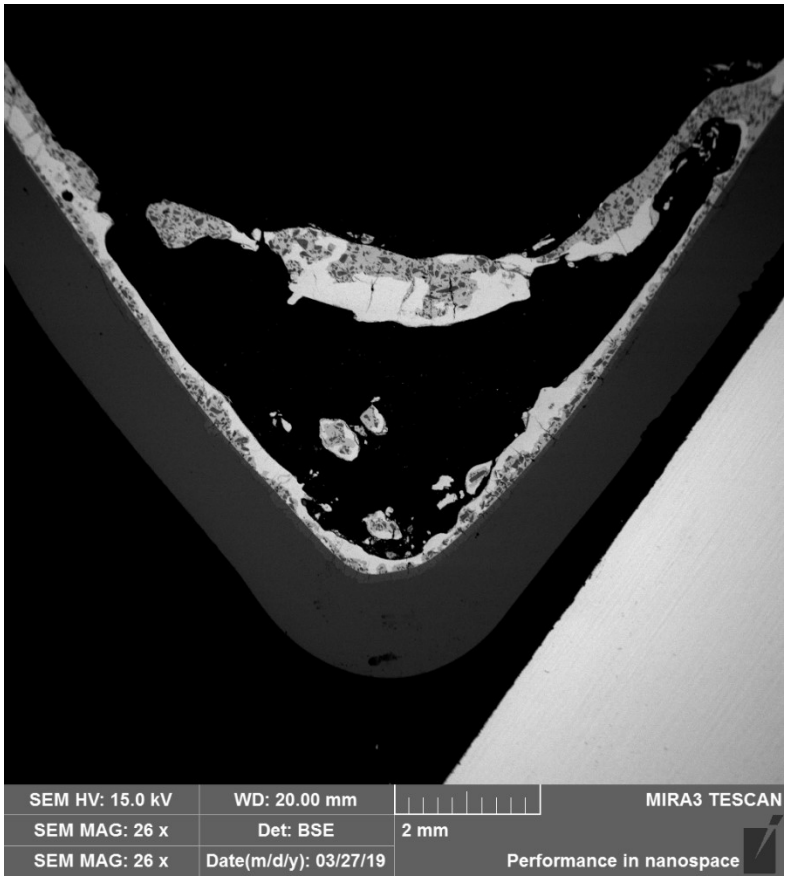

Sample 6 in air, 20 s.

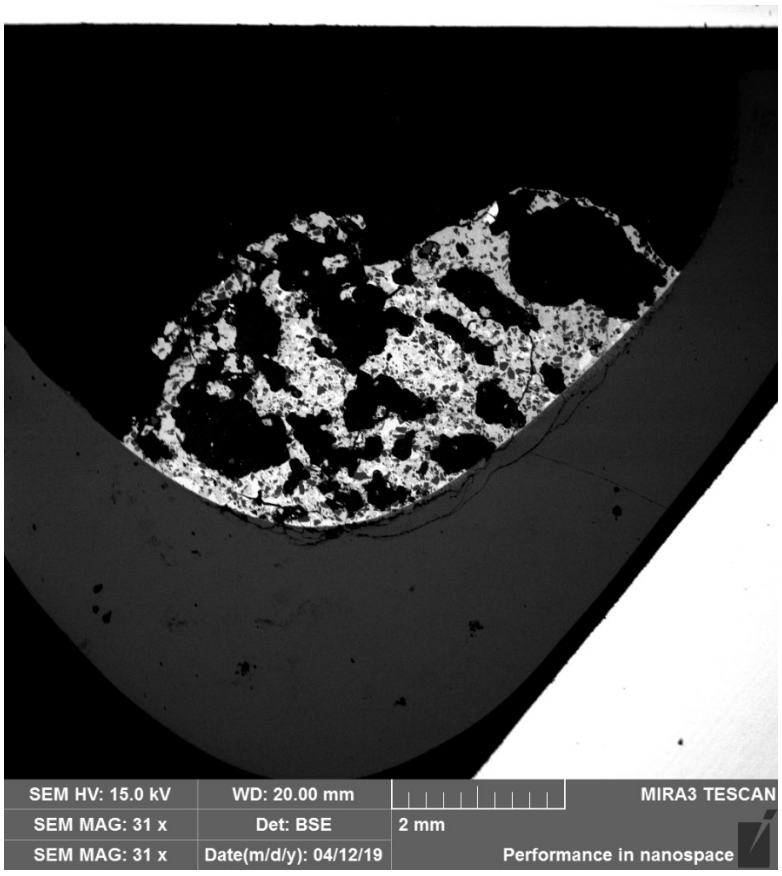

Sample 13 in air, 20 s.

30 s:

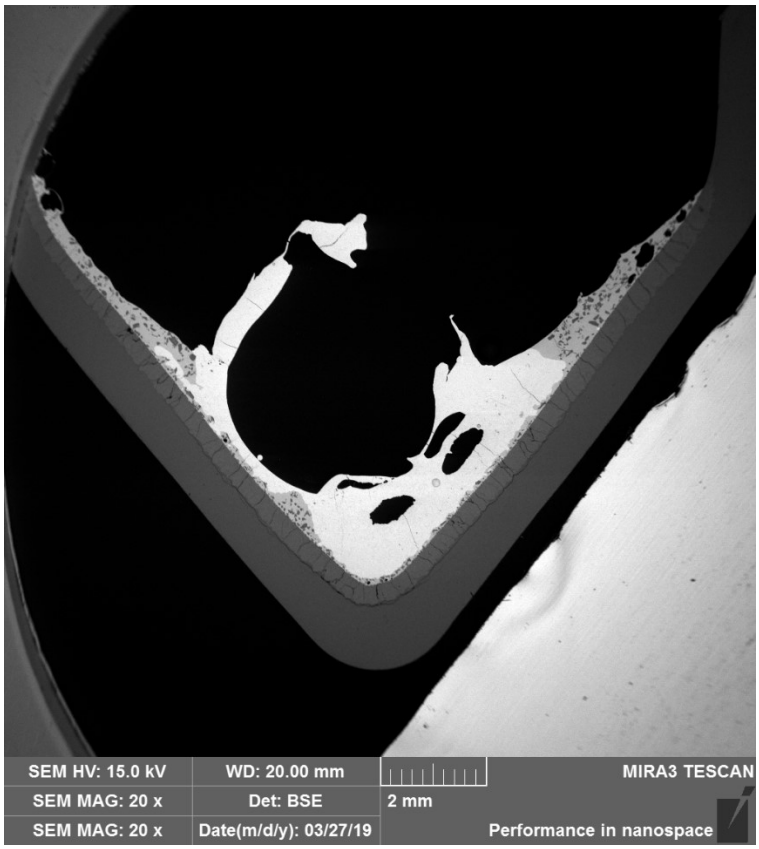

Sample 4 in air, 30 s.

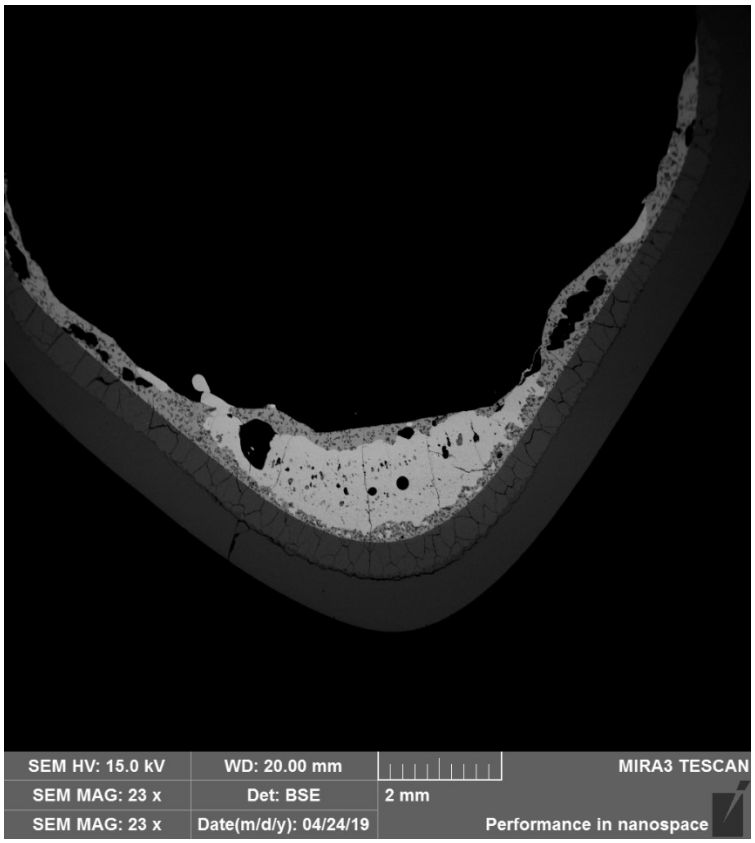

Sample 11 in air, 30 s.

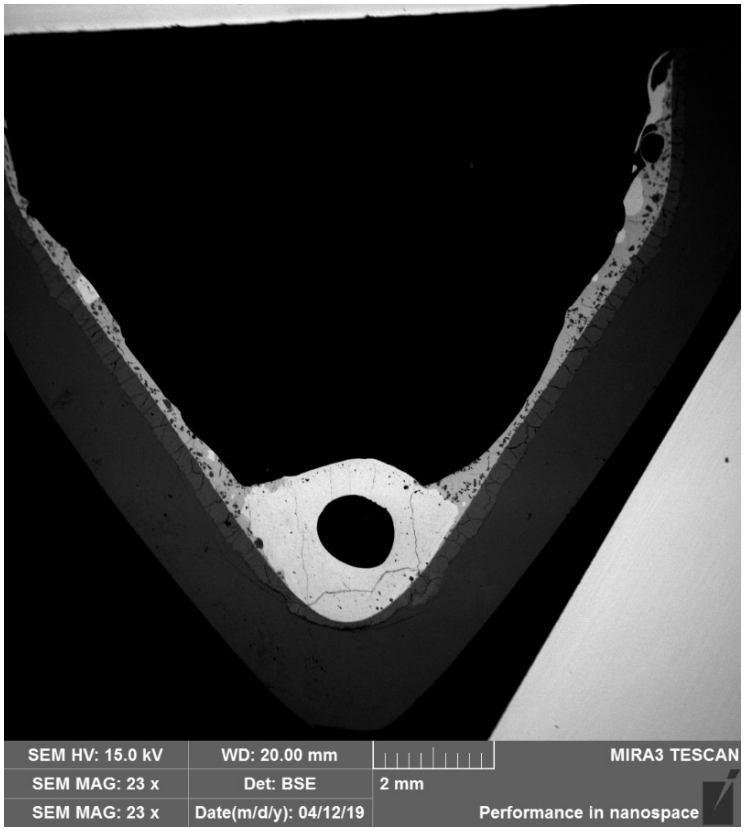

Sample 14 in air, 30 s.

60 s:

Sample 1 in air, 60 s.

Sample 2 in air, 60 s.

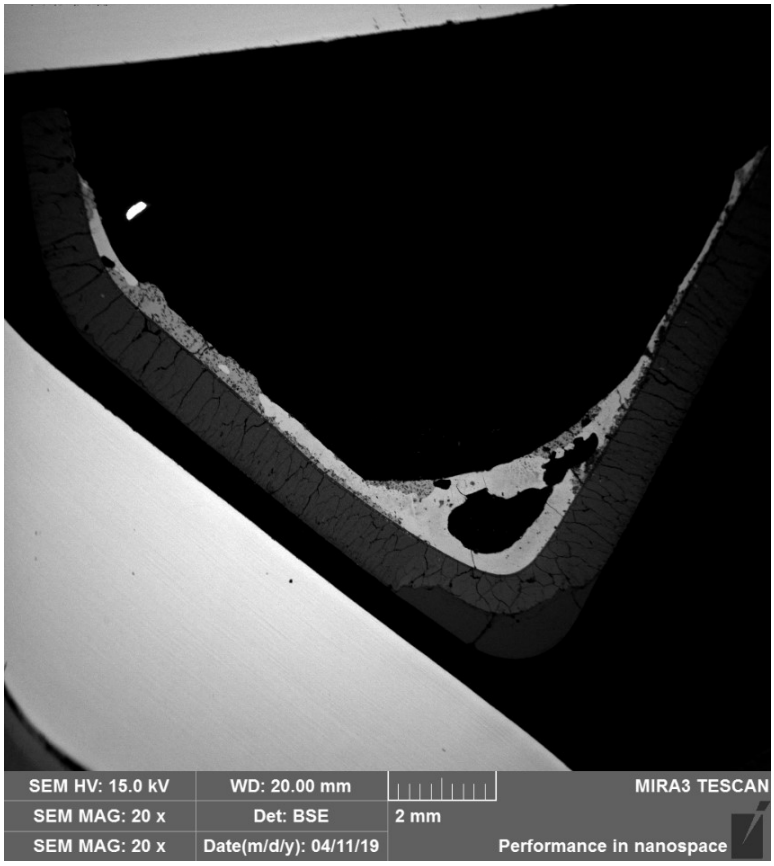

Sample 10 in air, 60 s.

150 s:

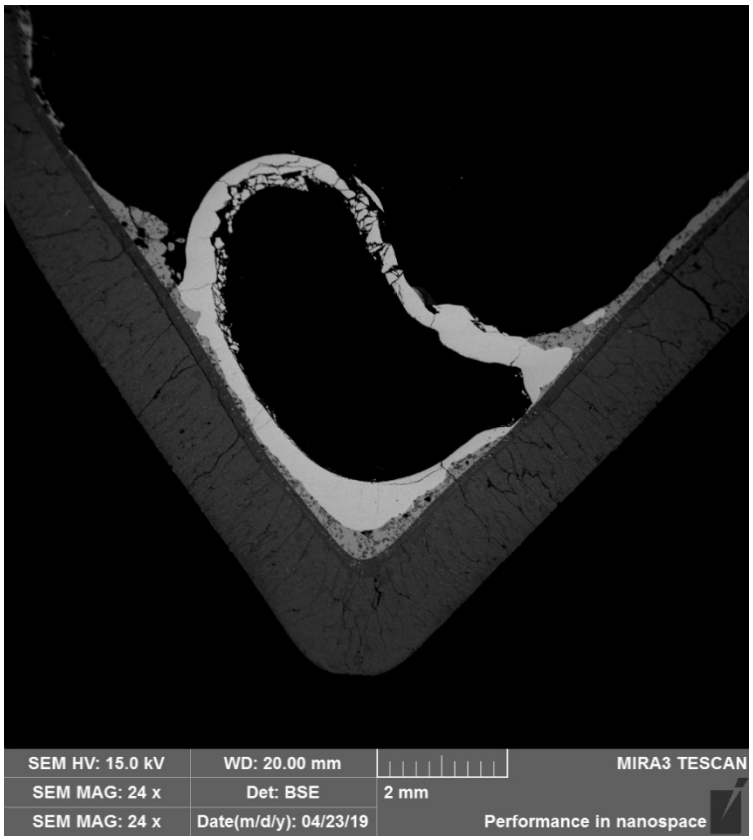

Sample 9 in air, 150s.

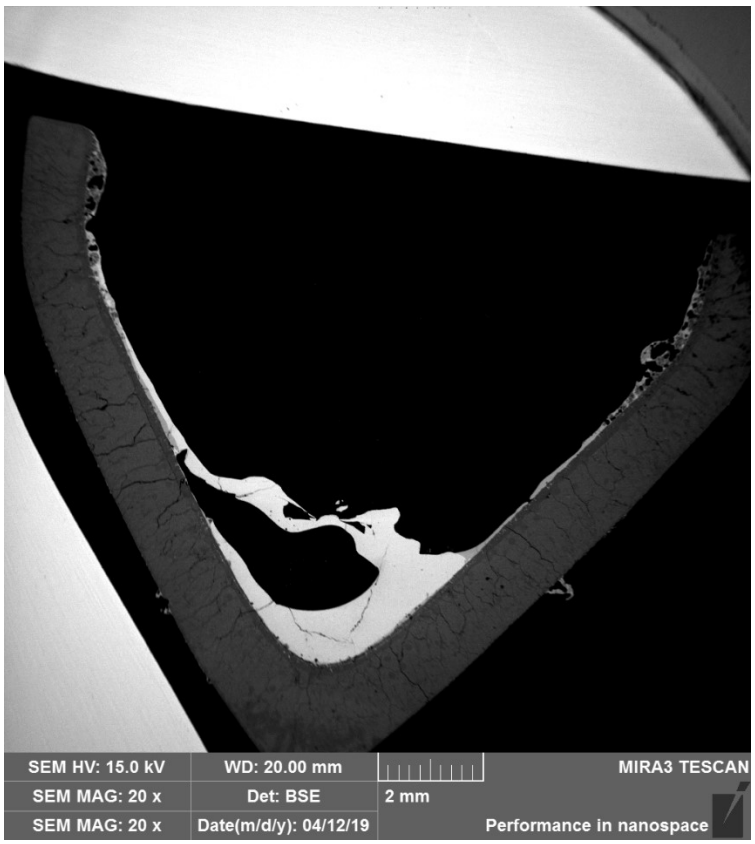

Sample 15 in air, 150 s.

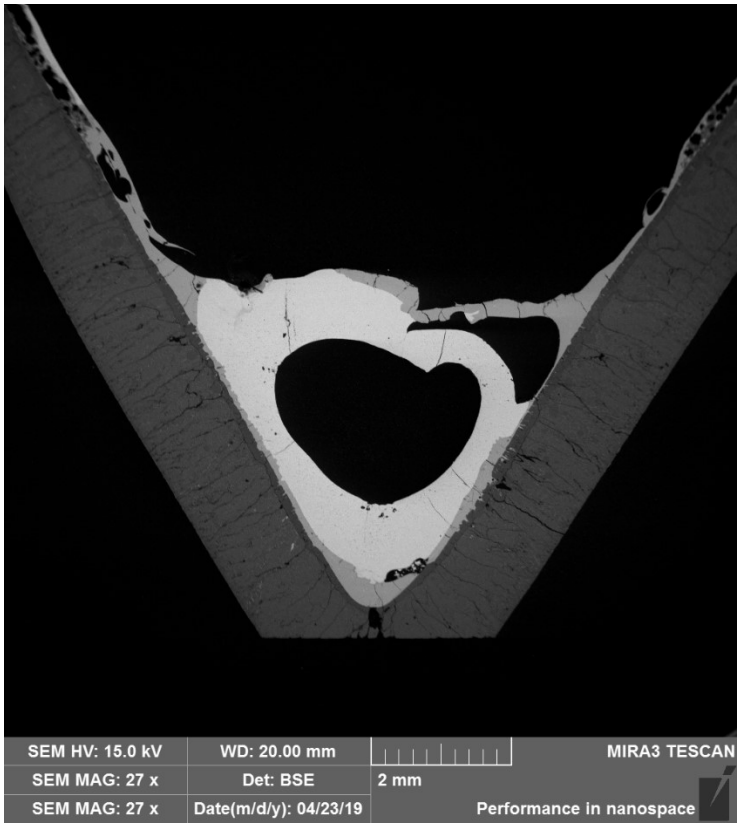

Sample 16 in air, 150 s.

300 s:

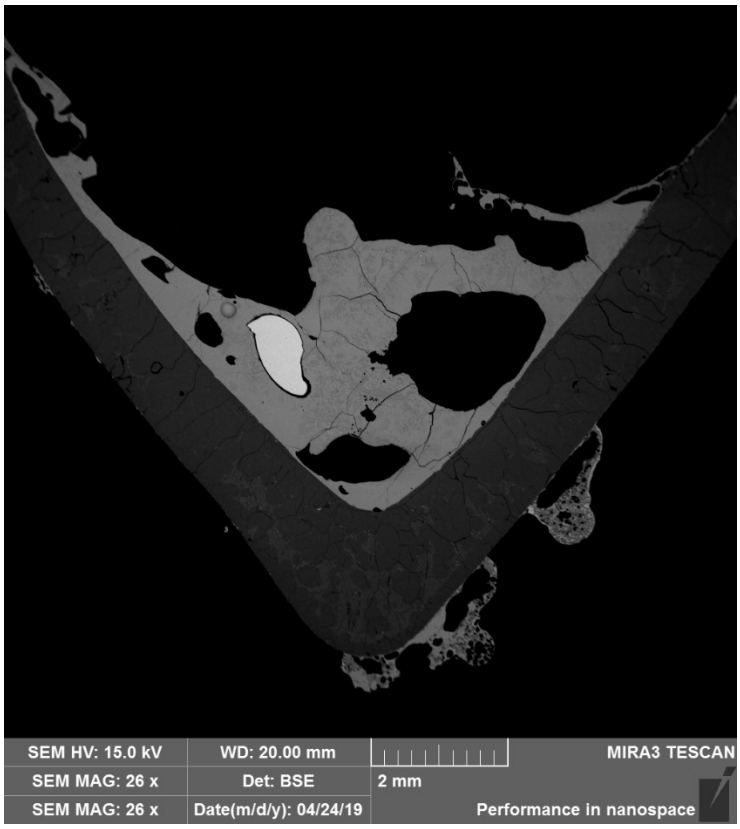

Sample 3 in air, 300 s.

Sample 8 in air, 300 s.

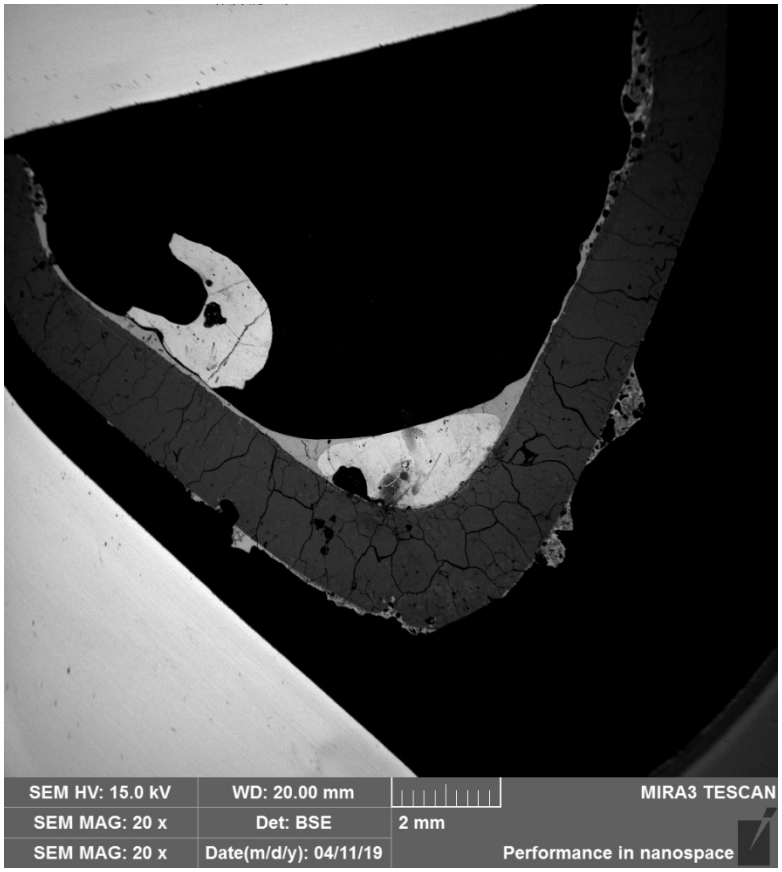

Sample 17 in air, 300 s.

Appendix II Cross sections of samples contacted in argon atmosphere

5 min:

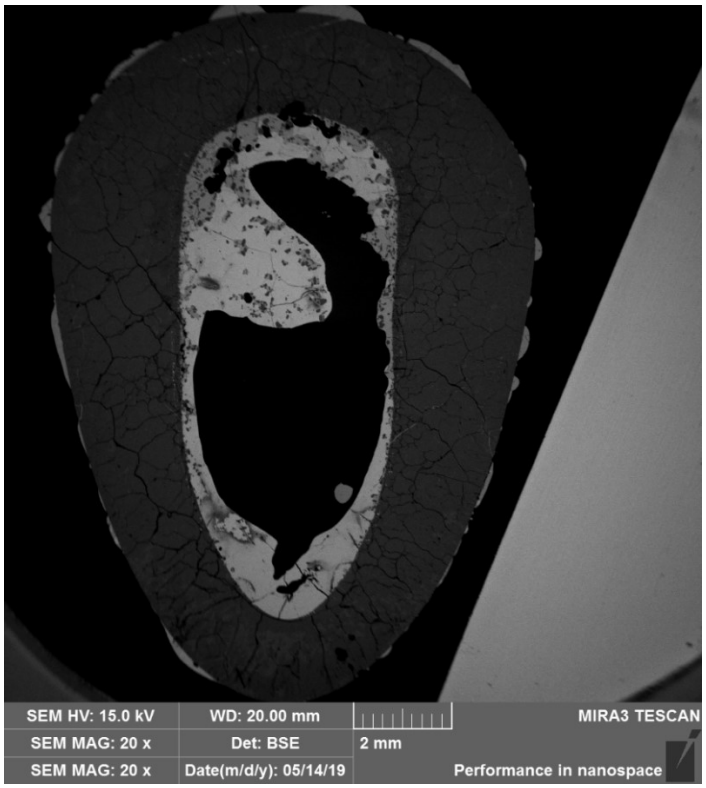

Sample 1 in Ar, 5 min.

Sample 2 in Ar, 5min.

10 min:

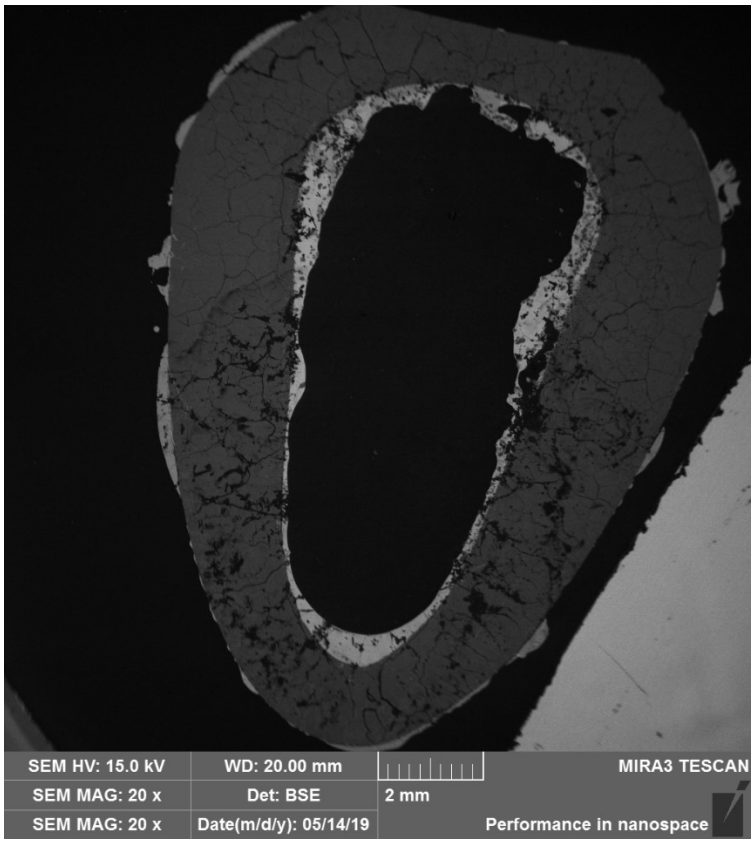

Sample 3 in Ar, 10 min.

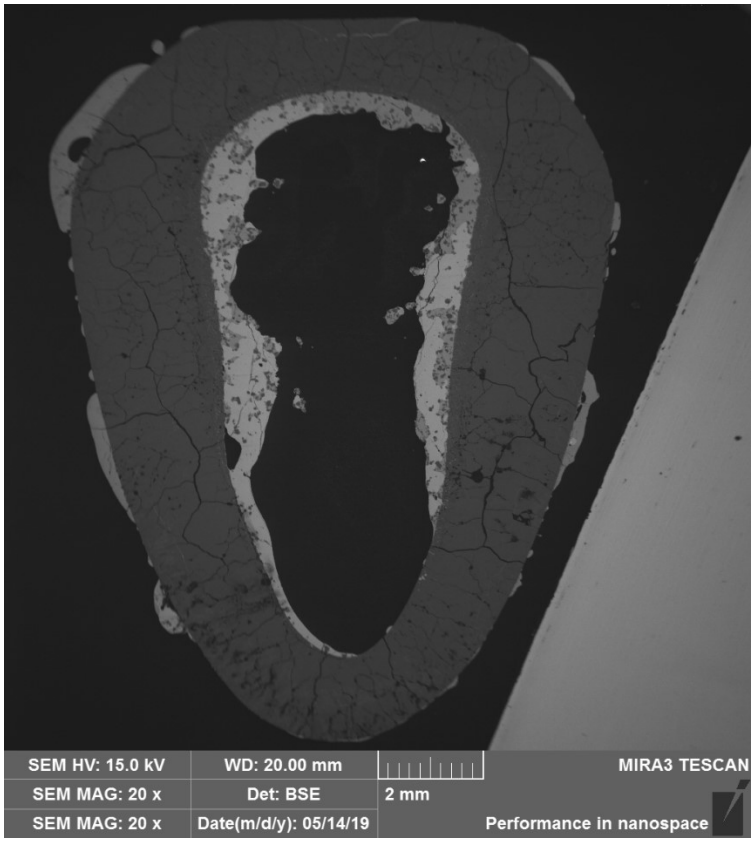

Sample 4 in Ar, 10 min.

20 min:

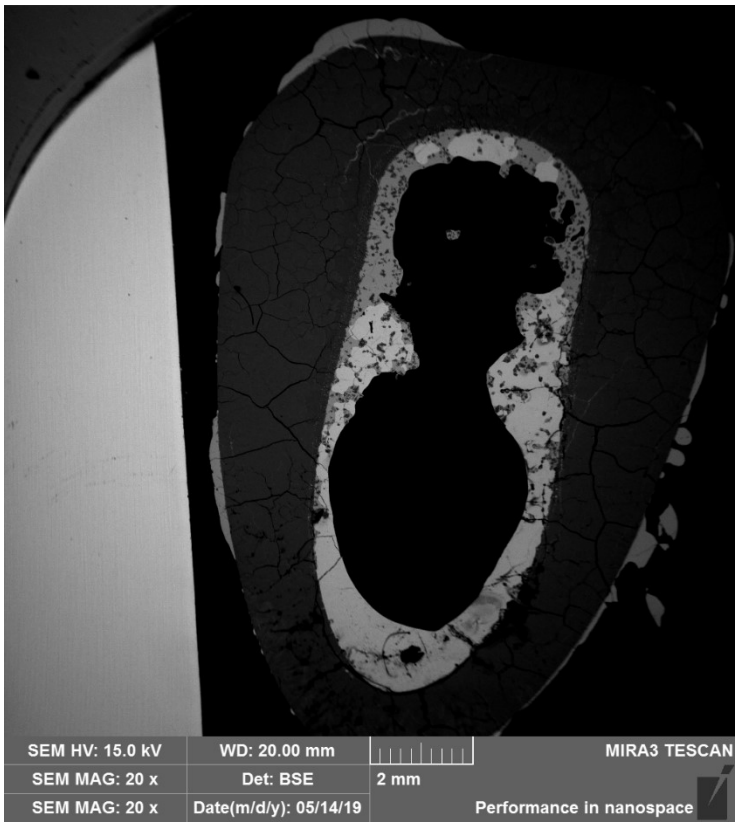

Sample 5 in Ar, 20 min.

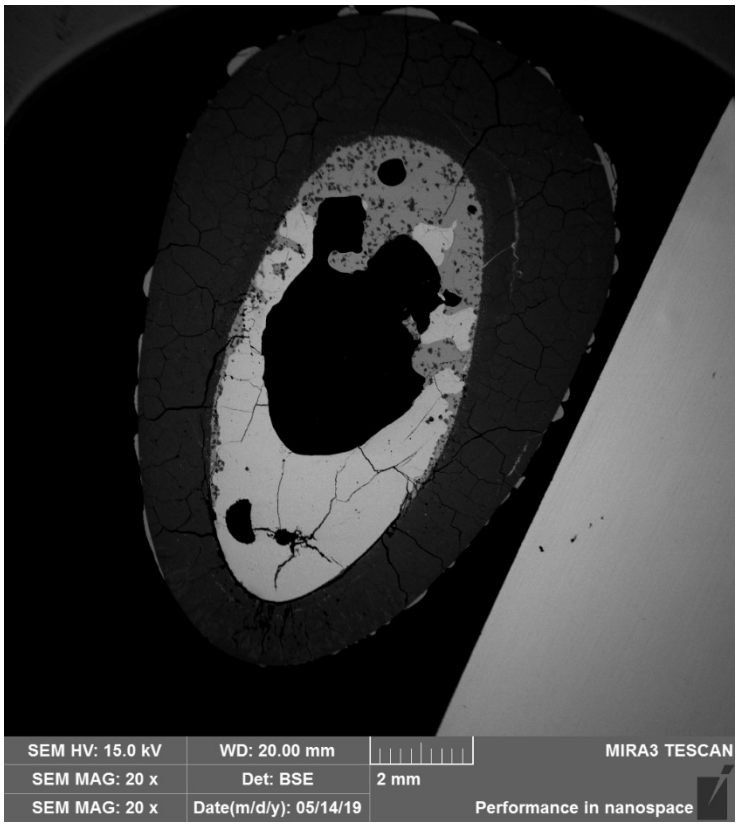

Sample 6 in Ar, 20 min.

40 min:

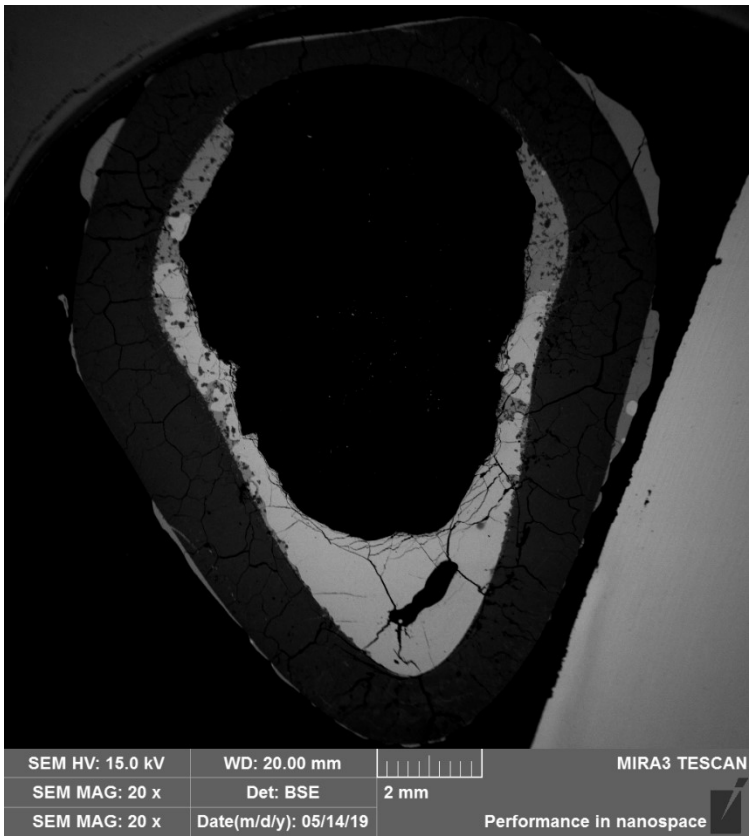

Sample 7 in Ar, 40 min.

Sample 8 in Ar, 40 min.

Appendix III LA-ICP-MS results for matte in air atmosphere

The values marked with red were not used in calculations of averages or standard deviations.

Element			**4/30s**					
Li6	<0.217	1,12	0,458	<0.199	1,19	0,8	<0.204	<0.28
Li7	0,066	<0.040	<0.040	<0.036	<0.044	<0.048	<0.037	<0.051
Mg25	9,97	10,34	10,68	12,24	12,97	17,29	12,48	9,64
Mg26	10,5	9,64	12,1	14,18	12,58	16,02	9,98	8,32
Si29	1789,2	1518,71	1909,86	1814,96	2183,21	2203,09	1793,98	1912,02
Fe57	392697,6	392697,6	392697,6	392697,6	392697,6	392697,6	392697,6	392697,6
Co59	6,38	6,32	6,29	6,75	6,03	6,01	6,1	6,15
Zn66	24824,97	23118,57	24423,09	24827,23	23963,94	23250,63	23509,18	24015,61
Zn68	20273,39	19196,72	19865,21	20385,41	19835,25	19039,35	19241,29	20373,48
La139	104,06	125,75	127,78	147,06	104,26	184,21	107,57	42.41
Nd143	99,32	118,78	122,03	144,38	100,8	188,11	104,65	42.82
Nd145	98,51	116,51	124,27	138,64	102,4	185,31	101,89	42.48
Nd146	99,36	123,75	122,52	143,17	104,24	190,43	103,08	44.05
Pb208	1107,76	1091,34	923,16	1119,84	783,82	1139,78	965,31	960,32
Element			**5/20s**					
Li6	<0.242	0,42	<0.31	0,57	<0.216	<0.216	<0.28	<0.241
Li7	<0.050	0,064	<0.051	<0.046	0,155	<0.044	<0.051	<0.051
Mg25	25,45	10,62	4,48	15,48	12,64	14,11	12,96	13,22
Mg26	26,81	9,64	5,53	15,26	12,48	12,37	10,73	12,43
Si29	2302,35	1557,74	1330,71	1834,76	1717,95	1727,81	1530,95	1672,93
Fe57	404590,4	404590,4	404590,4	404590,4	404590,4	404590,4	404590,4	404590,4
Co59	6,42	6,28	6,3	6,33	6,39	6,29	6,59	6,5
Zn66	28149,26	28745,29	27517,21	26433,26	26681,3	26227,06	28076,38	26201,83
Zn68	22868,75	23837,37	22942,44	22077,54	21547,6	21924,25	23125,16	21507,96
La139	327,54	141,18	72.84	189,42	160,28	167,52	181,69	198,17
Nd143	328,6	132,56	71.39	180,18	155,2	158	172,93	183,81
Nd145	319,02	132,63	70.59	177,22	150,67	159,69	170,49	183,66
Nd146	331,25	133,87	69.53	180,11	153,41	159,89	174,29	184,66
Pb208	1163,82	1266,17	917,37	1131,96	1117,35	1031,05	1269,87	1131,19
Element			**1/60s**					
Li6	0,74	<0.239	<0.35	0,64	<0.237	<0.227	<0.34	<0.30
Li7	<0.054	0,168	<0.062	<0.054	<0.049	0,051	0,095	<0.043
Mg25	11,04	12,59	11,44	9,21	10,26	13,04	11,85	12,41
Mg26	9,83	12,33	11,45	8,72	11,03	12,36	11,35	12,38
Si29	2232,56	2089,54	2290,48	2034,75	2143,9	2276,82	2137,39	2078,63
Fe57	393086,2	393086,2	393086,1	393086,2	393086,2	393086,1	393086,2	393086,2
Co59	6,58	6,74	6,89	6,62	6,7	6,62	6,81	6,71
Zn66	21604,65	21001,84	23280,98	20911,15	22014,18	20116,98	22272,78	20403,37
Zn68	17908,93	18082,25	19614,5	17635,86	18889,52	17040,36	18510,77	16845,55
La139	108,42	115,42	117,47	91,59	95,35	111,86	91,1	100,94
Nd143	107,24	112,05	112,02	89,71	92,35	110,01	91,63	93,49

Nd145	106,8	111,59	113,88	89,48	92,67	108,22	91,29	95,4		
Nd146	108,17	113,66	113,76	89,5	96,26	109,98	92,34	99,49		
Pb208	983,55	978,27	972,16	898,35	990,11	944,22	938,38	1024,02		
Element			**9/150s**							
Li6	0,39	<0.36	1,04	0,58	0,63	<0.32	<0.37	<0.33	<0.33	<0.34
Li7	0,097	<0.068	<0.066	<0.064	<0.065	<0.059	0,284	<0.066	0,072	0,086
Mg25	4,19	4,73	3,72	2,4	3,9	6,99	6,81	4,83	5	7,37
Mg26	4,06	4,83	3,82	3,36	5,22	7,2	7,05	5,81	4,11	7,87
Si29	1340,58	1382,64	1225,39	1037,41	1384,84	1425,31	1691,11	1373,98	1361,27	1723,06
Fe57	330901,2	330901,2	330901,2	330901,2	330901,2	330901,3	330901,3	330901,2	330901,2	330901,2
Co59	7,58	7,46	7,56	7,76	6,95	7,42	7,3	7,48	7,17	7,22
Zn66	17877,4	18022,56	17851,63	17343,12	17156,38	17428,91	18591,34	18590,09	17771,14	17651,89
Zn68	13732,34	13961,38	13811,5	13652,15	13144,66	13864,85	14297,4	14064,11	13731,13	13909
La139	49,59	70,24	49,86	46,29	42,86	84,85	79,81	55,99	55,04	82,46
Nd143	49,13	68,07	47,7	42,06	41,09	77,49	73,85	52,32	51,25	78
Nd145	48,44	68,81	48,41	43,72	39,64	77,94	73,75	51,22	52,6	79,18
Nd146	48,58	70,19	48,83	42,87	41,47	77,78	74,09	52,05	52,23	77,54
Pb208	629,59	693,11	645,56	829,98	632,92	728,28	593,44	586,05	584,82	639,62
Element			**6/20s**							
Li6	<0.31	<0.27	<0.56	<0.38	0,62	0,98	<0.37	0,54		
Li7	<0.062	0,146	<0.106	<0.076	<0.074	<0.065	0,264	<0.081		
Mg25	12,37	18,69	8,68	8,86	12,96	11,35	12,27	12,74		
Mg26	11,73	19,69	11,95	8,96	12,92	10,4	11,6	13,08		
Si29	1883,54	1908,55	1563,15	1674,35	1645,16	1819,91	1765,24	2074,49		
Fe57	404590,3	404590,3	404590,3	404590,3	404590,3	404590,3	404590,3	404590,3		
Co59	6,81	7,05	6,75	7,03	6,65	6,48	6,67	6,26		
Zn66	29565,7	31316,62	32729,95	30515,71	28587,23	29056,25	30442,37	29464,07		
Zn68	22541,04	24760,24	25915,59	23800,31	22240,87	22628,79	23485,75	23020,36		
La139	178	266.76	178,76	140,69	208,02	153,66	178,7	164,64		
Nd143	166,36	261.52	172,15	133,99	198,37	145,46	177,75	158,38		
Nd145	169,56	265.49	170,52	133,58	195,88	143,01	175,24	159,77		
Nd146	166,27	266.58	172,92	134,85	195,89	144,66	177,96	159,47		
Pb208	1218,96	1211,03	1257,82	1158,04	1190,84	1162,41	767,86	1083,67		
Element			**8/300s**							
Li6	<0.33	0,4	<0.33	0,74	<0.34	<0.36	0,87	<0.37	<0.33	
Li7	<0.067	<0.068	0,184	<0.067	<0.064	0,274	<0.078	<0.068	<0.068	
Mg25	4,35	4,87	4,37	6,07	4,99	4,49	3,26	3,82	4,2	
Mg26	3,66	5,35	4,3	6,39	3,51	4,76	3,29	5,08	3,3	
Si29	1276,15	1281,35	1347,9	1332,26	1248,13	1185,29	1234,49	1218,71	1248,28	
Fe57	311546,3	311546,3	311546,3	311546,3	311546,3	311546,3	311546,3	311546,3	311546,3	
Co59	7,68	7,41	7,62	7,48	7,77	7,59	7,7	7,69	7,52	
Zn66	15259,25	14870,98	15792,48	15179,72	15967,26	15364,02	16035,55	15078,32	15045,39	
Zn68	11832,29	11969,13	12365,35	11775,99	12570,77	12138,94	12724,6	11944,03	12086,69	
La139	43,02	51,56	45,34	61,07	46,13	42,58	34,26	41,69	39,47	
Nd143	42,51	48,74	45,47	58,59	44,14	41,23	33,43	40,6	38,78	
Nd145	41,99	48,08	44,27	57,89	44,65	41,9	33,84	41,29	37,24	

Nd146	42,05	49,59	44,3	57,83	44,36	42,45	32,96	41,39	38,42
Pb208	508,23	488,2	368,41	494,49	460,81	489,24	463,06	486,45	484,32
Element			**11/30s**						
Li6	<0.35	<0.35	<0.53	<0.46	0,92	<0.38	<0.33	<0.40	<0.39
Li7	<0.070	<0.065	<0.107	<0.091	<0.083	<0.075	0,071	<0.073	<0.076
Mg25	14,76	13,3	11,11	8,85	8,37	11,61	11,59	8,49	9,88
Mg26	15,08	13,98	9,45	5,67	7,21	13,33	10,82	10,75	10,33
Si29	2382,44	2114,15	2022,02	1527,22	1898,5	2427,54	2018,68	2121,26	1900,6
Fe57	393863,4	393863,4	393863,5	393863,5	393863,5	393863,5	393863,5	393863,5	393863,5
Co59	6,5	6,78	6,32	6,52	6,07	6,66	6,67	6,79	6,51
Zn66	26253,06	25039,73	26005,59	27647,57	28413,79	27096,48	27464,03	26576,89	26580,8
Zn68	20700,57	19481,24	20351,14	21136,03	21599,5	21154,69	21923,03	21832,49	21641,66
La139	183,04	162,74	144,76	126,66	110,79	126,01	117,83	102,35	108,23
Nd143	175,52	156,66	145,12	120,98	106,86	118,85	114,96	98,05	103,06
Nd145	174,18	156,73	141,6	117,43	106,03	119,28	114,57	98,32	102,4
Nd146	176,04	154,73	143,83	115,26	102,02	120,88	113,35	102,48	102,73
Pb208	1209,27	947,7	1259,73	1274,41	1052,64	1064,44	1125,57	1124,02	1211,15
Element			**2/60s**						
Li6	<0.32	1,08	<0.32	<0.28	0,36	<0.30	<0.31	<0.30	<0.29
Li7	<0.065	<0.063	0,091	<0.056	<0.071	<0.061	<0.064	<0.062	<0.058
Mg25	9,88	10,97	10,3	11,87	13,73	13,78	12,33	9,85	11,51
Mg26	11,07	10,55	11,09	13,24	13,54	14,71	14,73	10,87	13,05
Si29	2232,8	2168,32	2303,28	2330,65	2573,31	2333,55	2519	2346,37	2347,5
Fe57	397516,9	397516,9	397516,9	397516,9	397516,9	397516,9	397516,9	397516,9	397516,9
Co59	6,73	6,77	6,84	6,51	6,64	6,4	6,51	6,72	6,83
Zn66	22886,36	21757,37	23715,4	20165,82	23225,15	22868,26	22735,22	23931,31	23010,48
Zn68	18487,77	17547,08	18758,85	16053,54	18512,2	18404,02	18022,89	19167,42	18428,07
La139	104,98	99,99	105,9	135,31	133,15	134,42	134,13	100,97	114,91
Nd143	103,95	100,3	103,01	133,91	131,98	130,37	132,71	98,29	114,29
Nd145	103,05	98,51	102,58	133,62	129,8	127,94	131,96	99,6	112,78
Nd146	105,17	100,41	103,81	134,08	133,21	129,49	132,71	98,85	115,59
Pb208	965,77	878,18	928,79	1073,03	966,57	986,56	860,58	859,15	913,96
Element			**16/150s**						
Li6	<0.40	<0.30	0,7	<0.33	1,03	2,2	<0.39	<0.20	<0.30
Li7	<0.074	<0.063	<0.059	<0.067	<0.067	<0.067	<0.078	<0.039	<0.057
Mg25	1,47	<0.181	2,13	1,44	2,45	0,882	2,31	0,714	0,947
Mg26	0,48	0,48	3,37	0,75	2,29	0,6	<0.47	1,81	1,61
Si29	1111,94	823,25	1286,7	1188,84	1472,06	812,33	1028,03	1292,95	953,61
Fe57	354997,9	354997,9	354997,9	354997,9	354997,9	354997,9	354997,9	354997,9	354997,9
Co59	19,16	20,14	19,65	19,31	18,41	20,66	19,82	18,81	20,06
Zn66	19676,82	17477,12	18342,97	19610,18	18075,79	17781,92	19180,17	19559,98	19698,77
Zn68	16072,29	14103,22	14781,94	15896,29	14321,14	14381,34	15457,38	15025,01	16020,37
La139	10,91	11,57	29,04	6,36	14,46	14,52	29,65	4,19	9,6
Nd143	11,27	10,8	27,91	7,4	14,81	12,46	25,79	6,66	9,68
Nd145	11,89	11,16	28,68	7,13	15,43	12,61	26,75	6,05	9,63
Nd146	11,54	11,31	28,41	7,42	14,55	12,47	27,29	5,9	10,1

Pb208	954,72	1350,28	839,33	815,27	522,38	1163,12	968,73	876,78	867,85
Element			**17/300s**						
Li6	<0.31	0,56	<0.26	0,45	<0.256	<0.27	<0.29	<0.32	<0.33
Li7	<0.061	0,091	<0.051	0,093	0,052	<0.051	<0.055	<0.061	<0.060
Mg25	1,6	2,21	2,38	1,013	2,08	1,92	2,59	1,86	1,23
Mg26	1,19	2,86	2,01	1,54	2,74	2,64	2,85	2,73	1,91
Si29	1986,65	2002,67	2073,48	1591,09	1934,56	1973,17	2103,53	1898,91	1755,43
Fe57	368911,8	368911,8	368911,8	368911,8	368911,8	368911,8	368911,8	368911,8	368911,8
Co59	19,92	19,47	19,85	19,7	19,68	19,13	19,22	19,11	19,81
Zn66	16093,54	16318,85	15517,08	16211,55	15268,56	16394,93	15996,09	16360,69	17418,01
Zn68	12502,31	13230,17	12297,2	12886,46	12130,57	13147,91	12632,54	12878,12	13457,79
La139	20,88	21,54	21,98	12,21	18,03	19,09	23,04	17,41	13,55
Nd143	22,1	21,16	22,36	12,5	18,07	19,04	23,71	17,28	14,09
Nd145	22,5	21,39	21,95	12,74	18,03	19,37	22,57	17,77	14,17
Nd146	21,68	20,93	21,72	12,13	18,25	18,67	22,88	17,16	13,8
Pb208	454,87	511	426,23	490	462,13	446,08	441,28	445,42	477,93

Appendix IV LA-ICP-MS results for matte in argon atmosphere

The values marked with red were not used in calculations of averages or standard deviations.

Element	**Ar1B**		**5 min**					
Mg25	7,04	7,03	6,87	7,87	7,65	6,59	6,34	6,55
Mg26	6,29	6,95	6,64	8,7	7,84	6,57	5,56	8,33
Si29	1841,12	1829,29	1710,77	1848,3	1863,13	1790,33	1812,43	1877,88
Fe57	413762,8	413762,8	413762,8	413762,8	413762,8	413762,8	413762,8	413762,8
Co59	35,78	35,65	35,45	36,11	36,46	35,07	36,19	36,27
Zn66	11355,97	10588,1	9679,54	10475,77	10052,89	10172,36	9872,43	10780,86
Zn68	9010,76	8299,92	7346,36	7802,13	7748,94	7861,9	7846,12	8279,9
La139	73,35	73,07	72,18	72,74	73,9	74,09	71,5	74,41
Nd143	73,68	72,85	71,33	70,44	72,19	72,79	69,28	72,94
Nd145	72,62	72,87	69,93	69,34	71,54	72,04	69,5	71,91
Nd146	73,29	74,49	70,91	72,82	71,91	72,18	69,1	72,75
Pb208	363,21	339,75	287,49	307,09	300,28	295,71	303,13	321,58
Element	**Ar2**		**5 min**					
Mg25	7,89	8,04	8,19	8,98	8,19	8,38	8,47	9,42
Mg26	9,1	7,96	8,55	8,45	7,94	9,32	8,81	9,93
Si29	1812,15	1776,55	1756,2	1762,68	1728	1743,07	1657,89	1678,3
Fe57	413762,6	413762,6	413762,6	413762,6	413762,6	413762,6	413762,6	413762,6
Co59	36,8	35,83	37,07	36,66	35,45	36,66	36,12	36,79
Zn66	8766,13	8687,61	8630,13	8740,13	8288,74	8376,66	7889,81	7807,37
Zn68	6384,24	6272,66	6304,9	6725,02	6312,01	6316,39	5946,35	5779,07
La139	74,39	73,83	78,69	71,77	76,66	81,21	75,13	80,06
Nd143	74,13	75,13	78,39	70,03	74,93	78,93	73,93	78,47
Nd145	72,73	73,13	76,53	69,98	74,4	79,46	73,27	77,98
Nd146	73,63	75,74	77,68	71,56	75,4	77,62	74,95	74,88
Pb208	234,23	226,58	218,37	239,09	238,38	219,07	197,28	197,46
Element	**Ar3B**		**10 min**					
Mg25	5,73	6,79	6,16	5,95	6,37			
Mg26	6,64	6,35	7,5	6,75	7,34			
Si29	1481,12	1496,5	1543,38	1483,22	1571,5			
Fe57	409098,9	409098,9	409098,9	409098,9	409098,9			
Co59	35,02	34,35	32,98	33,3	33,96			
Zn66	1038,21	1032,35	1001,55	1027,02	1023,87			
Zn68	807,91	785,26	781,96	789,84	803,6			
La139	66,81	68,78	65,16	66,18	69,3			
Nd143	67,13	66,84	64	66,56	66,46			
Nd145	67,14	67,43	66,8	66,69	68,34			
Nd146	66,31	67,27	65,13	64,24	67,92			
Pb208	38,32	36,14	39,97	35,76	34,03			
Element	**Ar4A**		**10 min**					
Mg25	18,24	18,24	17,25	20,95	16,45	17,32	18,54	21,84

Mg26	23,37	26,39	23,53	23,92	22,15	22,13	24,51	29,63
Si29	1597,76	1510,94	1601,42	1778,35	1712,03	1756,49	1712,56	1802,44
Fe57	416716,4	416716,4	416716,4	416716,4	416716,4	416716,4	416716,4	416716,4
Co59	36,98	36,66	36,42	37,36	34,63	37,22	35,47	36,66
Zn66	1686,88	1671,34	1610,53	1651,04	1373,73	1472,41	1324,44	1574,03
Zn68	1317,44	1329,65	1298,49	1314,93	1080,78	1149,86	1054,1	1273,95
La139	77,03	75,67	75,99	81,12	62,99	61,27	70,28	75,4
Nd143	77,05	74,52	76,26	81,21	62,4	61,17	68,16	73,42
Nd145	75,38	76,7	75,96	81,83	62,57	60,14	68,75	74,24
Nd146	76,77	75,76	75,1	81,57	64,09	62,74	70,53	74,98
Pb208	36,1	37,31	35,1	37,89	30,81	30,75	30,18	33,35
Element	**Ar5B**		**20 min**					
Mg25	5,46	5,88	4,88	5,24	5,89	5,28	6,17	5,76
Mg26	9,31	7,22	5,21	4,99	7,13	6,42	5,96	6,17
Si29	1427,3	1441,89	1390,42	1394,68	1472,67	1461,58	1419,14	1436,64
Fe57	410575,8	410575,8	410575,8	410575,8	410575,8	410575,8	410575,8	410575,8
Co59	51,46	52,68	50,49	50,57	49,53	48,07	49,01	50,2
Zn66	213,28	219,07	219,02	200,32	194,1	176,58	175,32	175,7
Zn68	159,89	161,42	165,23	155,56	148,22	132,71	132,9	133,97
La139	57,57	62,97	58,49	58,44	65,77	67,12	62,74	66,29
Nd143	57,78	63,02	57,04	57,23	64,15	65,48	60,84	65,67
Nd145	57,98	63,9	57,36	58,12	64,41	66,11	61,59	66,26
Nd146	58,36	63,72	58,46	58,8	65,67	66,56	61,8	65,85
Pb208	12,87	12,45	12,25	12,3	11,26	10,45	10,57	9,98
Element	**Ar6B**		**20min**					
Mg25	5,9	5,72	6,37	5,74	6,22	7,26	4,43	5,13
Mg26	4,55	5,38	5,87	5,72	7,07	6,51	5,57	5,81
Si29	1585,37	1616,35	1672,03	1489,5	1559,97	1545,81	1425,63	1518,29
Fe57	413684,8	413684,8	413684,8	413684,8	413684,8	413684,9	413684,8	413684,8
Co59	36,5	36,88	36,62	37	35,1	36,79	36,45	34,72
Zn66	467,69	485,37	494,58	424,96	399,21	300,7	289,01	310,87
Zn68	353,25	371,39	386,77	319,18	307,71	232,18	213,45	233,5
La139	63,13	65,15	65,53	56,46	64,96	65,91	56,71	57,46
Nd143	64,14	64,39	63,43	54,66	64,71	64,96	56,72	56,98
Nd145	62,55	64,67	63,52	53,09	64,42	65,06	56,02	54,84
Nd146	62,85	64,84	65,69	56,49	64,85	68,03	57,5	56,61
Pb208	19,8	17,14	18,38	18,81	16,75	12,24	10,68	13,21
Element	**Ar7A**		**40 min**					
Mg25	3,32	5,6	4,99	6,8	7,01	6,9	7,22	7,08
Mg26	3,76	6,12	6,22	7,71	7,68	7,97	8,23	8,31
Si29	1170,58	1387,62	1413,38	1431,4	1492,32	1509,5	1558,02	1430,99
Fe57	426976,9	426976,9	426976,9	426976,9	426976,9	426976,9	426976,9	426976,9
Co59	35,14	36,23	34,76	36,91	36,57	36,17	35,81	36,82
Zn66	16,98	18,88	17,32	17,63	17,52	18,36	17,33	19,39
Zn68	12,64	13,8	13,09	14,21	13,26	13,16	13,28	13,95
La139	29,32	58,15	42,18	57,91	57,55	55,1	54,7	50,22

Nd143	30,1	58,09	42,86	56,06	58,04	54,94	54,48	50,73
Nd145	28,93	58,24	42,7	57,51	56,33	54,21	55,21	50,41
Nd146	29,36	58,52	43,94	56,72	56,04	53,32	53,2	50,97
Pb208	0,737	0,723	0,802	0,693	0,699	0,677	0,737	0,811
Element	**Ar8B**		**40 min**					
Mg25	9,54	8,5	9,03	7,42	8,91	9,67	10,4	9,56
Mg26	10,24	9,21	9,96	10,32	9,16	11,74	12,86	11,34
Si29	1371,28	1271,27	1249,57	1223,85	1347,66	1325,07	1390,07	1342,42
Fe57	405834,1	405834,1	405834,1	405834,1	405834,1	405834,1	405834,1	405834
Co59	37,28	36,68	35,37	35,06	35,2	35,93	34,69	35,43
Zn66	20,88	20,55	20,41	21,44	21,54	20,8	21,69	23,38
Zn68	15,22	15,69	14,64	16,61	15,64	15,88	17,51	17,03
La139	60,08	64,21	48,46	60,19	58,93	60,37	65,54	66,54
Nd143	59,93	60,7	48,33	57,95	57,87	58,74	63,61	64,77
Nd145	61,52	61,12	47,49	59,34	59,04	57,89	64,16	66,64
Nd146	60,03	60,35	48,1	57,62	58,73	57,63	64,06	65,18
Pb208	0,645	0,614	0,598	0,627	0,709	0,643	0,67	0,654

Appendix V EPMA results for slag in air atmosphere

Norm Weight%

Sample / Comment	O	Si	Mg	S	Fe	Cu	La	Pb	Zn	Nd
1_kuona_piste1	32,23	13,97	0,29	2,61	41,74	0,77	2,92	0,00	2,47	3,00
1_kuona_piste1	32,15	14,05	0,29	2,59	41,74	0,76	2,89	0,06	2,49	2,98
1_kuona_piste2	33,82	15,02	0,31	1,49	39,82	0,79	3,20	0,00	2,26	3,27
1_kuona_piste3	33,80	14,92	0,30	1,47	40,03	0,87	3,15	0,00	2,21	3,25
1_kuona_piste3	33,62	15,06	0,32	1,53	40,06	0,77	3,15	0,05	2,19	3,26
1_kuona_piste4	31,37	14,10	0,26	2,84	42,82	0,85	2,56	0,01	2,50	2,70
1_kuona_piste4	31,33	13,84	0,26	2,77	43,39	0,73	2,50	0,06	2,50	2,63
1_kuona_piste5	32,37	14,86	0,29	2,31	41,11	0,78	2,88	0,06	2,39	2,95
1_kuona_piste5	32,43	14,99	0,30	2,24	40,93	0,82	2,89	0,03	2,35	3,02
1_kuona_piste6	32,24	15,04	0,29	2,42	40,96	0,77	2,87	0,02	2,41	2,98
2_kuona_piste1	32,34	15,04	0,35	2,11	39,95	0,67	3,49	0,09	2,42	3,56
2_kuona_piste1	32,04	15,05	0,35	2,17	40,41	0,66	3,42	0,01	2,40	3,49
2_kuona_piste1	32,13	15,10	0,34	2,23	40,14	0,70	3,42	0,04	2,41	3,49
2_kuona_piste2	31,55	14,84	0,33	2,38	41,06	0,65	3,31	0,00	2,45	3,43
2_kuona_piste2	31,90	14,88	0,34	2,31	40,67	0,63	3,36	0,01	2,46	3,44
2_kuona_piste2	31,66	14,93	0,34	2,33	40,78	0,63	3,35	0,04	2,46	3,48
2_kuona_piste3	31,76	14,98	0,34	2,33	40,62	0,59	3,41	0,00	2,47	3,51
2_kuona_piste3	31,63	14,93	0,34	2,28	40,86	0,60	3,39	0,01	2,47	3,50
2_kuona_piste3	31,74	15,07	0,34	2,30	40,56	0,57	3,43	0,04	2,45	3,50
2_kuona_piste4	31,83	14,98	0,33	2,26	40,57	0,72	3,41	0,00	2,43	3,47
2_kuona_piste4	31,82	15,05	0,34	2,25	40,49	0,70	3,42	0,00	2,43	3,50
2_kuona_piste5	31,66	14,92	0,32	2,40	40,48	0,79	3,38	0,11	2,46	3,46
2_kuona_piste5	31,45	14,97	0,33	2,26	41,17	0,64	3,32	0,04	2,43	3,38
2_kuona_piste6	32,38	14,68	0,31	2,04	41,07	0,68	3,17	0,02	2,36	3,29
2_kuona_piste6	32,01	14,81	0,31	2,11	41,16	0,66	3,24	0,02	2,40	3,28
4-kuona_piste1	31,19	14,53	0,36	2,20	41,38	0,64	3,59	0,07	2,40	3,66
4_kuona_piste1	30,77	14,53	0,36	2,34	41,61	0,71	3,57	0,00	2,46	3,65
4_kuona_piste2	31,36	14,78	0,36	1,96	41,28	0,75	3,57	0,00	2,25	3,69
4_kuona_piste2	31,46	14,65	0,36	2,02	41,13	0,69	3,63	0,05	2,27	3,73
4_kuona_piste3	31,65	14,80	0,34	1,69	41,68	0,75	3,47	0,00	2,03	3,58
4_kuona_piste3	31,76	14,80	0,34	1,67	41,50	0,76	3,52	0,00	2,06	3,59
4_kuona_piste4	31,35	14,39	0,36	2,25	41,43	0,64	3,51	0,08	2,41	3,59
4_kuona_piste4	31,63	14,36	0,35	2,14	41,33	0,62	3,61	0,00	2,33	3,62
4_kuona_piste4	31,30	14,59	0,36	2,10	41,51	0,57	3,55	0,03	2,36	3,64
4_kuona_piste5	30,97	14,34	0,38	2,31	41,06	0,75	3,79	0,04	2,51	3,85
4_kuona_piste5	30,96	14,37	0,37	2,33	41,14	0,73	3,79	0,02	2,47	3,83
4_kuona_piste5	31,12	14,38	0,38	2,33	41,04	0,74	3,74	0,01	2,46	3,79
4 kuona_piste6	31,64	15,29	0,36	2,11	39,78	0,76	3,69	0,03	2,49	3,85
5_kuona piste1	30,96	11,54	0,34	0,66	48,06	0,37	3,16	0,00	1,60	3,31
5_kuona_piste1	30,89	11,05	0,34	0,62	48,86	0,40	3,07	0,01	1,57	3,18
5_kuona_piste1	30,44	10,39	0,31	0,75	49,83	0,87	2,86	0,08	1,53	2,94
5_kuona_piste2	30,95	12,57	0,42	0,71	44,56	0,38	4,07	0,02	2,27	4,06
5_kuona_piste2	30,84	12,50	0,41	0,75	44,87	0,37	4,02	0,08	2,18	3,98
5_kuona_piste2	31,13	12,44	0,43	0,51	44,86	0,37	4,00	0,02	2,21	4,03

5_kuona_piste3	29,87	11,74	0,43	1,42	45,18	0,49	4,16	0,02	2,39	4,30
5_kuona_piste3	29,77	11,51	0,40	1,65	44,74	0,50	4,43	0,02	2,38	4,60
5_kuona_piste3	29,80	11,88	0,41	1,59	44,28	0,45	4,47	0,03	2,42	4,66
5_kuona_piste4	31,04	12,56	0,35	1,21	45,27	0,35	3,39	0,06	2,31	3,47
5_kuona_piste4	30,81	12,64	0,34	1,12	45,48	0,35	3,41	0,03	2,31	3,51
5_kuona_piste4	30,98	13,22	0,35	1,23	44,14	0,40	3,56	0,07	2,34	3,70
5_kuona_piste5	29,91	12,37	0,41	1,96	44,13	0,45	4,04	0,06	2,46	4,21
5_kuona_piste5	29,77	12,17	0,40	1,97	44,63	0,46	3,99	0,00	2,45	4,15
5_kuona_piste5	29,84	11,45	0,39	1,78	46,08	0,44	3,76	0,00	2,36	3,91
5_kuona_piste6	31,64	12,72	0,35	0,36	46,02	0,46	3,34	0,06	1,64	3,40
5_kuona_piste6	31,46	12,26	0,35	0,37	46,98	0,50	3,18	0,00	1,62	3,29
5_kuona_piste6	31,34	12,48	0,34	0,49	46,50	0,72	3,23	0,00	1,59	3,31
6_kuona piste1	29,91	11,79	0,34	1,08	46,82	0,51	3,57	0,00	2,19	3,79
6_kuona_piste1	29,75	11,61	0,34	0,89	47,34	0,45	3,60	0,00	2,16	3,86
6_kuona_piste2	30,46	13,00	0,44	0,46	44,91	0,44	4,05	0,02	2,05	4,16
6_kuona_piste2	30,27	12,27	0,44	0,43	46,28	0,49	3,85	0,01	2,04	3,92
6_kuona_piste2	29,35	9,92	0,39	0,44	50,99	0,69	3,07	0,02	1,93	3,20
6_kuona_piste3	29,64	11,63	0,49	0,81	47,47	0,44	3,76	0,00	1,84	3,93
6_kuona_piste3	29,77	11,96	0,49	0,90	46,54	0,46	3,92	0,00	1,94	4,02
6_kuona_piste3	29,36	11,72	0,48	0,94	47,43	0,47	3,76	0,01	1,91	3,91
6_kuona_piste4	30,54	13,72	0,42	0,39	44,97	0,51	3,73	0,01	1,85	3,85
6_kuona_piste4	30,44	13,76	0,42	0,51	44,82	0,59	3,71	0,04	1,87	3,85
6_kuona_piste4	30,03	13,50	0,41	0,55	45,83	0,44	3,59	0,02	1,89	3,75
6_kuona_piste5	30,16	12,65	0,40	0,17	46,71	0,50	3,68	0,05	1,90	3,77
6_kuona_piste5	30,52	13,26	0,42	0,19	45,45	0,52	3,82	0,00	1,90	3,93
6_kuona_piste5	30,31	12,51	0,41	0,18	46,75	0,46	3,69	0,03	1,88	3,78
6_kuona_piste6	28,87	11,59	0,36	2,12	46,32	0,38	3,71	0,05	2,75	3,85
6_kuona_piste6	28,94	11,74	0,37	2,10	45,97	0,37	3,80	0,05	2,75	3,92
6_kuona_piste6	28,95	11,84	0,38	2,14	45,79	0,38	3,84	0,01	2,73	3,94
8_kuona_piste1	30,63	13,91	0,22	2,46	45,22	0,93	2,29	0,00	1,93	2,41
8_kuona_piste1	30,56	13,88	0,22	2,44	45,31	0,91	2,30	0,00	1,95	2,43
8_kuona_piste1	30,70	13,92	0,22	2,37	45,32	0,79	2,30	0,01	1,96	2,42
8_kuona_piste2	30,50	13,99	0,23	2,47	45,27	0,86	2,25	0,06	2,02	2,35
8_kuona_piste2	30,69	14,28	0,22	2,32	45,08	0,76	2,29	0,00	1,97	2,39
8_kuona_piste3	31,22	14,56	0,25	1,84	44,24	0,81	2,48	0,09	1,96	2,55
8_kuona_piste3	31,26	14,77	0,24	1,83	44,13	0,80	2,46	0,01	1,95	2,56
8_kuona_piste3	31,15	14,63	0,24	1,80	44,41	0,80	2,47	0,00	1,95	2,56
8_kuona_piste4	30,94	15,13	0,26	1,31	44,32	0,71	2,58	0,03	2,04	2,69
8_kuona_piste4	31,07	14,87	0,25	1,45	44,30	0,79	2,54	0,06	2,06	2,63
8_kuona_piste4	30,99	15,19	0,25	1,44	44,18	0,96	2,44	0,00	2,00	2,56
8_kuona_piste5	31,30	15,40	0,28	0,93	43,82	0,68	2,70	0,00	2,08	2,81
8_kuona_piste5	31,37	15,33	0,27	0,90	43,82	0,66	2,69	0,11	2,06	2,79
8_kuona_piste5	31,38	15,45	0,27	0,90	43,70	0,66	2,68	0,08	2,06	2,81
8_kuona_piste6	31,03	14,27	0,24	2,04	44,70	0,83	2,45	0,01	1,95	2,49
8_kuona_piste6	31,01	14,81	0,24	1,74	44,45	0,73	2,48	0,00	1,96	2,58
8_kuona_piste6	31,04	14,80	0,25	1,66	44,49	0,73	2,48	0,00	1,97	2,59
9_kuona piste1	31,28	15,59	0,23	1,76	43,60	0,84	2,30	0,00	2,05	2,36
9_kuona_piste1	31,50	15,57	0,22	1,74	43,48	0,86	2,23	0,00	2,05	2,36

9_kuona_piste1	31,43	15,66	0,22	1,74	43,43	0,87	2,27	0,01	2,02	2,36
9_kuona_piste2	32,70	16,20	0,22	0,40	43,51	0,80	2,14	0,04	1,74	2,25
9_kuona_piste2	33,07	16,07	0,22	0,41	43,28	0,74	2,19	0,00	1,75	2,28
9_kuona_piste2	32,64	16,23	0,22	0,51	43,35	0,79	2,20	0,03	1,75	2,29
9_kuona_piste3	32,70	16,27	0,21	0,49	43,38	0,83	2,12	0,01	1,74	2,24
9_kuona_piste3	32,65	16,23	0,21	0,48	43,42	0,85	2,13	0,06	1,74	2,23
9_kuona_piste3	32,77	16,15	0,22	0,51	43,41	0,85	2,14	0,00	1,72	2,24
9_kuona_piste4	30,74	15,37	0,25	2,29	43,25	0,82	2,48	0,07	2,17	2,56
9_kuona_piste4	30,79	15,39	0,25	2,33	43,14	0,84	2,47	0,01	2,18	2,60
9_kuona_piste4	30,64	15,39	0,25	2,31	43,36	0,83	2,51	0,00	2,12	2,60
9_kuona_piste5	30,68	15,35	0,24	2,35	43,40	0,89	2,40	0,00	2,17	2,51
9_kuona_piste5	30,60	15,34	0,24	2,34	43,48	0,87	2,43	0,05	2,16	2,48
9_kuona_piste5	30,68	15,28	0,24	2,38	43,48	0,83	2,38	0,05	2,20	2,48
9_kuona_piste6	31,31	15,69	0,24	1,83	42,94	0,86	2,44	0,00	2,12	2,56
9_kuona_piste6	31,44	15,79	0,24	1,80	42,69	0,87	2,45	0,00	2,15	2,57
9_kuona_piste6	31,31	15,78	0,24	1,73	42,90	0,80	2,51	0,03	2,12	2,59
11_kuona piste1	30,72	15,14	0,40	2,34	40,21	0,67	3,83	0,02	2,69	3,99
11_kuona_piste1	30,61	15,25	0,38	2,34	40,28	0,65	3,88	0,03	2,63	3,96
11_kuona_piste1	30,55	15,22	0,38	2,31	40,21	0,66	3,96	0,02	2,65	4,04
11_kuona_piste2	30,50	14,89	0,36	2,38	41,28	0,65	3,60	0,03	2,62	3,70
11_kuona_piste2	30,50	14,81	0,36	2,37	41,22	0,67	3,68	0,02	2,64	3,74
11_kuona_piste2	30,70	14,72	0,35	2,30	41,28	0,69	3,62	0,04	2,58	3,71
11_kuona_piste3	30,77	15,54	0,38	2,12	40,31	0,66	3,81	0,03	2,48	3,90
11_kuona_piste3	30,99	15,49	0,38	2,11	40,20	0,65	3,81	0,03	2,46	3,88
11_kuona_piste3	30,95	15,54	0,38	2,13	40,04	0,67	3,86	0,01	2,52	3,91
11_kuona_piste4	30,34	15,26	0,36	2,28	41,31	0,68	3,59	0,02	2,52	3,64
11_kuona_piste4	30,35	15,26	0,35	2,29	41,19	0,70	3,61	0,05	2,54	3,67
11_kuona_piste4	30,45	15,21	0,36	2,27	41,22	0,68	3,60	0,03	2,51	3,65
11_kuona_piste5	30,75	15,54	0,37	2,14	40,67	0,67	3,66	0,00	2,47	3,74
11_kuona_piste5	30,63	15,55	0,36	2,06	40,86	0,67	3,62	0,07	2,49	3,70
11_kuona_piste5	30,72	15,47	0,37	2,10	40,86	0,66	3,65	0,00	2,43	3,75
11_kuona_piste6	30,75	15,06	0,37	2,22	41,24	0,59	3,56	0,03	2,50	3,69
11_kuona_piste6	30,58	15,33	0,36	2,25	40,98	0,63	3,55	0,06	2,55	3,71
16_kuona piste1	30,76	14,07	0,22	1,95	45,42	0,93	2,10	0,03	2,29	2,23
16_kuona_piste1	31,37	14,36	0,23	1,38	45,06	0,66	2,21	0,08	2,35	2,31
16_kuona_piste2	30,82	13,99	0,22	1,77	45,50	0,83	2,18	0,08	2,33	2,28
16_kuona_piste2	30,73	13,88	0,23	1,79	45,71	0,86	2,13	0,03	2,35	2,29
16_kuona_piste2	30,75	13,92	0,22	1,82	45,75	0,79	2,16	0,00	2,33	2,27
16_kuona_piste3	32,30	14,82	0,23	0,34	44,14	0,84	2,31	0,11	2,48	2,43
16_kuona_piste3	32,12	14,87	0,23	0,32	44,39	0,83	2,31	0,02	2,48	2,43
16_kuona_piste3	32,24	14,88	0,23	0,32	44,28	0,82	2,30	0,02	2,47	2,43
16_kuona_piste4	30,71	13,85	0,22	1,95	45,74	0,66	2,21	0,02	2,34	2,31
16_kuona_piste4	30,40	13,69	0,22	2,14	45,93	0,74	2,22	0,02	2,36	2,28
16_kuona_piste5	30,83	14,03	0,22	1,83	45,26	0,80	2,26	0,03	2,35	2,37
16_kuona_piste5	30,90	13,85	0,22	1,97	45,31	0,82	2,22	0,00	2,38	2,34
16_kuona_piste6	32,50	14,79	0,24	0,45	44,04	0,69	2,33	0,05	2,45	2,46
16_kuona_piste6	32,33	14,80	0,23	0,46	44,22	0,67	2,29	0,06	2,48	2,46
16_kuona_piste6	32,49	14,80	0,24	0,43	44,01	0,73	2,34	0,03	2,47	2,47

17_kuona piste1	30,61	13,87	0,11	3,01	46,88	1,00	1,24	0,04	1,90	1,34
17_kuona_piste1	30,72	13,77	0,11	3,11	46,83	1,03	1,20	0,02	1,89	1,32
17_kuona_piste1	30,50	13,33	0,10	3,41	47,40	1,13	1,03	0,04	1,92	1,14
17_kuona_piste2	30,64	13,85	0,11	3,15	46,80	1,05	1,18	0,00	1,95	1,27
17_kuona_piste2	31,69	14,45	0,15	2,42	45,48	0,87	1,50	0,00	1,86	1,58
17_kuona_piste2	31,62	14,40	0,14	2,46	45,61	0,89	1,48	0,00	1,80	1,59
17_kuona_piste3	31,80	14,86	0,15	2,05	45,15	0,86	1,60	0,00	1,81	1,73
17_kuona_piste3	31,88	14,81	0,16	2,06	45,04	0,90	1,61	0,03	1,81	1,70
17_kuona_piste3	31,86	14,76	0,15	2,11	45,15	0,89	1,60	0,00	1,81	1,68
17_kuona_piste4	31,83	14,86	0,15	2,12	45,23	0,68	1,57	0,00	1,88	1,69
17_kuona_piste4	31,21	14,56	0,14	2,43	46,05	0,70	1,45	0,00	1,89	1,56
17_kuona_piste4	31,79	14,87	0,15	2,22	44,96	0,85	1,57	0,00	1,92	1,69
17_kuona_piste5	31,17	14,70	0,13	2,51	45,77	0,87	1,38	0,02	1,94	1,51
17_kuona_piste5	31,29	14,71	0,12	2,61	45,61	0,88	1,36	0,00	1,94	1,49
17_kuona_piste5	31,23	14,63	0,12	2,54	45,79	0,88	1,35	0,04	1,95	1,47
17_kuona_piste6	31,44	15,00	0,13	2,23	45,36	0,91	1,43	0,00	1,95	1,54
17_kuona_piste6	31,32	14,88	0,12	2,35	45,57	0,95	1,37	0,00	1,95	1,49
17_kuona_piste6	31,16	14,99	0,13	2,46	45,54	0,96	1,34	0,01	1,95	1,47

Appendix VI EPMA results for slag in argon atmosphere

	Norm Weight%									
Sample / Comment	O	Si	Mg	S	Fe	Cu	La	Pb	Zn	Nd
Ar1B_kuona_piste1	30,82	15,54	0,70	2,50	42,36	0,86	3,03	0,00	0,95	3,23
Ar1B_kuona_piste1	30,79	16,20	0,24	2,28	42,15	0,64	3,52	0,00	1,01	3,16
Ar1B_kuona_piste2	30,62	15,69	0,29	2,60	42,16	0,83	3,41	0,16	0,97	3,28
Ar1B_kuona_piste3	31,11	15,75	0,34	2,65	42,20	0,67	3,11	0,00	1,14	3,03
Ar1B_kuona_piste3	30,96	15,98	0,31	2,43	42,35	0,90	2,92	0,00	0,87	3,28
Ar1B_kuona_piste4	32,22	15,57	0,39	2,03	40,27	0,80	4,11	0,00	1,12	3,50
Ar1B_kuona_piste4	31,46	15,06	0,29	2,10	42,30	1,02	3,16	0,05	1,20	3,37
Ar1B_kuona_piste4	31,03	15,17	0,29	2,54	42,27	0,62	3,79	0,00	0,96	3,34
Ar1B_kuona_piste5	31,99	15,36	0,37	2,02	41,78	0,53	3,04	0,80	0,85	3,28
Ar1B_kuona_piste5	30,50	15,79	0,33	2,36	42,52	0,93	3,10	0,27	0,74	3,45
Ar1B_kuona_piste5	33,10	15,30	0,16	1,86	40,73	0,47	3,77	0,00	1,14	3,47
Ar1B_kuona_piste6	31,65	15,80	0,36	2,32	41,97	0,60	3,26	0,00	0,75	3,31
Ar1B_kuona_piste6	31,32	15,94	0,32	2,64	41,51	0,53	3,26	0,15	0,90	3,44
Ar2_kuona_piste1	31,61	15,18	0,33	2,36	41,82	0,68	3,46	0,01	1,08	3,46
Ar2_kuona_piste1	31,68	15,19	0,33	2,35	41,71	0,69	3,47	0,04	1,08	3,46
Ar2_kuona_piste2	31,81	15,26	0,33	2,34	41,59	0,67	3,48	0,00	1,00	3,51
Ar2_kuona_piste2	32,05	15,10	0,34	2,32	41,43	0,69	3,50	0,03	1,03	3,51
Ar2_kuona_piste3	31,85	15,14	0,33	2,34	41,65	0,69	3,45	0,03	1,01	3,50
Ar2_kuona_piste3	32,04	15,20	0,33	2,31	41,36	0,70	3,50	0,03	1,00	3,52
Ar2_kuona_piste4	31,10	15,33	0,35	2,40	42,20	0,67	3,40	0,00	1,09	3,46
Ar2_kuona_piste4	31,38	15,34	0,34	2,38	41,90	0,68	3,43	0,02	1,07	3,46
Ar2_kuona_piste5	31,64	15,26	0,33	2,33	41,85	0,69	3,46	0,00	0,95	3,48
Ar2_kuona_piste5	31,65	15,28	0,33	2,32	41,82	0,67	3,47	0,03	0,96	3,48
Ar2_kuona_piste6	31,05	15,37	0,33	2,37	42,20	0,70	3,47	0,00	1,08	3,43
Ar2_kuona_piste6	31,42	15,27	0,33	2,39	41,95	0,71	3,42	0,00	1,07	3,44
Ar3B_kuona_piste1	30,39	15,92	0,34	2,23	43,32	0,65	3,50	0,00	0,10	3,55
Ar3B_kuona_piste2	30,37	16,05	0,34	2,23	43,06	0,66	3,57	0,01	0,12	3,60
Ar3B_kuona_piste3	30,22	16,19	0,38	2,10	42,62	0,64	3,84	0,00	0,10	3,91
Ar3B_kuona_piste4	31,24	15,89	0,36	2,09	42,00	0,64	3,86	0,00	0,09	3,84
Ar3B_kuona_piste5	30,93	15,83	0,37	2,14	42,41	0,60	3,80	0,00	0,09	3,83
Ar3B_kuona_piste6	30,86	15,96	0,37	2,11	42,23	0,62	3,90	0,00	0,07	3,87
Ar3B_kuona_piste7	30,71	16,35	0,35	2,18	42,39	0,65	3,64	0,04	0,09	3,60
Ar3B_kuona_piste8	30,55	15,76	0,34	2,28	43,33	0,69	3,49	0,01	0,10	3,45
Ar4A_kuona_piste1	31,08	16,30	0,39	1,85	41,65	0,62	3,97	0,00	0,17	3,97
Ar4A_kuona_piste1	31,12	16,34	0,40	1,85	41,50	0,63	3,98	0,00	0,19	3,99
Ar4A_kuona_piste2	30,86	16,13	0,38	1,96	41,97	0,63	3,93	0,00	0,21	3,94
Ar4A_kuona_piste3	30,58	16,07	0,37	2,14	42,43	0,65	3,79	0,00	0,20	3,78
Ar4A_kuona_piste3	30,91	15,93	0,36	2,10	42,21	0,67	3,82	0,03	0,18	3,79
Ar4A_kuona_piste4	30,65	15,91	0,36	2,10	42,73	0,66	3,67	0,03	0,17	3,72
Ar4A_kuona_piste5	30,78	16,22	0,39	1,84	42,05	0,61	3,95	0,03	0,15	3,96
Ar4A_kuona_piste6	30,48	15,48	0,32	2,43	44,05	0,74	3,14	0,00	0,20	3,17
Ar4A_kuona_piste6	30,28	15,52	0,31	2,37	44,18	0,76	3,22	0,01	0,16	3,19
Ar5B_kuona_piste1	30,94	15,65	0,33	2,15	43,21	0,55	3,56	0,01	0,02	3,58
Ar5B_kuona_piste1	30,89	15,73	0,34	2,18	43,03	0,61	3,58	0,02	0,01	3,60

Ar5B_kuona_piste2	30,91	15,58	0,36	2,09	43,27	0,54	3,61	0,00	0,01	3,64
Ar5B_kuona_piste2	31,38	15,43	0,35	2,14	42,81	0,61	3,61	0,03	0,01	3,63
Ar5B_kuona_piste3	30,95	15,86	0,35	2,09	43,01	0,56	3,58	0,00	0,01	3,60
Ar5B_kuona_piste3	31,26	15,85	0,35	2,10	42,70	0,55	3,58	0,00	0,02	3,60
Ar5B_kuona_piste4	30,76	16,50	0,32	2,08	42,92	0,57	3,41	0,00	0,00	3,44
Ar5B_kuona_piste4	30,89	15,81	0,33	2,05	43,38	0,56	3,48	0,02	0,00	3,49
Ar5B_kuona_piste5	30,72	15,77	0,34	2,08	43,44	0,64	3,49	0,01	0,00	3,51
Ar5B_kuona_piste5	30,50	15,81	0,35	2,11	43,54	0,62	3,49	0,04	0,04	3,50
Ar5B_kuona_piste6	30,76	15,57	0,34	2,04	43,66	0,66	3,47	0,02	0,01	3,47
Ar5B_kuona_piste6	30,90	15,72	0,33	2,04	43,43	0,64	3,48	0,00	0,00	3,46
Ar6B_kuona_piste1	31,41	15,53	0,33	2,19	43,10	0,63	3,38	0,00	0,04	3,39
Ar6B_kuona_piste1	31,48	15,40	0,33	2,20	43,06	0,63	3,41	0,01	0,05	3,42
Ar6B_kuona_piste2	31,47	15,40	0,33	2,18	43,15	0,63	3,40	0,00	0,04	3,40
Ar6B_kuona_piste2	31,57	15,37	0,33	2,17	43,00	0,63	3,41	0,04	0,05	3,41
Ar6B_kuona_piste3	31,43	15,51	0,34	2,17	43,02	0,63	3,41	0,00	0,07	3,44
Ar6B_kuona_piste3	31,66	15,41	0,34	2,14	42,99	0,64	3,34	0,02	0,04	3,42
Ar6B_kuona_piste4	31,24	15,61	0,34	2,15	43,08	0,64	3,44	0,00	0,05	3,45
Ar6B_kuona_piste4	31,20	15,58	0,34	2,11	43,28	0,63	3,40	0,00	0,03	3,45
Ar6B_kuona_piste5	31,76	15,40	0,34	2,03	42,95	0,64	3,41	0,00	0,04	3,43
Ar6B_kuona_piste5	31,73	15,46	0,34	2,01	42,92	0,65	3,44	0,00	0,02	3,43
Ar6B_kuona_piste6	31,13	15,70	0,34	2,13	43,12	0,62	3,42	0,03	0,03	3,48
Ar6B_kuona_piste6	31,26	15,65	0,34	2,09	43,08	0,62	3,41	0,03	0,05	3,47
Ar7A_kuona_piste1	30,94	15,95	0,33	2,13	43,25	0,64	3,37	0,00	0,00	3,38
Ar7A_kuona_piste2	31,19	16,26	0,34	2,05	42,63	0,63	3,41	0,00	0,01	3,47
Ar7A_kuona_piste3	30,78	16,29	0,34	2,02	42,95	0,63	3,49	0,01	0,00	3,48
Ar7A_kuona_piste4	31,43	15,75	0,32	2,14	43,07	0,59	3,36	0,00	0,01	3,33
Ar7A_kuona_piste5	31,57	15,66	0,34	2,07	42,90	0,60	3,44	0,00	0,00	3,43
Ar7A_kuona_piste6	31,45	15,71	0,33	2,14	42,86	0,61	3,44	0,01	0,00	3,45
Ar8B_kuona_piste1	31,21	16,16	0,35	2,02	42,50	0,61	3,57	0,01	0,00	3,57
Ar8B_kuona_piste2	31,38	16,10	0,35	1,97	42,41	0,62	3,59	0,00	0,00	3,58
Ar8B_kuona_piste3	31,87	16,28	0,36	1,79	41,94	0,56	3,56	0,03	0,00	3,61
Ar8B_kuona_piste4	31,41	15,93	0,35	2,07	42,44	0,59	3,60	0,05	0,01	3,56
Ar8B_kuona_piste5	31,06	15,87	0,34	2,13	42,98	0,62	3,49	0,04	0,00	3,47
Ar8B_kuona_piste6	31,23	16,03	0,34	2,08	42,63	0,58	3,55	0,01	0,00	3,54

Appendix VII SEM-EDS results for Fe, Cu, S in matte in air atmosphere

Sample			**Fe**	**Norm. wt-%**				
19	39,84	39,99	39,15	40,64	39,57	40,64		
20	39,42	38,72	39,88	39,26				
21	39,06	38,26						
5	40,51	41,63	38,93	41,6	40,82	40,69	40,01	39,47
6	39,25	40,18	41,06	40,46	40,62	40,6	40,63	40,86
13	37,78	38,03	38,96	41,93	41,14	44,98		
4	37,31	39,72	38,5	39,52	38,31	40,83	40,67	
11	37,72	38,66	41,09	40,46	39,35	40,15	39,19	38,46
14	39,04	40,51	41,73	40,96	39,99	40,41	40,84	39,81
1	39,95	38,71	40,69	39,71	39,14	38,78	38,6	38,88
2	38,66	39,62	39,96	40,1	40,83	40,03	39,56	39,25
10	40,31	38,84	39,48	40,84	39,18	39,44	37,28	37,73
9	32,47	34,15	33,66	33,4	32,93	33,1	32,14	32,86
15	37,06	38,02	37,65	39,98	39,68	39,5	39,37	39,63
16	34,51	36,37	36,1	35,62	35,19	35,07	35,64	
3	0,28	0,43	0,29	0,32	0,42	0,21	0,44	
8	31,06	31,27	31,31	30,66	29,77	32,06	31,49	31,64
17	35,55	37,76	38,43	37,79	35,57	37,46	35,7	
			Cu	**Norm. wt-%**				
19	26,36	29,75	27,09	28,65	27,93	28,5		
20	28,09	28,65	30,44	28,81				
21	29,9	32,91						
5	30,5	28,68	31,75	28,88	30,13	30,17	31,03	31,82
6	30,09	30,63	29,37	30,03	29,85	30,09	29,96	29,25
13	31,46	30,55	29,91	27,93	28,12	24,75		
4	33,11	31,01	33,13	31,98	33,08	31,19	29,64	
11	33,4	33,08	30,6	30,02	32,45	31,95	32,19	33,42
14	32,68	31,99	30,31	30,99	32,35	31,79	31,42	32,13
1	32,58	33,88	31,95	33,19	33,17	33,8	33,86	33,52
2	33,35	32,36	31,6	31,98	30,44	30,69	31,26	31,66
10	31,82	32,83	32,39	31,35	32,93	32,07	34,39	34,73
9	40,37	39,52	39,1	40,02	38,96	39,98	40,5	40,3
15	34,77	33,97	34,27	32,04	32,78	32,17	33,02	32,44
16	38,39	37,33	36,8	36,86	37,61	37,24	37,15	
3	82,01	81,96	81,93	81,74	81,38	82,17	81,76	
8	42,11	42,49	41,45	42,32	43,71	40,98	41,29	41,33
17	37,37	34,98	34,58	34,61	38,02	35,32	37,57	
			S	**Norm. wt-%**				
19	24,89	24,3	22,87	24,26	23,02	24,11		
20	23,94	23,99	23,55	23,39				
21	23,59	23,92						
5	23,45	23,46	23,47	22,29	22,61	22,96	22,78	22,41

6	21,47	22,08	21,6	22,61	22,89	22,97	21,2	21,72
13	22,93	22,84	23,41	23,28	23,57	23,74		
4	21,32	21,31	21,54	21,58	22,55	22,19	19,88	
11	20,86	21,69	21,7	21,79	20,96	21,5	21,62	21,02
14	22,3	22,32	22,01	21,6	21,91	21,83	21,78	22,43
1	21,84	21,15	21,82	21,72	21,64	21,64	21,31	21,57
2	21,24	21,72	21,85	21,31	22,26	22,16	21,86	21,91
10	21,91	22,41	22,15	21,97	21,78	21,98	21,33	21,6
9	21,63	21,33	21,68	21,59	21,02	21,27	20,72	20,98
15	20,94	20,81	21,24	20,98	21,27	21,64	21,04	21,45
16	21,54	21,15	21,61	21,55	20,72	20,67	21,26	
3	16,98	16,78	17,04	17,14	17,16	16,89	17,04	
8	21,1	20,87	21,17	20,93	20,94	20,05	20,75	20,64
17	21,76	21,59	21,09	21,26	20,44	20,86	20,92	

Appendix VIII SEM-EDS results for Fe, Cu, S in matte in argon atmosphere

Sample			Fe	Norm. wt-%				
Ar1B	40,84	40,96	41,3	40,83	42,66	41,81	40,81	41,81
Ar2	41,52	41,71	42,12	41,69	41,07	41,58	40,58	40,73
Ar3B	40,21	40,28	40,38	41,38	41,64	40,64	41,74	41,03
Ar4A	42,03	42,15	41,56	41,7	41,92	42,17	40,78	41,04
Ar5B	42,99	42,69	42,95	42,44	39,26	39,29	39,34	39,51
Ar6B	40,58	39,91	41,04	40,62	41,68	42,62	41,92	42,59
Ar7A	41,83	41,6	41,12	42,35	45,43	41,95	43,7	43,6
Ar8B	40,79	40,33	39,94	39,86	39,84	41,62	43,42	38,84
			Cu	**Norm. wt-%**				
Ar1B	32,04	31,99	30,97	32	29,69	29,65	31,96	30,83
Ar2	29,07	29,44	28,85	29,21	29,35	29,18	30,16	29,79
Ar3B	32,32	32,54	32,06	31,24	30,9	32,11	30,47	31,69
Ar4A	30,26	30,78	30,75	31,07	30,81	30,06	31,98	31,75
Ar5B	30,76	30,98	30,71	31,76	35,09	35,22	35,21	34,83
Ar6B	32,8	33,99	32,68	33,2	31,81	30,73	31,91	30,72
Ar7A	31,88	31,91	32,81	31,34	27,84	31,57	29,7	29,55
Ar8B	32,71	33,55	34,14	33,83	34,17	31,81	29,89	35,18
			S	**Norm. wt-%**				
Ar1B	21,29	21,69	21,65	21,84	21,83	21,89	21,58	21,37
Ar2	23,15	23,19	23,15	23,3	23,31	23,11	23,18	23,25
Ar3B	21,25	21,66	21,27	21,8	21,7	21,36	21,87	21,37
Ar4A	22,45	22,24	22,12	22,14	21,7	22,28	21,61	21,8
Ar5B	21,1	21,28	21,46	21,1	20,75	20,75	20,8	20,61
Ar6B	21,1	20,41	20,83	20,88	21,7	21,79	21,4	21,75
Ar7A	21,33	21,44	21,19	21,58	21,57	20,98	21,37	21,31
Ar8B	21,36	21,15	21,21	21,3	20,53	20,98	21,32	20,6